

IntechOpen

Cortisol

Between Physiology and Pathology

Edited by Diana Loreta Păun



Cortisol - Between Physiology and Pathology

Edited by Diana Loreta Păun

Published in London, United Kingdom

Cortisol – Between Physiology and Pathology
<http://dx.doi.org/10.5772/intechopen.111262>
Edited by Diana Loreta Păun

Contributors

Vanessa Wandja Kamgang, Mercy Murkwe, Modeste Wankeu-Nya, John Bolodeoku, Tae Kyum Kim, Richard I. Dorin, Clifford R. Qualls, Orien L. Tulp, Ying Su, Ren-Shan Ge, Hong Xie, Vitaliy Vasylovskyy, Tetiana Nehreba, Nataliya Voloshyna, Maksym Chernenko, Tetiana Pohuliaieva

© The Editor(s) and the Author(s) 2024

The rights of the editor(s) and the author(s) have been asserted in accordance with the Copyright, Designs and Patents Act 1988. All rights to the book as a whole are reserved by INTECHOPEN LIMITED. The book as a whole (compilation) cannot be reproduced, distributed or used for commercial or non-commercial purposes without INTECHOPEN LIMITED's written permission. Enquiries concerning the use of the book should be directed to INTECHOPEN LIMITED rights and permissions department (permissions@intechopen.com).

Violations are liable to prosecution under the governing Copyright Law.



Individual chapters of this publication are distributed under the terms of the Creative Commons Attribution 3.0 Unported License which permits commercial use, distribution and reproduction of the individual chapters, provided the original author(s) and source publication are appropriately acknowledged. If so indicated, certain images may not be included under the Creative Commons license. In such cases users will need to obtain permission from the license holder to reproduce the material. More details and guidelines concerning content reuse and adaptation can be found at <http://www.intechopen.com/copyright-policy.html>.

Notice

Statements and opinions expressed in the chapters are those of the individual contributors and not necessarily those of the editors or publisher. No responsibility is accepted for the accuracy of information contained in the published chapters. The publisher assumes no responsibility for any damage or injury to persons or property arising out of the use of any materials, instructions, methods or ideas contained in the book.

First published in London, United Kingdom, 2024 by IntechOpen
IntechOpen is the global imprint of INTECHOPEN LIMITED, registered in England and Wales, registration number: 11086078, 5 Princes Gate Court, London, SW7 2QJ, United Kingdom

British Library Cataloguing-in-Publication Data
A catalogue record for this book is available from the British Library

Additional hard and PDF copies can be obtained from orders@intechopen.com

Cortisol – Between Physiology and Pathology
Edited by Diana Loreta Păun
p. cm.
Print ISBN 978-0-85466-092-6
Online ISBN 978-0-85466-091-9
eBook (PDF) ISBN 978-0-85466-093-3

We are IntechOpen, the world's leading publisher of Open Access books Built by scientists, for scientists

6,900+

Open access books available

184,000+

International authors and editors

200M+

Downloads

156

Countries delivered to

Our authors are among the
Top 1%

most cited scientists

12.2%

Contributors from top 500 universities



WEB OF SCIENCE™

Selection of our books indexed in the Book Citation Index
in Web of Science™ Core Collection (BKCI)

Interested in publishing with us?
Contact book.department@intechopen.com

Numbers displayed above are based on latest data collected.
For more information visit www.intechopen.com



Meet the editor



Diana Loreta Păun, MD, Ph.D., FACE, is an Associate Professor of Endocrinology at “Carol Davila” University of Medicine and Pharmacy and an endocrinologist at the National Institute of Endocrinology, Bucharest, Romania. Dr. Păun has acquired a comprehensive array of qualifications within her field, encompassing diabetology, osteoporosis, endocrine ultrasonography, and public health. She was General Manager of the Institute of Endocrinology from 2006 to 2015. Furthermore, since 2019, she has undertaken the role of Presidential Advisor for Health to the president of Romania. Dr. Păun is a fellow of the American College of Endocrinology, a former president of the Romanian Chapter of the American Association of Clinical Endocrinologists (AACE), and a member of the Romanian Society of Endocrinology, Romanian Society of Psychoneuroendocrinology, and the Romanian Association of Clinical Endocrinologists

Contents

Preface	XI
Chapter 1 Biological Effects of Cortisol <i>by Vanessa Wandja Kamgang, Mercy Murkwe and Modeste Wankeu-Nya</i>	1
Chapter Cortisol Measurement at Point of Care or Use: A Portable Fluorescence Immunoassay Method Using Capillary (Finger Prick) Samples <i>by John Bolodeoku and Tae Kyum Kim</i>	19
Chapter 3 Distribution of Cortisol in Human Plasma <i>in vitro</i> : Equilibrium Solutions for Free Cortisol Using Equations of Mass Conservation and Mass Action <i>by Richard I. Dorin and Clifford R. Qualls</i>	33
Chapter 4 Glucocorticoid Ablation Restores Glycemic and Thermogenic Parameters in Obesity <i>by Orien L. Tulp</i>	73
Chapter 5 Steroidogenesis of Corticosteroids, Genetic Mutation, and Endocrine Disruption Leading to Adrenal Insufficiency <i>by Ying Su, Ren-Shan Ge and Hong Xie</i>	91
Chapter 6 Efficacy of Glucocorticoid Therapy in Different Types of Multiple Sclerosis Progression <i>by Vitaliy Vasylovskyy, Tetiana Nehreba, Nataliya Voloshyna, Maksym Chernenko and Tetiana Pohuliaieva</i>	119

Preface

In an era of medical progress, a book that approaches cortisol from various perspectives represents an ambitious undertaking relevant to practitioners, whether they are endocrinologists or medical professionals from other specialties.

Cortisol is one of the most essential hormones in the body's economy due to its role in stress adaptation and metabolic effects.

The book delves into the physiology and pathophysiology of this hormone, presenting the current state of knowledge in the field and offering new perspectives with therapeutic implications. The first chapters are dedicated to the biology of cortisol, especially from the standpoint of its metabolic roles and its effects on bone, the cardiovascular system, the reproductive system, and the immune system. A significant part of the book focuses on laboratory investigations and cortisol measurement methods, presenting some new and original methods.

From a pathological perspective, the book discusses adrenal cortex disorders induced by genetic defects in enzymes involved in steroidogenesis, as well as the role of glucocorticoid excess in the development of insulin resistance and non-insulin-dependent diabetes.

Finally, the book addresses the evident therapeutic properties of glucocorticoids in challenging conditions such as multiple sclerosis.

The book explores the mysteries of cortisol while also providing, in an easily understandable format, the main advances made in understanding its mechanisms of action and the pathology of this fascinating hormone.

I would like to express my gratitude to all the chapter authors for their courage in addressing this complex and fascinating pathology and for their support in this endeavor. We hope that this book will answer multiple questions raised by cortisol and provide readers with valuable information for their everyday practice.

Diana Loreta Păun
“Carol Davila” University of Medicine and Pharmacy,
Department of Endocrinology,
Bucharest, Romania

Chapter 1

Biological Effects of Cortisol

*Vanessa Wandja Kamgang, Mercy Murkwe
and Modeste Wankeu-Nya*

Abstract

Cortisol is an essential steroid hormone, synthesized from cholesterol and released from the adrenal gland. Cortisol is mostly known for its implication in physiological changes associated with stressful circumstances. It has as main function to regulate our response to stress, via activation of the hypothalamic–pituitary–adrenal axis (HPA-axis). However, this hormone has a variety of effects on different functions throughout the body in normal circumstances or at its basal levels. Cortisol act on tissues and cells of the liver, muscle, adipose tissues, pancreas, testis, and ovaries. Moreso, it is also implicated in the regulation of various processes such as energy regulation, glucose metabolism, immune function, feeding, circadian rhythms, as well as behavioral processes. The body continuously monitors the cortisol levels to maintain steady levels (homeostasis). In this chapter, we attempt to describe the biological effects of cortisol on the various organs of the body in humans and other animal species, with emphasis on the action mechanism implicated at level of the cells of the main target tissues or organs.

Keywords: cortisol, steroid hormone, HPA axis, stress, biological effects

1. Introduction

Cortisol is a steroid hormone from the glucocorticoid family, produced in the adrenal glands [1, 2]. The secretion and release of cortisol is orchestrated by the hypothalamic-pituitary-adrenal (HPA) axis, one of the major neuro-endocrine systems of the organism. Briefly, the hypothalamic corticotropin releasing hormone CRH acts on the pituitary to cause release of ACTH, and ACTH then stimulates the adrenal gland (zona fasciculata and zona reticularis) to release glucocorticoids among which cortisol [3, 4]. The prominent glucocorticoid synthesized following the activation of the HPA axis in most mammals is cortisol; however in rodents and birds, corticosterone is the principal glucocorticoid secreted [5]. At optimal levels, cortisol works along with the other hormones of the body to maintain homeostasis. The secretion of cortisol follows a circadian rhythm; it is also essential for the survival of several living organisms [6]. Cortisol is a ubiquitous hormone, as it acts on almost every tissue and organs in the body (**Figure 1**), regulates numerous physiological processes including gluconeogenesis, protein catabolism, immune response, water balance, lipolysis, cardio-vascular function, reproduction, and skeletal growth [8].

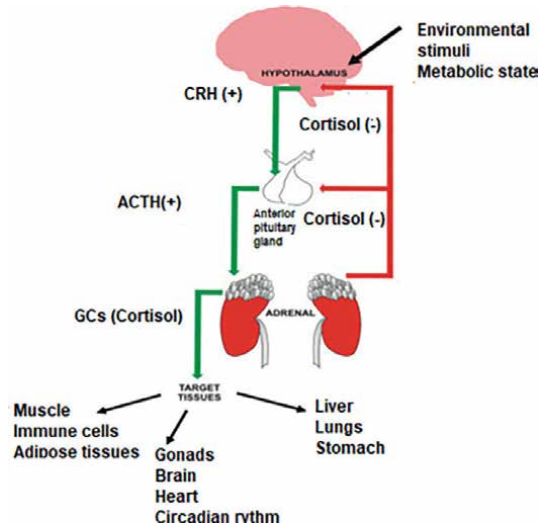


Figure 1.
The main biological effects of cortisol (Modified from Johnston III et al [7]).

Beyond these functions, in most living organisms, cortisol has a vital function: It is the key hormone involved in stress response; It is implicated in the physiological changes observed during an adaptive response (behavioral, cognitive, and physiological) necessary to deal with the upcoming actual stressor or stressful circumstances.

Along with other glucocorticoids (GCs), cortisol is known to display potent anti-inflammatory effects at pharmacological levels. Thus, glucocorticoids drugs are mostly used to treat inflammatory diseases nowadays. They are commonly prescribed to patients suffering from cancers affecting the lymphoid system such as lymphomas, leukemia and myelomas. They are also prescribed following organ transplantation to prevent rejection [9]. Because of these pleiotropic effects, the abnormal use of exogenous glucocorticoids as drugs may induce several adverse effects in the body such as growth retardation in children, immunosuppression, hypertension, inhibition of wound repair, osteoporosis, abdominal obesity, glaucoma and other metabolic disturbances [10]. Patients with Cushing syndrome, caused by either exogenous or endogenous cortisol excess show several functional disorders. Too much or too little cortisol can impact the body. Elevated cortisol provokes several physiological responses, including energy mobilization and homeostasis disturbance, thus implicating other actions of cortisol different from its actions in normal circumstances [2, 11]. An understanding of the biological actions of cortisol on various physiological processes may be an important step in developing new drugs to combat the deleterious impact of stress. The present chapter outlines the current knowledge on the effect of endogenous cortisol on target body cells, emphasis is made on the actions of cortisol under normal physiological conditions, (that is at baseline concentrations). We focus on some biological activity of cortisol on the immune system, cardiovascular system, reproductive systems, as well as its role in the lipid, sugar, and bone metabolism and on the sleep-wake cycle. Herein, to aid the understanding of the actions of cortisol, we review the various actions of cortisol across the tissues of the body, with emphasis on the action mechanism implicated at level of the cells of the main target tissues or organs [10, 12].

2. Cortisol and immunity

The survival of an organism heavily relies on homeostasis and for mammals, the immune and anti-inflammatory response play a major role in the maintenance of a constant internal milieu [3, 13]. The anti-inflammatory action of glucocorticoid hormones was discovered by Hench and colleagues over 50 years ago [14, 15].

Since the immune system has been known to be influenced by glucocorticoids, in the past and present centuries, glucocorticoids have been used to efficiently treat immune-related diseases [16]. Over the last half century synthetic GCs such as dexamethasone and prednisolone have been indicated as efficient for the treatment of many autoimmune, inflammatory, allergic disorders such as rheumatoid arthritis, ulcerative colitis, allergic rhinitis and are the most effective anti-inflammatory therapy for asthma [17]. Thus, to further improve effective therapies for various inflammatory diseases, the physiological pathways involved in the secretion and regulation of glucocorticoids as well as their action mechanism on the different components of the immune system has been studied. Among glucocorticoids, Cortisol specially is known to affect several components of the immune system such as the production of lymphocytes and granulocytes [1, 18]. Previous findings investigating the mechanisms of cortisol on the immune system of pigs indicate that an increase in cortisol levels may cause a decrease in circulating lymphocytes and granulocytes [19]. The biological actions of cortisol on the immune system are mostly initiated by a regulatory mechanism involving the central nervous system (CNS), neuroendocrine system, and immune system [10, 13].

The immune system of humans among other species can be challenged by difficult circumstances (stressors) such as infection, external aggression (injury), or the physiological or psychological response to such circumstances (stress responses) [3]. When the body is challenged with injury, during the early onset of infection, neural, endocrine and cytokines send signals from the site of inflammation converge to the periventricular nucleus of the hypothalamus to activate the secretion of corticotropin releasing hormone (CRH) into the hypophyseal portal system [10, 16]. For autoimmune diseases and tissue damage where various cytokines are produced, the secretion of cortisol also increases as the HPA axis is activated. Following the release of CRH, it triggers the anterior lobe of the pituitary gland to secrete and release the adrenocorticotropin hormone (ACTH) in the circulation, which then stimulate the expression and release of cortisol by the adrenal glands [1, 9, 20].

Previous studies have shown that changes in levels of cortisol after exercise or changes in circadian rhythms are marked by an increase in cytokine levels and production of leukocytes. Thus, after its secretion, cortisol mainly acts by modulating the transcription of genes involved in the inflammatory response [16]. The glucocorticoid receptor (GR) (NR3C1) mediates the end point tissue effect of glucocorticoids. After binding to their cytoplasmic receptor (GR), a ligand-inducible transcription factor, the GC-GR complex may regulate the expression of gene via several mechanisms after translocation into the nucleus. But first, the GC-GR complex binds to the promoter region of steroid-sensitive genes of the glucocorticoid-response elements found in the nucleus [21]. Foremost, it switches off multiple activated inflammatory genes that encode cytokines, chemokines, adhesion molecules inflammatory enzymes and receptors [22]. The mechanisms result in the decrease transcription of genes coding for

- inflammatory cytokines such as interleukines (IL2, IL3, IL4, IL-5, IL-6, IL-13, IL-15), Tumornecrosis factor (TNF- α) and other factors such as GM-CSF, SCF, TSLPTNF- α , GM-CSF, SCF, TSLP
- Chemokines such as CCL1, CCL5, CCL8: CCL1, CCL5, CXCL8
- Various inflammatory enzymes including Inducible nitric oxide synthase, (iNOS), inducible cyclooxygenase, inducible phospholipase A2 (cPLA2)
- Endothelin-1(inflammatory peptides) Inflammatory peptides: Endothelin-1
- Neurokinin-1, bradykinin B2 receptors (mediator receptors [9, 17]).

In addition to the “switch off” mechanism, the major action of cortisol is to activate many anti-inflammatory genes [22], resulting in the increase transcription (trans-activation) of:

- Lipocortin-1
- β 2-Adrenoceptors
- Secretory leukocyte inhibitory protein
- Glucocorticoid inducible Leucine zipper
- Anti-inflammatory or inhibitor cytokines IL-10, IL-12, IL-1 receptor agonist [12, 17]. The various anti-inflammatory action mechanism of cortisol also include the repression of the NFkB known as the major factor responsible for the regulation of cytokines and other elements of the immune response; thus resulting immunosuppression [6, 12].

3. Cortisol and glucose and lipid metabolism

3.1 Effects of cortisol and glucose metabolism

Cortisol mostly has a catabolic effect favoring liberation of energy stores, critical for adaptation to acute stress or illness. The maintenance of blood glucose homeostasis is among the central physiological functions regulated by glucocorticoids, and more specifically cortisol [23]. Cortisol and the other glucocorticoids influence all aspects of glucose metabolism by exerting their collective effects on the liver, endocrine pancreas, skeletal muscle, and adipose tissue [24]. Thus, disruption in cortisol rhythms often leads to disease, with chronic CORT excess (hypercortisolism) commonly associated with the impairment of glucose metabolism and the development of secondary type 2 diabetes [25].

Cortisol exerts its action after uptake of free hormone from the circulation and binding to intracellular corticoid receptors (GRs), being members of the steroid receptor hormone superfamily of nuclear transcription factors that regulate various physiological functions [26, 27].

In the liver, Cortisol is known to inhibit glucose utilization and accelerate hepatic gluconeogenesis, thereby preventing hypoglycaemia. Gluconeogenesis is the process by which glucose is generated from the non-carbohydrate substrates lactate, glycerol, and amino acids. Furthermore, cortisol also positively regulates hepatic gluconeogenesis, by stimulating the activation of key regulatory enzymes such as the glucose-6-phosphatase and the phosphoenolpyruvate carboxykinase. As in inflammation, this is achieved through the induction of the binding of GR to the glucocorticoid response elements in the promoter region of several genes encoding these enzymes [28], the rate limiting step of gluconeogenesis. In the liver, cortisol and other GCs also induce glycogen formation by increasing the activity of glycogen synthase [29].

In muscles, cortisol and the other GCs mainly impair insulin-stimulated glycogen synthesis by decreasing the activity of glycogen synthase. They also act to promote insulin resistance in skeletal muscle by regulation of a few GR target genes involved in the insulin-signaling cascade, that may lead to the malfunctioning or an apparent post-receptor defect with reduced downstream phosphoinositide-3-kinase and AKT activities. Further studies also showed that Cortisol may prevent hypoglycemia by stimulating glycogenolysis in muscle through epinephrine induced activation of glycogen phosphorylase [30]. Cortisol is thought to stimulate the generation of gluconeogenic precursors such as glycerol and gluconeogenic amino acids, by promoting lipolysis of triglyceride stores in adipose tissue and protein degradation in muscle [26].

In the adipocyte, cortisol acts by inhibiting glucose uptake and oxidation but also promotes lipolysis to provide glycerol as precursor for gluconeogenesis. The processes contributing to decreased glucose utilization by glucocorticoids in the adipocyte are less clear. However, currently, the modulation of glucose transporter GLUT4 function and the insulin signaling cascade are reported as plausible mechanisms involved herein [31]. Additionally, GCs are also involved in the differentiation and expansion of adipocyte precursors, a process that may further intensify insulin resistance and adipocyte dysfunction [24].

Cortisol is known as a potent regulator of the action metabolism of insulin secretion by pancreatic beta cells of the pancreas. Cortisol acts as a counter-regulatory hormone to insulin, and its effects may create an insulin resistance [26, 32]. Imbalanced cortisol concentrations in glycogen storage disease type I show evidence for a possible link between endocrine regulation and metabolic derangement [24]. Cortisol may impair Glucose-stimulated insulin secretion on multiple levels [30]. Primarily, it promotes the degradation of glucose transporter present in β cells, the GLUT2 and reduces expression levels of glucokinase [24, 33]. Additionally, the activity of glucose-6-phosphatase (G6P) is increased, further impairing the entry of G6P into the glycolytic cycle [34]. Cortisol also increases glucagon secretion in α cells [23, 24]. Once insulin resistance occurs, due to elevated levels of cortisol, glycogenesis is no longer stimulated and glucose storage by the liver as glycogen is thus inhibited; thereby contributing to the hyperglycaemic effects of cortisol [24].

3.2 Effects of cortisol on lipid metabolism

The implication of cortisol in lipid metabolism is well known. Previous experiments have shown that short-term administration of cortisol *in vivo* may promote adipose tissue lipolysis [35]. This could result from insulin resistance or inhibition of the action of insulin by glucocorticoid, as insulin is known to inhibit lipolysis [36]. Glucocorticoids are also thought to promote lipolysis by stimulating lipoprotein lipase

(LPL), thereby increasing the activity of lipolysis itself [37, 38]. Cortisol and glucocorticoids have been also shown to influence adipogenesis via the development of mature adipocytes, by stimulating the differentiation of pre-adipocytes into mature adipocytes and thus literally increasing the adipose tissue [39]. According to Lindroos *et al.* [40] Cortisol also acts by upregulating the glucocorticoid-dependent gene LIM domain only 3 (LMO3) known to influence the expression of 11 β -HSD1. Following its upregulation, LMO3 modulates adipocyte differentiation via PPAR γ which in turn regulates a set of adipocyte specific genes [40]. In addition to these, cortisol also influences de novo lipogenesis (DNL); a process whereby endogenous free fatty acids (FFAs) are produced from dietary carbohydrates [41]. The increase in DNL hepatic rates may decrease the available cytosolic triacylglycerol (TAG) pool, thereby increasing the export of TAGs to adipose tissues, resulting in hepatic steatosis (fatty liver) [42].

4. Cortisol effects on bone metabolism and bone growth

4.1 Cortisol effects on bone metabolism

In chronic stress circumstances, GCs have been shown to cause several adverse effects on the skeleton. However, at physiological levels, GCs play an important anabolic role as they appear to be vital for normal skeletogenesis and bone mass accrual [43, 44]. In normal physiologic conditions, endogenous cortisol regulates the expression of target genes through GR signaling within bone cells, affecting bone mineral density and the rate of bone loss [44]. The effects of cortisol on bone depend on intracellular enzymes, namely 11 β -HSDs (1 and 2), that interconvert (Figure 2) cortisol between its inactive and active forms i.e., cortisol and cortisone [45–47]. 11 β -HSD1, promotes the conversion of cortisone to cortisol in the presence of NADPH, whereas 11 β -HSD2 in the presence of its cofactor nicotinamide adenine

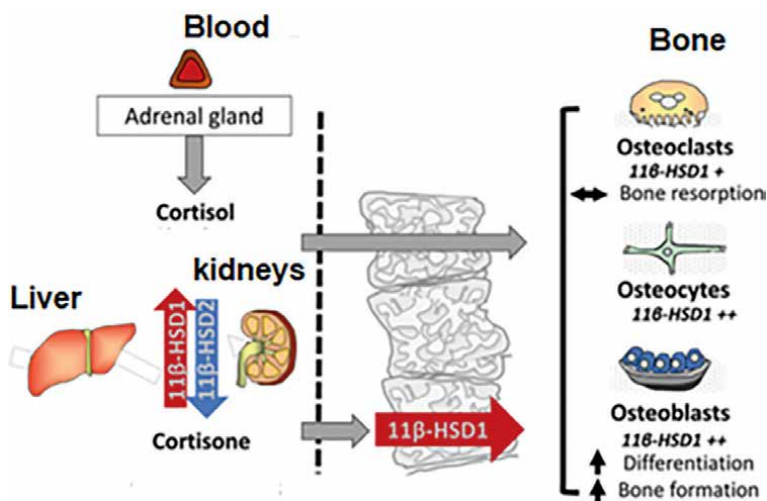


Figure 2. Cortisol and bone metabolism: Actions of corticosteroids through the conversion of cortisone to cortisol and their effect in osteoclasts, osteocytes and osteoblasts (Modified from Martin *et al.* [45]).

dinucleotide (NAD), potentially inactivates cortisol to cortisone that is inactive in bone [43, 46, 48]. Previous research studies have demonstrated that the anabolic role of cortisol on bone mainly involves bone modeling and remodeling, as it promotes osteoblastogenesis to maintain the bone architecture. Osteoblasts (the bone forming cells) and osteocytes (long-lived cells related to osteoblasts which are resident within bone tissue) are the primary cortisol target cells in bones [43, 45, 49]. Within bone cells, via the Wnt/b-catenin pathway cortisol stimulates mesenchymal cells (usually derived from bone marrow) to differentiate into mature osteoblasts and thus increase bone formation [43]. Also, cortisol stimulates expression of a range of cellular markers of osteoblast function, including osteocalcin and alkaline phosphatase [47]. Cortisol was also proven to additionally drive differentiation of osteoclasts from mesenchymal precursors and enhance the bone resorption activity of mature osteoclasts [50]. The mechanism herein implicates the production of receptor activator of nuclear factor kappa-B ligand (RANKL) and the suppression of the expression of the RANKL decoy receptor osteoprotegerin (OPG). Although cortisol has a stimulatory effect on osteoblasts at low doses, they are inhibitory at higher doses, where they instead promote apoptosis of osteoblasts [47, 51].

4.2 Cortisol effects on bone growth

Major insights into the role of cortisol on bone are limited to their metabolism, although findings have shown that they appear to be essential for normal bone growth and maintenance though not directly implicated in endochondral ossification [52]. Findings show glucocorticoids among which cortisol may have negative as well as positive effects on bone growth. Glucocorticoids were demonstrated to inhibit proliferation of chondrocytes in the resting and proliferation zones of the growth plate of bone through the inhibition of pro-proliferative growth hormone (GH) and Insulin-like growth hormone 1 (IGF-I), as well as inhibition of ERK-dependent AP-1 activation; but may increase or decrease their differentiation [52, 53].

5. Cortisol and circadian rhythm

Circadian rhythm is a pattern that occurs throughout a period of 24-h comprising light-dark cycles wherein physiological functions adjust or synchronize with the beginning or ending of each cycle of the environment [54, 55]. As in many other mammals, in human, the circadian system coordinates physiology and behaviors to adapt daily to the environment.

Adaptation here is achieved via endogenous circadian clocks, with the central circadian pacemaker (CCP) located in the suprachiasmatic nucleus (SCN) of the hypothalamus being the main clock and other peripheral clock located in other tissues of the body (**Figure 3**). The latter will then enable the body to act like a finely harmonized clock. The circadian clock is sustained by linked of transcriptional-translational feedback loops comprising clock genes namely CLOCK and BMAL1 [57, 58]. The expression of these genes activates the synthesis of other proteins that act on their own targets to produce an integrated output over the 24-h cycle [56]. Under normal conditions or fully circadian-aligned conditions the CCP, synchronizes peripheral clocks throughout the body using hormonal and neural signals [8, 59] that

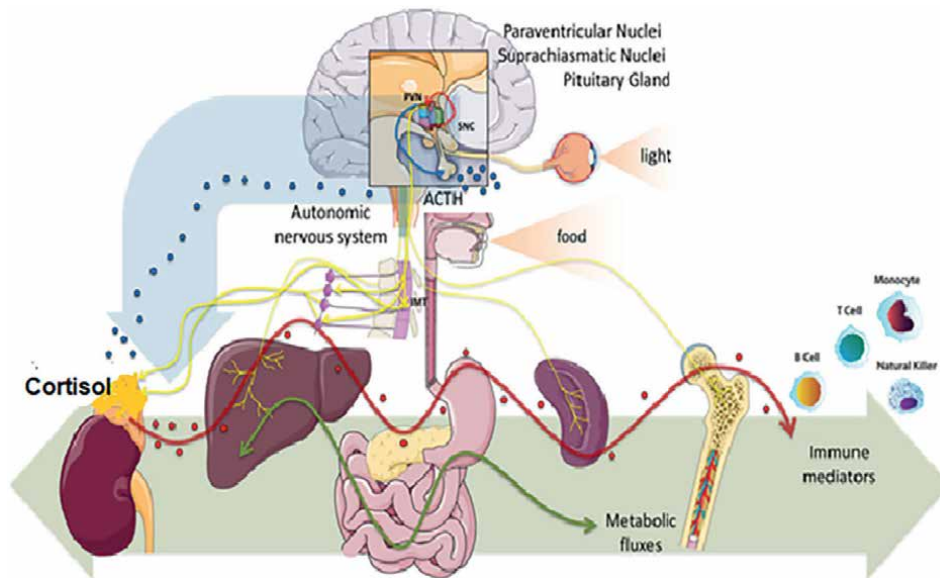


Figure 3. Schematic representation of the circadian rhythm synchronization between the central circadian pacemaker (CCP) and peripheral clock located in other tissues of the body. Cortisol secretion is stimulated via interactions between the CCP (thick blue arrow) from the suprachiasmatic master clock nuclei (SCN) and autonomic nervous system (yellow lines) and hypothalamic pituitary axis, (blue lines and circles). Following this, cortisol (red line and circles) enhances the activity of the main circadian via synchronizing systems (thick green arrow) comprising multiple signals from metabolic fluxes, cytokines, and peripheral modulation of the ligand-activated glucocorticoid receptor (modified from Minnetti et al. [56]).

participate in the entrainment of peripheral clocks by the master genes and, hence, with the light: darkness cycle. Cortisol appears to be the main metabolic or hormonal central synchronizing signal between the CCP and peripheral clocks in body tissues. In mammals, cortisol secretion is also subjected to a circadian rhythm. In normal individuals, without the occurrence of any stressors, the secretion of cortisol follows a distinct pattern; with very low or undetectable levels at midnight, to progressively increasing levels that build up overnight to peak in the morning [55, 60]. Following this, cortisol levels then decline slowly throughout the day [61]. To date, the exact mechanism through which cortisol enhances the activity of the main circadian oscillator is not well elucidated. However, it has been shown that the pivotal role of cortisol in the synchronization circadian is achieved via direct interaction between the cell-autonomous clocks in the metabolic tissues of the body i.e., the principal storage sites for glycogen, protein, and fat of the liver, muscle, and adipose tissue; or ligand-activated glucocorticoid receptor that bind to nuclear GRE at the level of regulatory regions of *Bmal1*, *Cry1*, *Per1* and *Per2* known as core clock genes [8]. Evidence of the crucial role of cortisol in circadian rhythmicity of the body are demonstrated in cases of diseases such as Cushing syndrome characterized by increased levels of cortisol, may result in a disturbed circadian rhythm seen through physical frailty, mood disorders, impaired spatial cognition and memory deficits [8, 62]. Whilst Addison's disease where there are reduced levels of cortisol is a condition characterized by attention deficit hyperactivity disorder, and dyslexia. Circadian rhythm impairments. Also studies to evaluate the consequences of circadian misalignment have shown that cortisol secretion was impaired and delayed in most individuals undergoing shift in behavioral cycles.

6. Cortisol and cardiovascular system

6.1 Actions of cortisol on the heart

Among its numerous effects on different tissues of the body, cortisol is also known to have effects on cardiac and vascular tissues. Diseases related to excess cortisol such as hypercortisolism (Cushing's syndrome) are usually associated with central obesity, insulin resistance, dyslipidemia, and alterations in clotting and platelet function but also hypertension, myocardial infarct size, ventricular remodeling post-acute myocardial infarction; the later representing risk factors of cardiovascular diseases [63–65]. The effects of cortisol on the cardiovascular system are not only linked to excess cortisol but cortisol is an important modulator of numerous processes with relevance for cardiovascular health [60, 66]. The effects of cortisol on the cardiovascular system are mostly potentiating effects. Further, cortisol has been shown to influence visceral-afferent signals or heartbeat even though the mechanisms underlying this action have not yet been clearly elucidated. Previous studies on knockout mice suggest that glucocorticoids also regulate cardiac function through the binding of mineralocorticoid receptor (MR), a nuclear receptor that appear to exert antagonistic transcriptional regulatory effects on the contractile function of the heart [4, 67, 68].

6.2 Actions of cortisol on vascular smooth muscles

The actions of cortisol on cardiovascular system do not only affect the heart but also comprise effects on vascular smooth muscles. Glucocorticoids are known to regulate the vascular tone [69]. They have been reported to enhance or potentiate the action of vasoconstrictor hormones namely Angiotensin II and norepinephrine. The potentiation action of glucocorticoids implicates receptor and non-receptor mechanisms. Studies investigating the receptor mechanisms have demonstrated that since corticosteroids are transcription factors, they could possibly induce synthesis of receptors for vasoconstrictors. For instance, for α -adrenergic receptors, Storm and Webb [70] have demonstrated that receptor number might be increased and binding affinity unchanged; whereas Schiffrin *et al.* [71] showed that in contrast to α -adrenergic receptors, angiotensin II surface receptors appear to be upregulated by corticosteroids. The non-receptor mechanisms have been shown to target vasoconstrictor synthesis by increasing the formation of angiotensinogen or by inducing the activity of angiotensin converting enzyme. In addition to increase vasoconstrictors synthesis, glucocorticoids may act on ion transport as to influence the membrane potential of vascular smooth muscle cells [69, 72].

7. Effects on the reproductive system

The biological effects of cortisol on reproduction are diverse as cortisol act in both male and female. In mammalian female, GR receptors are present in follicular cells of ovaries. Even though ovaries are site of synthesis of other steroid hormones namely progesterone and 17 alpha-hydroxy-progesterone but specific enzymes catalyzing the synthesis of cortisol are absent. In ovaries the activity of cortisol is modulated or regulated by the binding of other steroid hormones (progesterone and 17 alpha-hydroxy-progesterone) on GR receptors. Consequently, when the ovarian steroids bind to cortisol-binding protein receptors, there will be an increase of

unbound cortisol. Thus, increased levels of the latter increasing its availability to act on the follicles. Ovarian steroids also contribute to regulating the expression of two types of 11 beta-hydroxysteroid dehydrogenase (i.e. 11 beta-HSD type 1 and type 2). Consequently, a high concentration of cortisol available for biological action may be present in the preovulatory follicle just prior to ovulation [73]. Under normal physiological circumstances, cortisol levels increase in the preovulatory follicle just prior to ovulation [74, 75]. This preovulatory increase has been shown to promote receptive behavior, stimulate gonadotropins and facilitate ovulation [76, 77]. It has been suggested that cortisol may function to reduce the inflammatory-like reactions occurring in connection with ovulation [78].

In addition to its anti-inflammatory action, cortisol in the follicular fluid at ovulation may also affect the function of the oviduct and induce the formation and function of the corpus luteum, whereas the surrounding developing follicles may experience negative effects [73]. In cattle, findings from Komiya *et al.* show that cortisol may act to maintain corpus luteum function at early and midluteal stages by suppressing or regulating the apoptosis of luteal cells [79].

In females, the biological actions of cortisol are not only limited to the ovary. The actions of cortisol are also important in the uterine biology during pregnancy and labor [80]. This hormone is important for early pregnancy as previous studies have shown that glucocorticoids can promote proliferation in a variety of cell types in the uterus. Cortisol is known to increase the expression of some growth factors via the Wnt/ β -catenin and PI₃K/AKT signaling pathways and to promote proliferation of bovine endometrial epithelial cells (BEECs) [79]. Peterson *et al.* [81] demonstrated that dexamethasone administered at low doses to human lens epithelial cells in cultures may induce a moderate proliferation of these cells. The role of cortisol in the immune response is also crucial in establishing endometrial receptivity. In addition to this, cortisol may also be important during the decidualization process, as the glucocorticoid signaling in uterus may be required for the cell-fate decision of stromal cells [80]. Besides these actions, in mammals, GC levels increase towards parturition, and are partially involved in its onset through the promotion of prostaglandins. Studies in sheep have indicated that glucocorticoids may drive the shift to estrogen-primed contractile myometrium via the placental enzyme P450 17 α -hydroxylase. Following this, prostaglandins may induce myometrial contractions, ripening of the cervix and trigger the rupture of foetal membrane [80]. In species such as cattle, goat and sheep, GCs are low throughout pregnancy and only rise prior to parturition [82].

In males, glucocorticoids physiological levels and stress-induced cortisol are known to influence the testicular function. Previous studies have shown that cortisol influences the production of androgens by modulating the biosynthesis of enzymes and testicular LH receptors [73, 83]. In adrenalectomized rats, testosterone production was shown to increase. The number of spermatids also decreased and was restored after dexamethasone treatment. Moreover, in zebrafish (*Danio rerio*), studies in ex-vivo culture system demonstrated that cortisol may stimulate spermatogenesis i.e., spermatogonia proliferation and differentiation. This is achieved through using paracrine pathway (androgen independent manner) through the modulation of transcription of some genes involved in the testicular function. Further findings also demonstrated that cortisol promotes meiosis and spermiogenesis, thus increasing the number of spermatozoa in the testes [84]. In a previous study carried out on fragments of immature Japanese eel fish, Ozaki *et al.* demonstrated that cortisol activate spermatogonia differentiation and DNA replication via 11-ketotestosterone [85]. Besides the testicular function, cortisol also modulates or regulates the erectile

function and sexual behavior in humans. In a recent study by Rahardjo *et al.* [86] demonstrated that cortisol may act as a mediator of the erectile function, by acting as an antagonist of the normal sexual response in adults. Their results also highlighted that an impaired secretion of cortisol may induce erectile dysfunction. Moreso, cortisol was also proven that cortisol might be an important modulator of sexual behavior. Although the mechanism are still unclear, Rodriguez-Nieto *et al.* [87] suggested cortisol may act as a neuromodulator and may associates with the anteromedial prefrontal cortex region during the approach before sexual stimuli. It appears that the response to cortisol response varied among individuals in sexual inhibition and mood from sexual activity.

8. Conclusion

From this chapter describing the biological actions of cortisol, it can be concluded that cortisol plays a very important role in the various physiological processes in the body, important for its development and its homeostasis. Therefore, from the knowledge summarized herein, the importance of the use of cortisol derived drugs in decreasing the inflammation process is clearly understood. From this chapter it appears that the effects of cortisol on glucose metabolism are very vital for homeostasis as its various actions also influence lipid metabolism and may be at the origin of metabolic diseases. This chapter also shows the implication of cortisol in bone metabolism and growth even though more is still to be elucidated especially regarding the biological actions of cortisol on growth that is not very well known. The actions of cortisol on vascular systems, circadian rhythm and reproductive system further explains the disturbances observed due to environmental stimuli (stress). Transcriptional activation, modification of receptors, changing enzyme activity, stimulation of release or production, appear as the mechanisms, via which cortisol mostly exert its action; however, some pathways are still unknown. This suggests that many more experiments need to be performed to fully understand the pathways involved in the actions of cortisol in the different target tissues. Finally, because of all the different processes cortisol has effects on, there also are different possible changes in cortisol levels which may affect several systems in the body. Thus, corticosteroids treatments may have important adverse effects inhibiting processes important for the body. This confirms the necessity of carrying out further research on the various actions of cortisol, describing mechanisms involved to better corticosteroid-based treatments.

In spite of the knowledge about the biological actions of cortisol, there is still a lot to understand. Hence, every little discovery counts and will eventually help to explain physiological mechanisms in cortisol-related syndromes.

Acknowledgements

The authors would like to thank the Universities of Bamenda and Douala for the facilities which enabled them to write this chapter.

Conflict of interest

The authors declare no conflict of interest.

Author details


Vanessa Wandja Kamgang^{1*}, Mercy Murkwe¹ and Modeste Wankeu-Nya²

1 Department of Biology, Higher Teacher Training College, University of Bamenda, Bambili, Cameroon

2 Faculty of Science, Department of Animal Organisms Biology, University of Douala, Douala, Cameroon

*Address all correspondence to: vanessa.wandja@gmail.com

IntechOpen

© 2023 The Author(s). Licensee IntechOpen. This chapter is distributed under the terms of the Creative Commons Attribution License (<http://creativecommons.org/licenses/by/3.0>), which permits unrestricted use, distribution, and reproduction in any medium, provided the original work is properly cited. 

References

- [1] Chrousos GP. The hypothalamic–pituitary–adrenal axis and immune-mediated inflammation. *New England Journal of Medicine*. 1995;**332**(20):1351-1363
- [2] Sapolsky RM, Romero LM, Munck AU. How do glucocorticoids influence stress responses? Integrating permissive, suppressive, stimulatory, and preparative actions. *Endocrine Reviews*. 2000;**21**(1):55-89
- [3] Miller DB, O’Callaghan JP. Neuroendocrine aspects of the response to stress. *Metabolism-Clinical and Experimental*. 2002;**51**(6):5-10
- [4] Oakley RH, Cruz-Topete D, He B, Foley JF, Myers PH, Xu X, et al. Cardiomyocyte glucocorticoid and mineralocorticoid receptors directly and antagonistically regulate heart disease in mice. *Science Signaling*. 2019;**12**(577):eaau9685
- [5] Ralph C, Tilbrook A. Invited review: The usefulness of measuring glucocorticoids for assessing animal welfare. *Journal of Animal Science*. 2016;**94**(2):457-470
- [6] McKay LI, Cidlowski JA. Molecular control of immune/inflammatory responses: Interactions between nuclear factor- κ B and steroid receptor-signaling pathways. *Endocrine Reviews*. 1999;**20**(4):435-459
- [7] Johnstone WM III, Honeycutt JL, Deck CA, Borski RJ. Nongenomic glucocorticoid effects and their mechanisms of action in vertebrates. *International Review of Cell and Molecular Biology*. 2019;**346**:51-96
- [8] O’Byrne NA, Yuen F, Butt WZ, Liu PY. Sleep and circadian regulation of cortisol: A short review. *Current Opinion in Endocrine and Metabolic Research*. 2021;**18**:178-186
- [9] Straub RH, Cutolo M. Glucocorticoids and chronic inflammation. *Rheumatology*. 2016;**55**(suppl. 2):ii6-ii14
- [10] Rhen T, Cidlowski JA. Antiinflammatory action of glucocorticoids—New mechanisms for old drugs. *New England Journal of Medicine*. 2005;**353**(16):1711-1723
- [11] Rabasa C, Dickson SL. Impact of stress on metabolism and energy balance. *Current Opinion in Behavioral Sciences*. 2016;**9**:71-77
- [12] Oakley RH, Cidlowski JA. The biology of the glucocorticoid receptor: New signaling mechanisms in health and disease. *The Journal of Allergy and Clinical Immunology*. 2013;**132**(5):1033-1044
- [13] Thau L, Gandhi J, Sharma S. Physiology, cortisol. In: StatPearls. Treasure Island, FL: StatPearls Publishing; 2022
- [14] Hench PS, Slocumb CH, Barnes AR, Smith HL, Polley HF, Kendall EC. The effects of the adrenal cortical hormone 17-hydroxy-11-dehydrocorticosterone (compound E) on the acute phase of rheumatic fever: Preliminary report. In: *Proceedings of Staff Meetings*. Vol. 24, No. 11. Rochester, Minnesota: Mayo Clinic; 1949. pp. 277-297
- [15] Saklatvala J. Glucocorticoids: Do we know how they work? *Arthritis Research Therapy*. 2002;**4**(3):1-5
- [16] Webster JI, Tonelli L, Sternberg EM. Neuroendocrine regulation of immunity.

Annual Review of Immunology.
2002;**20**(1):125-163

[17] Barnes PJ. Anti-inflammatory actions of glucocorticoids: Molecular mechanisms. *Clinical Science*. 1998;**94**(6):557-572

[18] Griffin JFT. Stress and immunity: A unifying concept. *Veterinary Immunology and Immunopathology*. 1989;**20**(3):263-312

[19] de Groot J, de Jong IC, Prella IT, Koolhaas JM. Immunity in barren and enriched housed pigs differing in baseline cortisol concentration. *Physiology & Behavior*. 2000;**71**(3-4):217-223

[20] Sheridan JF, Dobbs C, Brown D, Zwilling B. Psychoneuroimmunology: Stress effects on pathogenesis and immunity during infection. *Clinical Microbiology Reviews*. 1994;**7**(2):200-212

[21] Vandevyver S, Dejager L, Tuckermann J, Libert C. New insights into the anti-inflammatory mechanisms of glucocorticoids: An emerging role for glucocorticoid-receptor-mediated transactivation. *Endocrinology*. 2013;**154**(3):993-1007

[22] Barnes PJ, Adcock IM. How do corticosteroids work in asthma? *Annals of Internal Medicine*. 2003;**139**(5_Part_1):359-370

[23] Wang Z, Mick GJ, Xie R, Wang X, Xie X, Li G, et al. Cortisol promotes endoplasmic glucose production via pyridine nucleotide redox. *The Journal of Endocrinology*. 2016;**229**(1):25-36

[24] Bauerle KT, Harris C. Glucocorticoids and diabetes. *Missouri Medicine*. 2016;**113**(5):378

[25] Zavala E, Gil-Gómez CA, Wedgwood KC, Burgess R, Tsaneva-

Atanasova K, Herrera-Valdez MA. Dynamic modulation of glucose utilisation by glucocorticoid rhythms in health and disease. *BioRxiv*. 2020;**28**:2020-2022

[26] Christiansen JJ, Djurhuus CB, Gravholt CH, Iversen P, Christiansen JS, Schmitz O, et al. Effects of cortisol on carbohydrate, lipid, and protein metabolism: Studies of acute cortisol withdrawal in adrenocortical failure. *The Journal of Clinical Endocrinology & Metabolism*. 2007;**92**(9):3553-3559

[27] Yajurvedi H. Stress and glucose metabolism: A review. *Imaging Journal of Clinical and Medical Sciences*. 2018;**5**:008-012

[28] Yabaluri N, Bashyam MD. Hormonal regulation of gluconeogenic gene transcription in the liver. *Journal of Bioscience (Bangalore)*. 2010;**35**(3):473-484

[29] Kuo T, McQueen A, Chen T-C, Wang J-C. Regulation of glucose homeostasis by glucocorticoids. *Glucocorticoid Signaling: From Molecules to Mice to Man*. 2015;**872**: 99-126

[30] Kuo T, Harris CA, Wang J-C. Metabolic functions of glucocorticoid receptor in skeletal muscle. *Molecular and Cellular Endocrinology*. 2013;**380**(1-2):79-88

[31] Lee RA, Harris CA, Wang J-C. Glucocorticoid receptor and adipocyte biology. *Nuclear Receptor Research*. 2018;**2018**:5

[32] Rossi A, Simeoli C, Salerno M, Ferrigno R, Della Casa R, Colao A, et al. Imbalanced cortisol concentrations in glycogen storage disease type I: Evidence for a possible link between endocrine regulation and metabolic derangement.

Orphanet Journal of Rare Diseases.
 2020;**15**:1-8

[33] Borboni P, Porzio O, Magnaterra R, Fusco A, Sesti G, Lauro R, et al. Quantitative analysis of pancreatic glucokinase gene expression in cultured β cells by competitive polymerase chain reaction. *Molecular and Cellular Endocrinology*. 1996;**117**(2):175-181

[34] Khan A, Ostenson C, Berggren P, Efendic S. Glucocorticoid increases glucose cycling and inhibits insulin release in pancreatic islets of ob/ob mice. *American Journal of Physiology-Endocrinology and Metabolism*. 1992;**263**(4):E663-E6E6

[35] Divertie GD, Jensen MD, Miles JM. Stimulation of lipolysis in humans by physiological hypercortisolemia. *Diabetes*. 1991;**40**(10):1228-1232

[36] Dinneen S, Alzaid A, Miles J, Rizza R. Metabolic effects of the nocturnal rise in cortisol on carbohydrate metabolism in normal humans. *The Journal of Clinical Investigation*. 1993;**92**(5):2283-2290

[37] Ottosson M, Vikman-Adolfsson K, Enerbäck S, Olivecrona G, Björntorp P. The effects of cortisol on the regulation of lipoprotein lipase activity in human adipose tissue. *The Journal of Clinical Endocrinology & Metabolism*. 1994;**79**(3):820-825

[38] Samra JS, Clark ML, Humphreys SM, MacDonald IA, Bannister PA, Frayn KN. Effects of physiological hypercortisolemia on the regulation of lipolysis in subcutaneous adipose tissue. *The Journal of Clinical Endocrinology & Metabolism*. 1998;**83**(2):626-631

[39] Halvorsen Y-DC, Bond A, Sen A, Franklin DM, Lea-Currie YR, Sujkowski D, et al. Thiazolidinediones

and glucocorticoids synergistically induce differentiation of human adipose tissue stromal cells: Biochemical, cellular, and molecular analysis. *Metabolism-Clinical and Experimental*. 2001;**50**(4):407-413

[40] Lindroos J, Husa J, Mitterer G, Haschemi A, Rauscher S, Haas R, et al. Human but not mouse adipogenesis is critically dependent on LMO3. *Cell Metabolism*. 2013;**18**(1):62-74

[41] Hillgartner FB, Salati LM, Goodridge AG. Physiological and molecular mechanisms involved in nutritional regulation of fatty acid synthesis. *Physiological Reviews*. 1995;**75**(1):47-76

[42] Macfarlane DP, Forbes S, Walker BR. Glucocorticoids and fatty acid metabolism in humans: Fuelling fat redistribution in the metabolic syndrome. *The Journal of Endocrinology*. 2008;**197**(2):189-204

[43] Zhou H, Cooper MS, Seibel MJ. Endogenous glucocorticoids and bone. *Bone Research*. 2013;**1**(1):107-119

[44] Suarez-Bregua P, Guerreiro PM, Rotllant J. Stress, glucocorticoids and bone: A review from mammals and fish. *Frontiers in Endocrinology*. 2018;**9**:526

[45] Martin CS, Cooper MS, Hardy RS. Endogenous glucocorticoid metabolism in bone: Friend or foe. *Frontiers in Endocrinology*. 2021;**12**:733611

[46] Cooper MS. Glucocorticoids in bone and joint disease: The good, the bad and the uncertain. *Clinical Medicine*. 2012;**12**(3):261

[47] Hardy RS, Zhou H, Seibel MJ, Cooper MS. Glucocorticoids and bone: Consequences of endogenous and

exogenous excess and replacement therapy. *Endocrine Reviews*. 2018;**39**(5):519-548

[48] Sher LB, Woitge HW, Adams DJ, Gronowicz GA, Krozowski Z, Harrison JR, et al. Transgenic expression of 11 β -hydroxysteroid dehydrogenase type 2 in osteoblasts reveals an anabolic role for endogenous glucocorticoids in bone. *Endocrinology*. 2004;**145**(2):922-929

[49] Hofbauer LC, Rauner M. Minireview: Live and let die: Molecular effects of glucocorticoids on bone cells. *Molecular Endocrinology*. 2009;**23**(10):1525-1531

[50] Weinstein RS, Jilka RL, Parfitt AM, Manolagas SC. Inhibition of osteoblastogenesis and promotion of apoptosis of osteoblasts and osteocytes by glucocorticoids. Potential mechanisms of their deleterious effects on bone. *The Journal of Clinical Investigation*. 1998;**102**(2):274-282

[51] Dempster D, Moonga B, Stein L, Horbert W, Antakly T. Glucocorticoids inhibit bone resorption by isolated rat osteoclasts by enhancing apoptosis. *The Journal of Endocrinology*. 1997;**154**(3):397-406

[52] Hartmann K, Koenen M, Schauer S, Wittig-Blaich S, Ahmad M, Baschant U, et al. Molecular actions of glucocorticoids in cartilage and bone during health, disease, and steroid therapy. *Physiological Reviews*. 2016;**96**(2):409-447

[53] Zaman F, Chrysis D, Huntjens K, Fadeel B, Säwendahl L. Ablation of the pro-apoptotic protein Bax protects mice from glucocorticoid-induced bone growth impairment. *PLoS One*. 2012;**7**(3):e33168

[54] Selfridge JM, Moyer K, Capelluto DG, Finkelstein CV. Opening

the debate: How to fulfill the need for physicians' training in circadian-related topics in a full medical school curriculum. *Journal of Circadian Rhythms*. 2015;**2015**:13

[55] Mohd Azmi NAS, Juliana N, Azmani S, Mohd Effendy N, Abu IF, Mohd Fahmi Teng NI, et al. Cortisol on circadian rhythm and its effect on cardiovascular system. *International Journal of Environmental Research in Public Health*. 2021;**18**(2):676

[56] Minnetti M, Hasenmajer V, Pofi R, Venneri MA, Alexandraki KI, Isidori AM. Fixing the broken clock in adrenal disorders: Focus on glucocorticoids and chronotherapy. *The Journal of Endocrinology*. 2020;**246**(2):R13-R31

[57] Nader N, Chrousos GP, Kino T. Circadian rhythm transcription factor CLOCK regulates the transcriptional activity of the glucocorticoid receptor by acetylating its hinge region lysine cluster: Potential physiological implications. *The FASEB Journal*. 2009;**23**(5):1572

[58] Moreira AC, Antonini SR, de Castro M. Mechanisms in endocrinology: A sense of time of the glucocorticoid circadian clock: From the ontogeny to the diagnosis of Cushing's syndrome. *European Journal of Endocrinology*. 2018;**179**(1):R1-R18

[59] Reppert S, Weaver DR. Coordination of circadian timing in mammals. *Nature*. 2002;**418**:935-941

[60] Timmermans S, Souffriau J, Libert C. A general introduction to glucocorticoid biology. *Frontiers in Immunology*. 2019;**10**:1545

[61] Chan S, Debono M. Replication of cortisol circadian rhythm: New advances in hydrocortisone replacement therapy.

- Therapeutic in Advanced Endocrinology Metabolism. 2010;**1**:129-138
- [62] Alexandraki KI, Grossman AB. Novel insights in the diagnosis of Cushing's syndrome. *Neuroendocrinology*. 2010;**92**(Suppl. 1):35-43
- [63] Bain R, Fox J, Jagger J, Davies M, Littler W, Murray R. Serum cortisol levels predict infarct size and patient mortality. *International Journal of Cardiology*. 1992;**37**(2):145-150
- [64] Pilz S, Theiler-Schwetz V, Trummer C, Keppel MH, Gröbler MR, Verheyen N, et al. Associations of serum cortisol with cardiovascular risk and mortality in patients referred to coronary angiography. *Journal of the Endocrine Society*. 2021;**5**(5):bvab017
- [65] Walker BR. Glucocorticoids and cardiovascular disease. *European Journal of Endocrinology*. 2007;**157**(5): 545-559
- [66] Liu B, Zhang T-N, Knight JK, Goodwin JE. The glucocorticoid receptor in cardiovascular health and disease. *Cell*. 2019;**8**(10):1227
- [67] Cruz-Topete D, Oakley RH, Cidlowski JA. Glucocorticoid signaling and the aging heart. *Frontiers in Endocrinology*. 2020;**11**:347
- [68] Amram AV, Cutie S, Huang GN. Hormonal control of cardiac regenerative potential. *Endocrine Connections*. 2021;**10**(1):R25-R35
- [69] Ullian ME. The role of corticosteroids in the regulation of vascular tone. *Cardiovascular Research*. 1999;**41**(1):55-64
- [70] Storm DS, Webb RC. Alpha-adrenergic receptors and 45Ca^{2+} efflux in arteries from deoxycorticosterone acetate hypertensive rats. *Hypertension*. 1992;**19**(6_pt_2):734-73814
- [71] Schiffrin EL, Gutkowska J, Genest J. Effect of angiotensin II and deoxycorticosterone infusion on vascular angiotensin II receptors in rats. *American Journal of Physiology-Heart and Circulatory Physiology*. 1984;**246**(4):H608-HH14
- [72] Perry PA, Webb RC. Agonist-sensitive calcium stores in arteries from steroid hypertensive rats. *Hypertension*. 1991;**17**(5):603-611
- [73] Andersen CY. Possible new mechanism of cortisol action in female reproductive organs: Physiological implications of the free hormone hypothesis. *The Journal of Endocrinology*. 2002;**173**(2):211-217
- [74] Schiml PA, Rissman EF. Cortisol facilitates induction of sexual behavior in the female musk shrew (*Suncus murinus*). *Behavioral Neuroscience*. 1999;**113**(1):166
- [75] Fanson KV, Keeley T, Fanson BG. Cyclic changes in cortisol across the estrous cycle in parous and nulliparous Asian elephants. *Endocrine Connections*. 2014;**3**(2):57-66
- [76] Ralph C, Lehman M, Goodman RL, Tilbrook A. Impact of psychosocial stress on gonadotrophins and sexual behaviour in females: Role for cortisol? *Reproduction*. 2016;**152**(1):R1-R14
- [77] Atkinson HC, Waddell BJ. Circadian variation in basal plasma corticosterone and adrenocorticotropin in the rat: Sexual dimorphism and changes across the estrous cycle. *Endocrinology*. 1997;**138**(9):3842-3848
- [78] Hillier S, Tetsuka M. An anti-inflammatory role for glucocorticoids

in the ovaries? Journal of Reproductive Immunology. 1998;**39**(1-2):21-27

[79] Dong J, Li J, Li J, Cui L, Meng X, Qu Y, et al. The proliferative effect of cortisol on bovine endometrial epithelial cells. Reproductive Biology and Endocrinology. 2019;**17**(1):1-9

[80] Whirledge S, Cidlowski JA. Glucocorticoids and reproduction: Traffic control on the road to reproduction. Trends in Endocrinology & Metabolism. 2017;**28**(6):399-415

[81] Petersen A, Carlsson T, Karlsson J, Jonhede S, Zetterberg M. Effects of dexamethasone on human lens epithelial cells in culture. Molecular Vision. 2008;**14**:1344

[82] Khan J, Ludri R. Hormone profile of crossbred goats during the periparturient period. Tropical Animal Health and Production. 2002;**34**(2):151-162

[83] Whirledge S, Cidlowski JA. A role for glucocorticoids in stress-impaired reproduction: Beyond the hypothalamus and pituitary. Endocrinology. 2013;**154**(12):4450-4468

[84] Tovo-Neto A, Martinez ER, Melo AG, Doretto LB, Butzge AJ, Rodrigues MS, et al. Cortisol directly stimulates spermatogonial differentiation, meiosis, and spermiogenesis in zebrafish (*Danio rerio*) testicular explants. Biomolecules. 2020;**10**(3):429

[85] Ozaki Y, Higuchi M, Miura C, Yamaguchi S, Tozawa Y, Miura T. Roles of 11 β -hydroxysteroid dehydrogenase in fish spermatogenesis. Endocrinology. 2006;**147**(11):5139-5146

[86] Rahardjo HE, Becker AJ, Märker V, Kuczyk MA, Ückert S. Is cortisol an endogenous mediator of erectile dysfunction in the adult male?

Translational Andrology and Urology. 2023;**12**(5):684

[87] Rodríguez-Nieto G, Sack AT, Dewitte M, Emmerling F, Schuhmann T. The modulatory role of cortisol in the regulation of sexual behavior in young males. Frontiers in Behavioral Neuroscience. 2020;**14**:197

Cortisol Measurement at Point of Care or Use: A Portable Fluorescence Immunoassay Method Using Capillary (Finger Prick) Samples

John Bolodeoku and Tae Kyum Kim

Abstract

In this chapter, we describe a quantitative fluorescence immunoassay (FIA) for the quantitative determination of cortisol in finger prick samples using a handheld device (ichroma™ M3). It gives a signal which is directly proportional to the cortisol concentration in plasma samples with a performance time between 10 and 15 min. The assay has a working range of 50–800 nmol/L. The precision of the assay (repeatability, within-laboratory, lot to lot, between person, between sites) is <7.1%. There is very little cross-reactivity (+/– 5%) with Cortisone, Corticosterone, Progesterone, Prednisone, Testosterone, Prednisolone, Deoxycortisol, DHEA, Dexamethasone. With minimal interference (+/– 5%) from D-glucose, L-Ascorbic acid, Bilirubin, Haemoglobin, Cholesterol and Triglyceride. There is very good agreement between the cortisol estimates of the bioMerieux Mini VIDAS (reference) and ichroma™ M3. In addition, cortisol estimations could also be performed on whole blood K²-EDTA, whole blood K³-EDTA and whole blood Li-Heparin samples. The ichroma™ cortisol method was able to detect the circadian rhythm in a healthy volunteer using finger prick samples and handheld device.

Keywords: assay, blood cortisol, immunoassay, method comparison, ichroma, point of care or use testing

1. Introduction

Cortisol, often referred to as the “stress hormone,” plays a crucial role in the body’s response to stress and regulates various physiological processes. The measurement of cortisol levels is a significant aspect of understanding stress-related conditions, adrenal function, and overall health. Total cortisol distribution is composed of corticoid binding globulin cortisol (80–90%), albumin bound cortisol

(10–15%) and free cortisol (3–5%). It enters the circulatory system and is detectable in several body fluids such as urine, blood, sweat, interstitial fluid (ISF), hair and saliva, with each of these body fluids having their advantages and weaknesses [1, 2].

Cortisol has been measured in sweat. There is a strong correlation between cortisol levels in sweat and hair. However, there is a challenge in accessing reliable and repeatable samples to measure cortisol in sweat. In addition, there are a number of factors that influence sweating [1].

Urinary cortisol is measured in its free form and usually a 24-h urine collection. Thereby making the 24-h urinary free cortisol measurement, it is not affected by diurnal variation or the confounding effect of cortisol binding proteins [2]. This biofluid is a relatively non-invasive and painless source to detect cortisol. However, the collection of the urine over a 24-h period and the special considerations related to the container, can make it inconvenient and the reliability of measurement of estimating and interpretation of free cortisol. In addition, several factors such as pregnancy and medications can interfere with the concentration of cortisol in urine [1].

Salivary cortisol is the most recognised source for cortisol measurement. In addition, it is also like blood cortisol has a circadian variation, with the highest levels in the morning and lowest at midnight. Saliva can be collected quite easily. However, the drawback to this popular source is that the cortisol present in the saliva is in the free form and in much smaller concentrations than in the blood. In some instances, large volumes of saliva are required [1, 3–6].

Blood for cortisol detection has been the oldest form of body fluid sampled. Sampling blood requires the puncture of veins, sample preparation, which is a painful and involves procedure, and causes stress prior to and during sampling that might elevate cortisol levels and increase the turnaround time [1].

There are a number of methods to measure blood cortisol used in numerous commercial kits and on automated laboratory platforms as immunoassays (IA) and enzyme immunoassays (EIA), luminescence and fluorescence assays, which are available. However, there remains several problems in the so-called direct immunoassays if pre-analytical measures are not carried out before the assay [7]. In addition, automated immunoassays measure cortisol but lack specificity and show significant inter-assay differences [8].

Cortisol immunoassays have been shown to demonstrate good precision and correlation with Liquid Chromatography Mass Spectrometry (LC-MS/MS) [6]. These assays have high performance, are easily performed, and are cost effective. However, they are performed on desk top analysers and use serum samples that require centrifugation, thereby making it a bit of a challenge for these assays to be used to measure cortisol at point of care or use. Recently, a fluorescence immunoassay (FIA) for the quantitative determination of cortisol was used to measure cortisol in peripheral and cord blood [7]. Using the same FIA, the ichroma™ cortisol assay and desktop device ichroma™ II, we determined the serum blood cortisol concentrations in a male population attending a prostate cancer screening program between 10:00 hrs and 18:00 hrs, showing cortisol concentrations between 98.85–643.3 nmol/L. The median concentration was 337.2 nmol/L, see **Figure 1** (data on file).

The ichroma™ cortisol is a fluorescence immunoassay (FIA) for the quantitative determination of cortisol in human whole blood using a handheld device. In this chapter, we would show the performance characteristics of this assay and present some data on cortisol profiles obtained using finger prick samples.

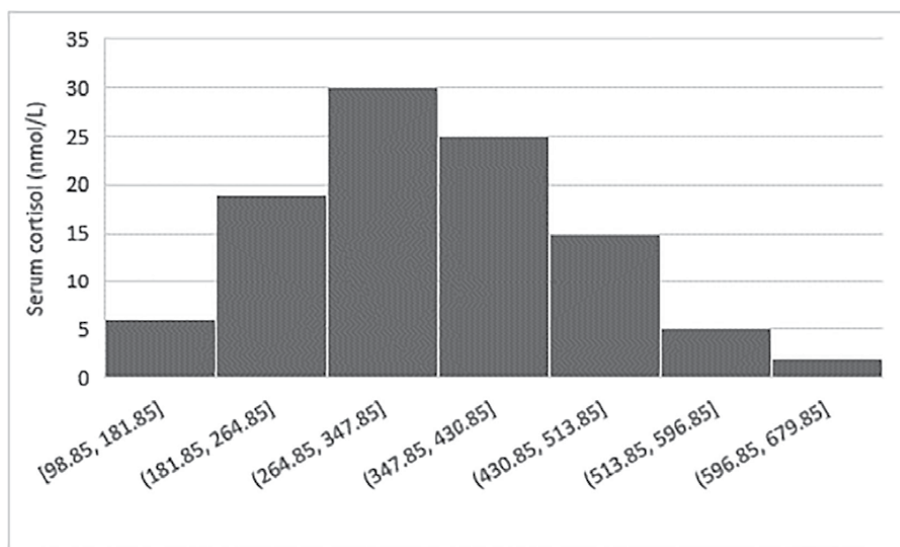


Figure 1.
Showing serum cortisol concentrations from 102 males attending prostate cancer screening program using ichroma™ cortisol reagents and ichroma™ II desk top device.

2. Performance characteristics

2.1 Sensitivity

Limit of Blank (LoB) 5.07 nmol/L
Limit of Detection (LoD) 6.28 nmol/L
Limit of Quantitation (LoQ) 50.0 nmol/L

2.2 Specificity

2.2.1 Cross reactivity

Standards were made up at cortisol concentrations of 70, 270 and 650 nmol/L. One set of standards were controls and another set were test standards where the following molecules (Cortisone, Corticosterone, Progesterone, Prednisone, Testosterone, Prednisolone, Deoxycortisol, DHEA and Dexamethasone) were added to the standards at much higher concentrations than their normal physiological concentrations in the blood. Cortisol was measured in both the control and test samples and the cross reactivity (%) was calculated. Cross reactivity % = (mean of test samples – mean of control samples/ mean of control samples x 100). The cross reactivity in the cortisol 70 nmol/L concentration ranged between –0.9 and 3.1%, in the 270 nmol/L concentration ranged between –3.04 and 2.2% and in the 650 nmol/L concentration ranged between –3.5 and 1.8% (see **Table 1**).

2.2.2 Interference

Standards were made up at cortisol concentrations of 70, 270 and 650 nmol/L. One set of standards were controls and another set were test standards where the

Cortisol concentration	70 nmol/L	270 nmol/L	650 nmol/L
Cross reactant	Cross-reactivity (%)	Cross-reactivity (%)	Cross-reactivity (%)
Cortisone	−0.4	2.2	−0.4
Corticosterone	0.8	−2.4	−2
Progesterone	3.1	−0.7	0.8
Prednisone	2.1	−3.4	0.1
Testosterone	−1.1	−0.5	−1.1
Prednisolone	1.2	−1.3	−3.5
Deoxycortisol	0.2	−0.1	0.8
DHEA	1.2	0.1	1.4
Dexamethasone	−0.9	0.3	1.8

Cross-reactivity with Cortisone, Corticosterone, Progesterone, Prednisone, Testosterone, Prednisolone, Deoxycortisol, DHEA, Dexamethasone is acceptably low (+/− 5%).

Table 1.

Showing cross reactivity % of cortisone, corticosterone, progesterone, prednisone, testosterone, prednisolone, Deoxycortisol, DHEA, dexamethasone with ichroma™ cortisol assay method.

following molecules (D-glucose, Ascorbic acid, Bilirubin (unconjugated), Haemoglobin, Cholesterol, Triglyceride and Biotin)) were added to the standards at much higher concentrations than their normal physiological concentrations in the blood. Cortisol was measured in both the control and test samples and the interference (%) was calculated. Interference % = (mean of test samples – mean of control samples/ mean of control samples x 100). The acceptable interference was +/− 5%.

The data shows that the interference in the cortisol 70 nmol/L concentration ranged between −1.8 and 0.8%, in the 270 nmol/L concentration ranged between −2.3 and 4.3% and in the 650 nmol/L concentration ranged between −1.3 and 0.2%. All meeting the acceptance criteria of +/−5% (see **Table 2**).

2.3 Precision

The precision (coefficient of variation %) was estimated for the following:

- Repeatability (within-run precision)
- Within-laboratory precision (Total precision)
- Lot to lot precision
- Between persons precision
- Between sites precision
- Between reader precision

Cortisol concentration	70 nmol/L	270 nmol/L	650 nmol/L
Interferent	Interference (%)	Interference (%)	Interference (%)
D-glucose	-1.8	4.3	-0.1
L-Ascorbic acid	0.7	-1	-0.1
Bilirubin	-0.4	-1.2	-0.6
Haemoglobin	0.8	0.1	-1.3
Cholesterol	-0.2	2.8	0.2
Triglyceride	-0.2	-2.3	1.2

Interference from D-glucose, L-Ascorbic acid, Bilirubin, Haemoglobin, Cholesterol and Triglyceride was minimal (+/-5%).

Table 2.
Showing interference % of D-glucose, ascorbic acid, bilirubin (unconjugated), haemoglobin, cholesterol, triglyceride and biotin with ichroma™ cortisol assay method.

The data shows that the coefficients of variation (CV) for repeatability, total precision, lot to lot, between person, between site and between reader is 6.1, 6, 5.8, 6, 5.8 and 6.1%, respectively for cortisol concentration 70 nmol/L.

The data shows that the coefficients of variation (CV) for repeatability, total precision, lot to lot, between person, between site and between reader is 5.9, 5.7, 5.9, 5.8, 6 and 4.6%, respectively for cortisol concentration 270 nmol/L.

The data shows that the coefficients of variation (CV) for repeatability, total precision, lot to lot, between person, between site and between reader is 5.4, 5.7, 5.7, 6.1, 7.1 and 6%, respectively for cortisol concentration 560 nmol/L.

All CVs met the acceptance criteria of CV +/- 15% (**Table 3**).

3. Accuracy

Six standards (samples 1–6) were made up, with the expected value of 80, 220, 360, 500, 640 and 800 nmol/L of cortisol. This was measured 3 times using ichroma™ Cortisol assay and the average determined, the recovery (%) was calculated as the average divided by the expected concentration multiplied by 100.

An acceptance criterion of recovery +/- 20% was set.

The data shows that for the expected cortisol value of 80, 220, 360, 500, 640 and 800 nmol/L, there was 99.9, 100.3, 97.6, 99.2, 98.9 and 99.8% recovered, respectively. The recovery met the acceptance criteria of +/-20% (see **Table 4**).

4. Correlation

Cortisol concentrations of 100 clinical samples were independently tested with the ichroma™ Cortisol reagents and ichroma™ M3 versus the comparator method (bioMerieux Mini VIDAS using VIDAS Cortisol reagent). Comparability was investigated with correlation coefficient analysis and Bland-Altman plots.

A				
Concentration (nmol/L)	Repeatability		Total Precision	
	Average	CV (%)	Average	CV (%)
70	70.18	6.1	70.1	6
270	265.66	5.9	268.41	5.7
560	648.22	5.4	641.68	5.7
B				
Concentration (nmol/L)	Lot to lot precision		Between –person	
	Average	CV (%)	Average	CV (%)
70	69.98	5.8	69.54	6
270	269.67	5.9	270.12	5.8
560	649.34	5.7	650.87	6.1
C				
Concentration (nmol/L)	Between-site		Between-reader	
	Average	CV (%)	Average	CV (%)
70	69.57	5.8	69.86	6.1
270	271.04	6	272.39	4.6
560	641.2	7.1	645.22	6

Table 3.
Showing precision at concentration.

Expected value (nmol/L)	Lot 1	Lot 2	Lot 3	Average	Recovery (%)
80	79.33	81.29	79.18	79.93	99.9
220	220.14	223.66	217.96	220.59	100.3
360	345.1	354.35	355.02	351.49	97.6
500	503.43	488.16	496.42	496	99.2
640	628.84	626.54	644.09	633.16	98.9
800	815.38	816.27	763.145	798.27	99.8

Table 4.
Showing recovery % of standards to determine accuracy.

4.1 bioMerieux Mini VIDAS (reference) and ichroma™ M3

The samples covered a measuring range of 51.4–780.08 nmol/L. The correlation analysis for the bioMerieux Mini VIDAS (reference) and ichroma™ M3 with samples ($n = 100$), resulted in a slope of 0.9489 [95% confidence interval (CI) 0.9210–0.9636] and an intercept of 2.527 nmol/L. The correlation coefficient was 0.9462 (**Figure 2a**).

The Bland-Altman difference plot of the bioMerieux Mini VIDAS (reference) and ichroma™ M3 with samples ($n = 100$) showed a mean bias of 21.98 nmol/L (SD –112.5 to 156.5) (**Figure 2b**).

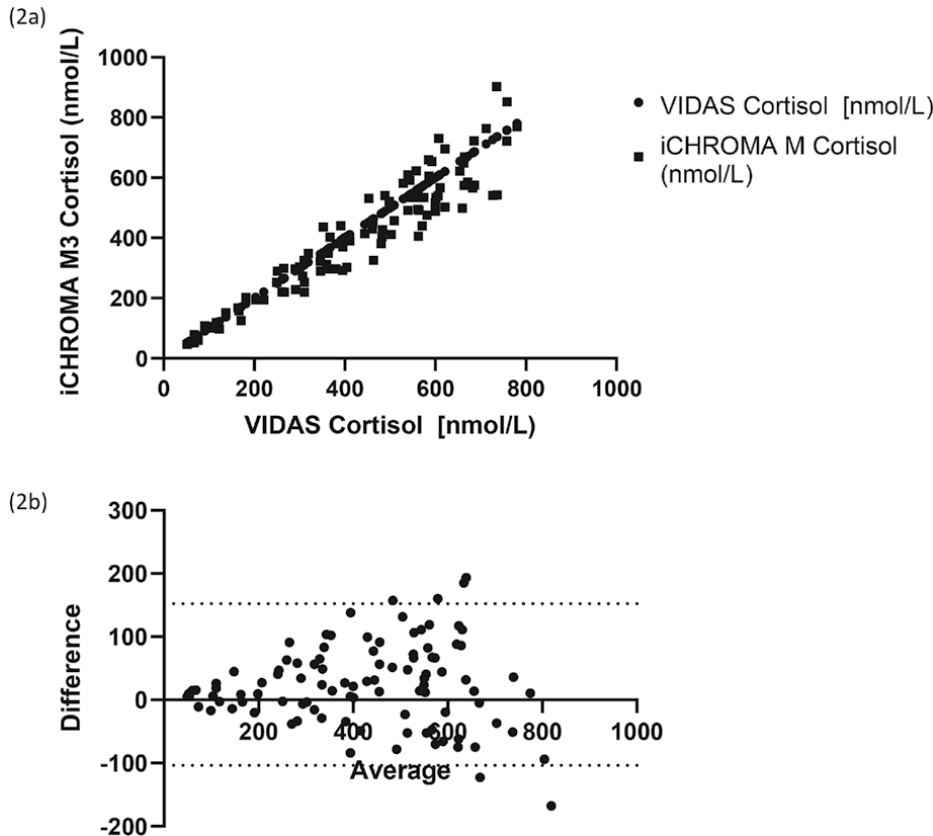


Figure 2.
Comparison results (a) and Bland-Altman plots (b) of the bioMerieux Mini VIDAS (reference) and ichroma™ M3.

According to the test results, the correlation coefficient (R) between the reference analyser (bioMerieux Mini VIDAS) and the analyser for ichroma™ M3) met the acceptance criteria (Slope: 1 ± 0.1 and Correlation coefficient (R): ≥ 0.9).

5. Specimen comparability

Fifty-one samples were collected for serum measured by the reference analyser (bioMerieux Mini VIDAS). These results were compared to the same fifty-one samples collected in the following tubes that were measured on the ichroma™: whole blood K²-EDTA, whole blood K³-EDTA and whole blood Li-Heparin. The acceptance criteria (slope 1 ± 0.1 and correlation coefficient $R \geq 0.9$) was determined.

The data shows that the slope for the cortisol estimations from the ichroma™ using whole blood K²-EDTA, whole blood K³-EDTA and whole blood Li-Heparin samples versus cortisol estimates from the serum samples using the reference analyser were between 0.9867 and 0.9904, see **Table 5**.

	Slope	Correlation (R)
Serum vs. Whole blood (K2-EDTA)	0.9886	0.9987
Serum vs. Whole blood (K3-EDTA)	0.9867	0.9989
Serum vs. Whole blood (Li-heparin)	0.9904	0.9988

Table 5.
Showing slope and correlation between serum cortisol measured using the reagents and the bioMerieux Mini VIDAS versus the respective whole blood samples measured using the ichroma™ cortisol assay and reader.

All slopes and correlations met the acceptance criteria (slope 1 +/-1 0.1 and correlation coefficient R >=0.9).

6. Reference range

See Table 6.

6.1 Clinical applications of ichroma™ cortisol assay and M3 handheld device

Aim: The purpose of this study was to determine the blood cortisol concentrations over a period of 24 h from finger prick sample using a handheld device.

7. Materials and methods

7.1 Reagents

See Figure 3.

Time	Reference Range (nmol/L)
Morning	151.6–793.3
Afternoon	67.9–473.1

Table 6.
Showing reference ranges of assay method.

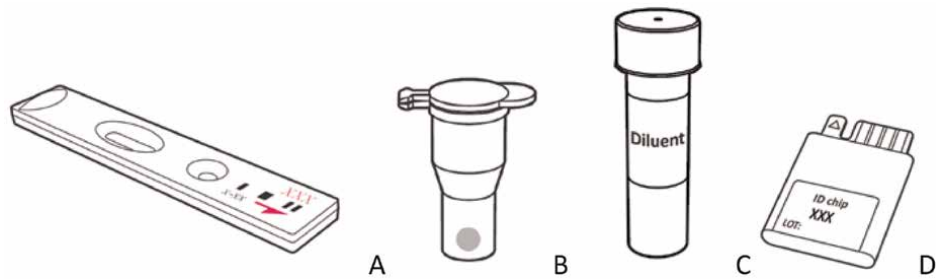


Figure 3.
A – The cartridge contains the membrane called a test strip which has cortisol BSA conjugate an anti- mouse IgG to test lines, and streptavidin at the control line. Dimension = 89.90 (W) × 15.75 (L) × 4.40 (H) mm B – The detection tube has a granule containing anti cortisol fluorescent conjugator, BSA biotene fluorescent conjugate, bovine serum albumin (BSA) as a stabiliser and sodium azide as a preservative in phosphate buffered saline (PBS). Dimension = 11.8 (W) × 23.8 (H) mm. C – The detector diluent contains bovine serum albumin (BSA) as a stabiliser, tween 20 as detergent, sodium azide as a preservative in phosphate buffered saline (PBS) and is in a vial. Dimension = 20 (W) × 59 (H) mm. D × ID chip. Dimension = 24 (W) × 34 (L) × 5 (H) mm.



Figure 4.
Showing hand-held Boditech ichroma M3 device.

7.2 Device

See **Figure 4.**

7.3 Test procedure

Established standard method for ichroma™ Cortisol as follows.

1. Take 150 μL of detector diluent using a pipette and dispense it to the detector tube containing a granule. When the granule form is completely dissolved in the tube, it becomes detection buffer.
2. (The detection buffer must be used immediately. Do not exceed 30 s.)
3. Take sample (50 μL of whole blood or 30 μL of serum/plasma/control) using a pipette and dispense it to a tube containing the detection buffer. Close the lid of the detector tube and mix the sample thoroughly by shaking it about 10 times.
4. (The sample mixture must be used immediately. Do not exceed 30 s.)
5. Take 75 μL of the sample mixture and dispense it into the sample well of the cartridge.
6. Insert the sample-loaded cartridge into the slot of the i-Chamber or an incubator (25°C).
7. Leave the sample-loaded cartridge in the i-Chamber or an incubator for 10 min.
8. Scan the sample-loaded cartridge immediately when the incubation time is over.
9. To scan the sample-loaded cartridge, insert it into the cartridge holder of the instrument for ichroma™ tests. Ensure proper orientation of the cartridge before pushing it all the way inside the cartridge holder. An arrow is marked on the cartridge especially for this purpose.

- 10. Press the ‘Select’ or tap the ‘Start’ button on the instrument for ichroma™ tests to start the scanning process.
- 11. The instrument for ichroma™ tests will start scanning the sample-loaded cartridge immediately.
- 12. Read the test result on the display screen of the instrument for ichroma™ tests.

8. Method

Finger prick samples were taken from a healthy volunteer hourly from 05:00 h to 03:00 h over a 1-month period. They were collected in lithium heparin tubes. The cortisol measurements were made using the ichroma™ Cortisol POC method on the handheld device (ichroma™ M3) were performed immediately as described in the test procedure.

9. Results

The 24-h cortisol profile revealed a circadian pattern starting with higher levels of 193.02–462 nmol/L in the morning (6-8 am), dropping to 93.3–157.01 nmol/L by noon, keeping it steady in the afternoon 123.33–150.81 nmol/L dropping in the evening till midnight at levels of 50–137.85 nmol/L **Figures 5 and 6** and **Table 7**.

10. Discussion

Cortisol as a glucocorticoid affects the metabolism of carbohydrates, proteins, and fats, but especially glucose. Cortisol tests are carried out on patients who have conditions affecting adrenal glands. Cortisol levels follow a circadian rhythm rising in the

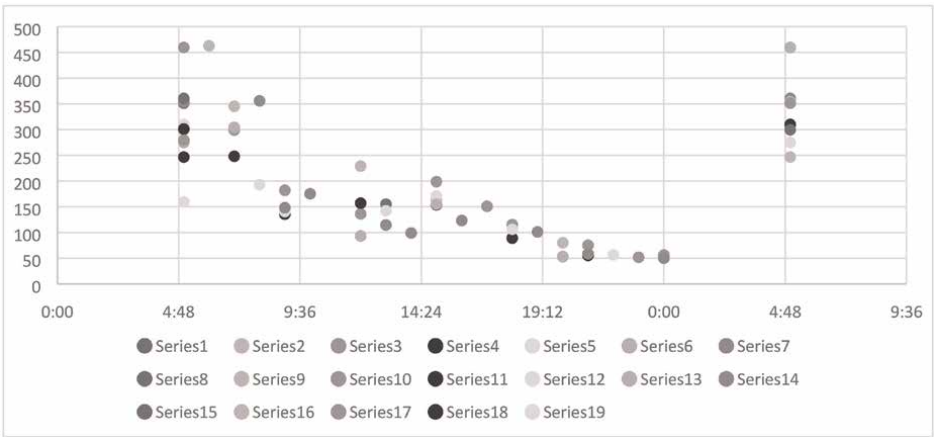


Figure 5.
Showing the cortisol estimations over the course of the month at the respective time.

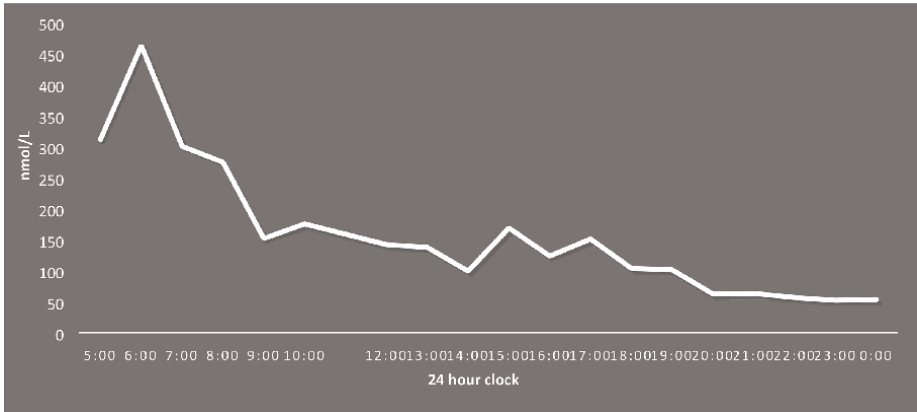


Figure 6.
Showing the mean cortisol estimations over the course of the month at the respective time.

Time of the day	Morning 6–8 am	Noon 12–1 pm	Afternoon 4 – 5 pm	Nighttime 10–12 midnight
Cortisol (nmol/L)	193.02–462	93.3–157.01	123.33–150.81	50–56.45

Table 7.
Showing cortisol estimates over the course of the month grouped into morning (6:00–8:00 h), noon (12:00–13:00 h), afternoon (16:00–17:00 h) and Nighttime (20:00–00:00 h).

early hours of the day and falling later on during the day. It peaks at its highest level between 6 and 8 AM and gradually falls, reaching its lowest point around midnight. Cortisol levels are usually collected at 8 AM and again at 4 PM. It should be noted that normal values may be adjusted in individuals who have worked during the night and slept during the day for long periods of time [1–3].

Cortisol immunoassays have been able and shown to demonstrate good precision and correlation with Liquid Chromatography Mass Spectrometry (LC-MS/MS) [6]. These assays have high performance, are easily performed, and are cost effective. However, they are performed on desk top analysers and use serum samples that require centrifugation, thereby making it a bit of a challenge for these assays to be used to measure cortisol at point of care. In this chapter, we describe a quantitative fluorescence immunoassay (FIA) for the quantitative determination of cortisol in human whole blood/serum/plasma using a handheld device (ichroma™ M3). It gives a signal which is directly proportional to the cortisol concentration in plasma samples with a performance time between 10 and 15 min. This technique provides a practical measurement range of concentration range of 0–900 nmol/L. It has a working range of 50–800 nmol/L.

A limitation of immunoassays is their specificity with interference of structurally similar compounds, for example endogenous steroids. In addition, different immunoassays show high inter-assay variation [6–9]. This assay has shown very good precision <7.1% (repeatability, within-laboratory, lot to lot, between person, between sites and between devices). In addition, there is very little cross-reactivity (+/– 5%) with Cortisone, Corticosterone, Progesterone, Prednisone, Testosterone, Prednisolone, Deoxycortisol, DHEA, Dexamethasone. With minimal interference (+/– 5%) from D-glucose, L-Ascorbic acid, Bilirubin, Haemoglobin, Cholesterol and Triglyceride. There

is very good agreement between the cortisol estimates of the bioMerieux Mini VIDAS (reference) and ichroma™ M3. In addition, cortisol estimations could also be performed on whole blood K²-EDTA, whole blood K³-EDTA and whole blood Li-Heparin samples. This makes this immunoassay method quite suitable for point of care or use testing.

The 24-h blood profiling conducted on the healthy volunteer using this point of care our use device and method on finger prick samples revealed a circadian pattern starting with higher levels of 193.02–462 nmol/L in the morning (6–8 am), dropping to 93.3–157.01 nmol/L by noon, keeping it steady in the afternoon 123.33–150.81 nmol/L dropping in the evening till midnight at levels of 50–137.85 nmol/L. This pattern is consistent with the profiles described in a number of studies [10–12] including the normative profile described by Dmitrieva et al. study, although in this study the data is from salivary samples which is considered an ultrafiltrate of blood which accounts for the cortisol concentration levels are lower than what is expected in the blood. The normative profile was the most observed profile in a study of 1101 adults living in the US. Salivary cortisol at waking was 13.4 nmol/L, increasing to 20.4 nmol/L at 30 min post waking, then declining to 6.0 nmol/L before lunch and dropping to 1.5 nmol/L prior to bedtime see **Figure 7**.

For some time, the optimum monitoring of cortisol has been advocated to support the replacement of cortisol in patients with adrenal insufficiency [13], to replace cortisol appropriately. We appreciate that replacement with steroid replacement in patients does not mimic the circadian rhythm of cortisol. This can be seen in the figure below which shows much higher concentrations of cortisol observed in the afternoon and mid-afternoon samples of the patient on steroids compared to the afternoon and mid-afternoon samples of a healthy volunteer (**Figure 8**).

With this method, a better understanding of blood cortisol in the patients receiving glucocorticoid therapy, patients with abnormalities of the adrenal gland and patients with abnormalities of the pituitary gland affecting ACTH production would prove valuable. In addition, there would be value in monitoring and understanding the kinetics of blood cortisol concentrations in athletes in sports medicine and understanding stress in many situations.

In this chapter, we have shown the performance characteristics (analytical sensitivity, analytical specificity, interference, precision, accuracy, and correlation) of a

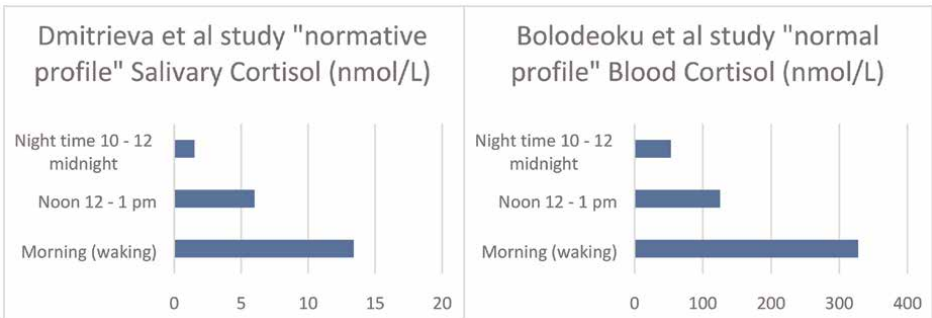


Figure 7. Showing “normative profile” described in Dmitrieva et al. with salivary cortisol concentrations and normal profile described by Bolodeoku et al. with blood cortisol concentrations.

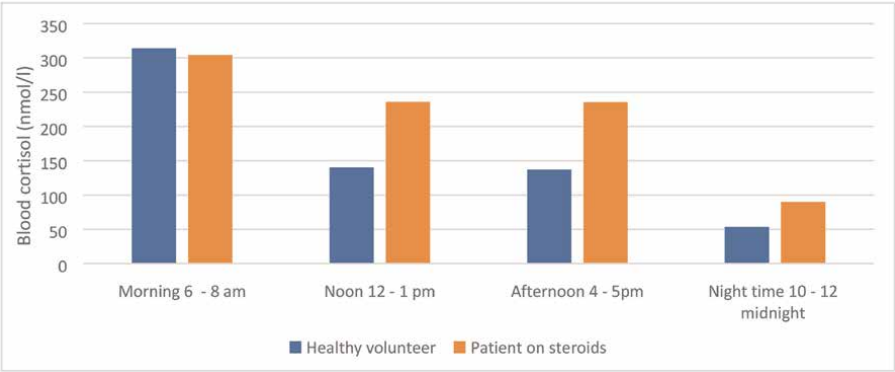


Figure 8.
Showing morning, afternoon, mid-afternoon and night-time blood cortisol concentrations in a healthy volunteer and patient taking steroids (data on file).

hand-held blood cortisol measuring device and assay method met the acceptance criteria. In addition, the cortisol method was able to determine blood cortisol profiles obtained using finger prick samples.

Author details


John Bolodeoku^{1*} and Tae Kyum Kim²

1 JB Consulting MDP Limited, Regus, Berkshire, United Kingdom

2 Boditech Med Inc, Chuncheon-si, Gangwon-do, Korea

*Address all correspondence to: john.bolodeoku@jbconsultingmdp.com

IntechOpen

© 2023 The Author(s). Licensee IntechOpen. This chapter is distributed under the terms of the Creative Commons Attribution License (<http://creativecommons.org/licenses/by/3.0>), which permits unrestricted use, distribution, and reproduction in any medium, provided the original work is properly cited. 

References

- [1] Kaushik A, Vasudev A, Arya SK, Pasha SK, Bhansali S. Recent advances in cortisol sensing technologies for point-of-care application. *Biosensors & Bioelectronics*. 2014;**53**:499-512. DOI: 10.1016/j.bios.2013.09.060
- [2] Choi MH. Clinical and technical aspects in free cortisol measurement. *Endocrinology Metabolism (Seoul)*. 2022;**37**(4):599-607. DOI: 10.3803/EnM.2022.1549
- [3] El-Farhan N, Rees DA, Evans C. Measuring cortisol in serum, urine and saliva – Are our assays good enough? *Annals of Clinical Biochemistry*. 2017; **54**(3):308-322. DOI: 10.1177/0004563216687335
- [4] Turpeinen U, Hämäläinen E. Determination of cortisol in serum, saliva and urine. *Best Practice & Research. Clinical Endocrinology & Metabolism*. 2013;**27**(6):795-801. DOI: 10.1016/j.beem.2013.10.008
- [5] Inder WJ, Dimeski G, Russell A. Measurement of salivary cortisol in 2012 – Laboratory techniques and clinical indications. *Clinical Endocrinology*. 2012;**77**(5):645-651. DOI: 10.1111/j.1365-2265.2012.04508.x
- [6] Klee GG. Interferences in hormone immunoassays. *Clinics in Laboratory Medicine*. 2004;**24**:1-18
- [7] Briegel J, Sprung CL, Annane D, Singer M, Keh D, Moreno R, et al. Multicenter comparison of cortisol as measured by different methods in samples of patients with septic shock. *Intensive Care Medicine*. 2009;**35**: 2151-2156
- [8] El-Farhan N, Pickett A, Ducroq D, Bailey C, Mitchem K, Morgan N, et al. Method-specific serum cortisol responses to the adrenocorticotrophin test: Comparison of gas chromatography-mass spectrometry and five automated immunoassays. *Clinical Endocrinology*. 2013;**78**: 673-680
- [9] Krasowski MD, Drees D, Morris CS, Maakestad J, Blau JL, Ekins S. Cross-reactivity of steroid hormone immunoassays: Clinical significance and two-dimensional molecular similarity prediction. *BMC Clinical Pathology*. 2014;**14**:33
- [10] Dmitrieva NO, Almeida DM, Dmitrieva J, Loken E, Pieper CF. A day-centered approach to modeling cortisol: Diurnal cortisol profiles and their associations among U.S. adults. *Psychoneuroendocrinology*. 2013; **38**(10):2354-2365. DOI: 10.1016/j.psyneuen.2013.05.003
- [11] Bhake RC et al. Continuous free cortisol profiles—Circadian rhythms in healthy men. *The Journal of Clinical Endocrinology & Metabolism*. 2019; **104**(12):5935-5947. DOI: 10.1210/jc.2019-00449
- [12] Adam EK, Hawkey LC, Kudielka BM, Cacioppo JT. Day-to-day dynamics of experience–cortisol associations in a population-based sample of older adults. *Proceedings of the National Academy Science USA*. 2006;**103**(45):17058-17063. DOI: 10.1073/pnas.0605053103
- [13] Hindmarsh PC, Honour JW. Would cortisol measurements be a better gauge of hydrocortisone replacement therapy? Congenital adrenal hyperplasia as an exemplar. *International Journal of Endocrinology*. 2020;**2020**:2470956. DOI: 10.1155/2020/2470956

Distribution of Cortisol in Human Plasma *in vitro*: Equilibrium Solutions for Free Cortisol Using Equations of Mass Conservation and Mass Action

Richard I. Dorin and Clifford R. Qualls

Abstract

Cortisol is secreted by the human adrenal cortex and circulates in plasma as free or protein-bound cortisol. Corticosteroid binding globulin (CBG) and albumin are the principal binding proteins (BPs) for cortisol in human plasma. Plasma concentrations of total cortisol (sum of protein-bound and free cortisol) are typically measured *in vitro*. Determination of free cortisol adds clinical and diagnostic value to total cortisol concentration. However, direct measurement of free cortisol concentrations involves laborious separation methods, limiting clinical utility. The development and application of physiologic protein-ligand binding models and equations provide an alternative approach to assessment of free cortisol concentrations *in vitro*. In this chapter, we introduce a matrix notation to represent relevant mass action and mass conservation equations. The matrix notation is also used to summarize and compare several contemporary models of interest, including cubic, quadratic, and quartic polynomial equations. Second, we introduce Feldman's equations for competitive ligand-protein binding interactions, which are represented by matrices for multiple ligands and multiple BPs, including illustrative 2×2 matrix; we also discuss iterative solution strategies for coupled polynomial equations. Third, we develop a theorem for albumin-cortisol binding and review related assumptions that have been used to simplify polynomial equations and their equilibrium solutions.

Keywords: cortisol, hydrocortisone, corticosteroid binding globulin, protein-ligand binding, albumin, computer-assisted numerical methods, matrix notation

1. Introduction

"A model should be as simple as it can be but no simpler." Albert Einstein
"All models are wrong; some are useful." George Box

1.1 Modeling the distribution of cortisol between free and protein-bound compartments in human plasma at equilibrium in the test tube (*in vitro*)

Several mathematical models have been put forward for the purpose of estimating equilibrium concentrations of free cortisol (X_F) in the test tube (*in vitro*). The minimum input data needed to estimate X_F include serum/plasma concentrations of total cortisol (X_{TotF}) and total corticosteroid binding globulin (X_{TotCBG}). Since X_{TotF} is known (measured experimentally), it is reasonable to consider that the problem is determining X_F as the fraction (or percentage) of the total cortisol, that is, (X_F/X_{TotF}) . Though the clinician is primarily interested in free cortisol concentration (X_F), these polynomial models also yield estimates of CBG-bound (X_{FC}) and albumin-bound (X_{FA}) cortisol concentrations, which are generally of secondary interest.

1.2 Cortisol in captivity

Sampling of blood from the vascular volume by venipuncture is conventional and useful. Here we use *in captivity* in reference to the contained environment of the *in vitro* condition (and not in reference to BP-bound ligand as in Bikle et al. [1]). Once plasma/serum is removed from the well-mixed vascular compartment and placed in the test tube, there is no longer input or output of cortisol from the system; that is, *in vitro* rates of cortisol appearance, elimination, and diffusion are all zero. Moreover, X_{TotF} remains constant in the test tube; that is, $dX_{TotF}/dt = 0$ *in vitro*. By contrast, apart from the steady state, $dX_{TotF}/dt \neq 0$ *in vivo*. We also note that the distribution of cortisol between free and protein-bound compartments quickly reaches equilibrium (or steady state) *in vitro*. A modeling perspective on the relationship between the dynamic and equilibrium conditions for cortisol *in vitro* is given in Appendix 1.

Thus, the *in vitro* assessment of cortisol captures a momentary *snapshot* or *still life* view of the dynamic, *in vivo* system. Despite these differences between the *in vitro* and *in vivo* conditions, analysis of cortisol distribution between free, CBG-bound, and albumin compartments *in vitro* yields information that can be usefully projected back to the dynamic model. This transition of parameters of interest from the *in vitro* equilibrium condition to the *in vivo* dynamic condition involves dividing association equilibrium constants into cognate on- and off-rate constants. Thus, the *in vivo* model uses on- and off-rate constants rather equilibrium association constants and differential equations (see [2]) rather than the iterative equilibrium equations discussed herein.

1.3 Motivations for estimating free cortisol concentrations by numerical modeling

Plasma or serum free cortisol concentrations (X_F) are generally difficult to measure, as they require pre-analytic separation procedures, such as equilibrium dialysis or ultrafiltration, at controlled temperature (37°C). These constraints have motivated interest in using numerical methods as an alternative approach to estimate X_F . Clinical laboratories routinely measure concentrations of total cortisol (X_{TotF}) and total albumin (X_{TotA}). Laboratory measurement of total CBG concentration (X_{TotCBG}) is less routine, but immunoassays are commercially available. In a typical scenario using contemporary methods, estimates of X_F can be obtained using a formula in which

(i) X_{TotF} and X_{TotCBG} are measured, (ii) association rate constants are taken from the literature, and (iii) a value for albumin concentration is assumed (or measured) [3, 4].

In the present chapter we review equations for several contemporary models for estimation of X_F , including the cubic equation (Section 2) as well as quadratic and quartic polynomial equations (Section 3). These models all use principles of mass action and mass conservation. However, to the extent that they focus on cortisol to the exclusion of all other ligands that may compete for CBG and/or albumin binding, they may be regarded as *too simple*. In Section 4, we review the work of Feldman and co-workers [5, 6], which outline a system of integrated equations of mass action and conservation. These integrated equations can be applied to a variety of protein-ligand binding problems, including the binding of cortisol and other ligands to serum binding proteins (BPs), such as CBG and albumin. We shall refer to these as Feldman equations. We also introduce an alternative representation of Feldman equations using nxm matrix (K) notation. The matrix notation is introduced for the 3-compartment model (1×2 , cubic solution) in Section 2.

1.4 Free, CBG-bound, and albumin-bound cortisol as a 3-compartment model

A minimal model for equilibrium solutions considers a single ligand (cortisol) and its two principal BPs in human plasma, namely CBG and albumin [2, 4, 7]. Whereas CBG-cortisol binding is specific, high-affinity, and saturable, albumin-cortisol binding is non-specific, low affinity, and non-saturable at physiologic concentrations of plasma cortisol [8]. The three compartments for cortisol in the vascular (plasma) volume (*in vitro*) include: (i) free (X_F), (ii) CBG-bound (X_{FC}), and (iii) albumin-bound (X_{FA}) cortisol (see Section 2). In this formulation, total cortisol represents the sum of three plasma compartments ($X_{\text{TotF}} = X_F + X_{\text{FC}} + X_{\text{FA}}$), illustrating the principle of mass conservation. An analytic solution (i.e., solution obtained using algebraic formula) for X_F may be obtained by a cubic equation, as previously described [4]. At a minimum, realistic modeling of cortisol distribution between free, CBG-bound, and albumin-bound compartments *in vitro* must take account of the different concentrations and binding characteristics of CBG and albumin. Thus, one- or two-compartment models may be *too simple* to realistically represent relevant physiology of cortisol in plasma and are not considered further in this chapter.

1.5 CBG-cortisol binding affinities are affected by temperature

CBG-cortisol binding affinity is sensitive to variation in temperature [9–13]. For purposes of this chapter, we focus on protein-ligand binding reactions at 37°C. In cortisol-binding studies performed using human serum at 37°C, values for the equilibrium dissociation constant for CBG-cortisol binding have been reported in the literature to be in the range of 12.5–33 nmol/L [3, 14–17]. As temperature is increased from 37 to 40°C, CBG-cortisol affinity decreases substantially (by $\approx 50\%$) [9–13]. Thus, in febrile patients, free cortisol concentrations *in vivo* are expected to be greater than those (i) predicted by equations developed using affinity constants obtained for conditions at 37°C or (ii) measured experimentally at 37°C (e.g., by equilibrium dialysis).

1.6 Competitive protein-ligand binding models for multiple BP's and multiple ligands

The problem of obtaining an accurate estimate of X_F becomes more challenging when one considers the possibility of other cortisol-binding proteins in human

plasma, such as orosomucoid (α – 1-acidic glycoprotein, AAG) or elastase-cleaved CBG [18–20]. And the problem is compounded further considering the possibilities of ligands other than cortisol that circulate at sufficiently high concentration and bind CBG with sufficiently high affinity that, through their collective activities, they effectively compete with cortisol for CBG (and/or albumin) binding [14, 21, 22]. If ligands that effectively compete for CBG binding are not accounted for, model predicted X_F may significantly underestimate actual (experimentally measured) X_F . In Section 4 we review a generalized approach for modeling competition for CBG-cortisol (and albumin-cortisol) binding. These are represented by the 2×2 matrix, with several examples of ligands competing for CBG-cortisol binding reaction given in Section 5. Interestingly, once the Feldman equations are applied to two (or more) ligands, they are no longer tractable to analytic solutions. We discuss this problem of *coupled polynomial equations* and solution by iteration in Section 4. In Section 4, we also present Duality theorem that provides for transposition of matrix expression between $n \times m$ and $m \times n$ formats. We also provide theorems for existence and uniqueness of iterative solutions for the characteristic polynomial, which is developed more generally to existence and uniqueness of *iterative* solutions in Appendix 2. In Appendix 3, we further review matrix approaches to the characteristic polynomial, which includes use of singular value decomposition and vector-based matrix operations.

1.7 Re-parameterization of albumin-bound cortisol concentration (X_{FA}) results in simplifications to model equations and model solutions

Cortisol-albumin binding is characterized by low specificity and low affinity; moreover, since concentrations of albumin ($\mu\text{mol/L}$) greatly exceed those of cortisol (nmol/L), simplifications in modeling albumin-bound cortisol may be possible. Indeed, Tait and Burstein as well as Coolens and co-workers suggest that the concentration of albumin-bound cortisol (X_{FA}) is linearly related to X_F by a simple constant of proportionality (N) [3, 7]. By combining two parameters as a single parameter to estimate the concentration of X_{FA} , Coolens' simplification reduces the order of the polynomial by one, such that analytic solutions using the cubic equation can now be obtained by a simpler (quadratic) equation (see Section 2). It may be noted that Coolens' assumption only considers a single ligand (cortisol) binding to albumin. Since $X_{\text{TotA}} \gg X_{\text{TotF}}$, the assumption that $X_{\text{TotA}} \approx$ 'free albumin' (X_A) seems reasonable enough. However, when one considers the myriad other ligands that bind albumin in non-specific fashion, the assumption that $X_{\text{TotA}} \approx X_A$ is less certain. A general theorem for albumin-cortisol binding, by which multiple ligands may compete for albumin-cortisol binding, is developed in Section 6. These considerations also raise the practical question of whether N is in fact constant (within and between individuals) and exactly what value of N should be used as the constant of proportionality (X_{FA}/X_F).

It also is uncertain whether there is a single or multiple cortisol binding sites per albumin molecule. In Appendix 4, we use the matrix format to represent equations for multiple albumin-cortisol binding sites having different but independent cortisol binding affinities.

1.8 The clinical conundrum

One might imagine that having measured concentrations of X_{TotF} , X_{TotCBG} , and X_{TotA} in hand, estimation of X_F (as a percent of X_{TotF}) should be a simple enough task. After all, cortisol binds CBG with simple 1:1 stoichiometry and the binding properties of CBG

and cortisol are well characterized [10, 15, 16, 23–26]. Similarly, purified albumin is readily available and cortisol binding properties have been reported [4, 17, 27–30]. For example, in Section 6 we review albumin-cortisol binding data obtained in a purified solution of human serum albumin [27].

However, we find in practice that estimation of X_F in human plasma using contemporary models remains an inexact science. These model solutions for X_F often match experimentally measured free cortisol; however, their performance may be inconsistent in certain individuals, populations, and conditions. Changing affinities and variation in concentrations of competing ligands in conditions such as critical illness and septic shock may further challenge clinical application of contemporary numerical methods to estimate X_F .

Before introduction to the $n \times m$ matrix notation for Feldman equations, let us briefly review our use of the terms *equilibrium concentration* and *bioavailable cortisol*.

1.9 Definition of equilibrium concentrations in the test tube (which is a thought experiment)

To be clear about what is meant by the term *equilibrium (or steady state) solutions in vitro*, let us consider as a thought experiment a sample of human plasma having median normative concentrations of CBG and albumin from which cortisol has been removed (e.g., by charcoal adsorption). Thus, in this theoretical plasma sample $CBG \approx 600$ nmol/L, $albumin \approx 600,000$ nmol/L, and $total\ cortisol = 0$ nmol/L. To 0.1 mL of this sample, let us add 1 μ L of (free) cortisol at a concentration of 10,000 nmol/L, which when diluted in the 100 μ L sample volume yields a final total cortisol concentration of ≈ 100 nmol/L after mixing. Immediately following addition of (free) cortisol to the sample, there is a (brief) dynamic phase during which concentrations of X_F , X_{FC} , and X_{FA} are rapidly changing. A new steady state is quickly achieved in the test tube, after which period concentrations of X_F , X_{FC} , and X_{FA} (in the test tube) remain constant. Modeling studies suggest that steady state occurs rapidly in this example [4]. When we speak of equilibrium solutions, we are referring to cortisol concentrations at these equilibrium (or steady state) conditions. See Appendix 1 for further discussion of dynamic and steady state conditions *in vitro*.

1.10 Parsing the problem: bioavailable cortisol ($X_F + X_{FA}$)

In studies of *in vitro* testosterone distribution among free (X_T), SHBG-bound (X_{TS}), and albumin-bound (X_{TA}) testosterone compartments, X_{TS} can be separated from X_T and X_{TA} by ammonium sulfate precipitation. The term *bioavailable testosterone* has been commonly used to denote the non-SHBG-bound fraction of testosterone (i.e., free and albumin-bound testosterone), where $X_{TotT} = X_T + X_{TS} + X_{TA}$ and $bioavailable\ testosterone\ (T_{bioavail}) = (X_{TotT} - X_{TS}) = (X_T + X_{TA})$. In the present chapter, we use the term *bioavailable cortisol* ($F_{bioavail}$) to denote the sum of free and albumin-bound cortisol ($X_F + X_{FA}$). Our use of the term is restricted to these concentrations without any intended endorsement of proposed biological activity of albumin-bound cortisol related to capillary transit times [31–34]. In fact, from a modeling perspective of systemic concentrations of cortisol *in vivo*, X_{FA} does not diffuse between vascular and extravascular compartments;

rather, X_{FA} varies in time-dependent fashion in dynamic equilibrium with X_F and X_{FC} (in the plasma compartment) [2, 8, 35]. Nonetheless, the concept of bioavailable cortisol may be useful to cortisol *in vitro*, as it parses the problem of estimating free cortisol into two tasks. The first task is determination of the concentration of bioavailable cortisol as a fraction of (measured) total cortisol (X_{TotF}), where bioavailable cortisol = $(X_{TotF} - X_{FC}) = (X_F + X_{FA})$. Once bioavailable cortisol concentration has been determined, the second task is selecting the correct constant of proportionality ($N = X_{FA}/X_F$) by which bioavailable cortisol can be apportioned between X_F and X_{FA} fractions.

2. Matrix notation for cubic equation (1×2 matrix)

A simple formulation of the $n \times m$ matrix shown in **Table 1** includes free ligand (row), free concentrations of BPs (columns), and protein-bound cortisol concentrations (inner cells). The principle of mass action is represented by the 1:1 stoichiometric formulae in each inner cell in the matrix, where concentrations of CBG-bound cortisol (FC) and albumin-bound cortisol (FA) are expressed as mass action formulae using equilibrium association constants for CBG-cortisol (K_{11}) and albumin-cortisol (K_{12}) binding reactions at 37°C. For example, the *inner cell* for steady state concentration of FC (dotted ellipse) is the product of (i) molar concentrations of the reactants, free cortisol (F) and free CBG (C), and (ii) the equilibrium association (affinity) constant for CBG-cortisol binding (K_{11}). Note that the equilibrium association constant is expressed in units of concentration⁻¹ (L/nmol, nM⁻¹). Thus, inner cell entries are of the form $K_{11} \cdot C \cdot F$. By the same token, the *inner cell* for steady state

Matrix 1x2	C = Free CBG	A = Free Albumin	
F = Free Cortisol	$K_{11} F \cdot C$	$K_{12} F \cdot A$	Tot F
	Tot C	Tot A	

Measured Otherwise Known To be solved

The three total concentrations are: total cortisol (TotF), total CBG (TotC), and total albumin (TotA) are measured (light red). The affinity constants for CBG-cortisol (K_{11}) and albumin-cortisol (K_{12}) binding are obtained from the literature or otherwise estimated (yellow). The free cortisol concentration (F) is estimated as cubic solution derived from the equilibrium equations of Feldman and co-workers [5] (light blue). The dashed boxes and ellipses are in this table to illustrate the discussion in the text. Briefly, ellipses enclose the mass action formulae for cortisol binding to CBG and albumin. Boxes enclose conservation of mass formulae. The horizontal box (dotted rectangle) indicates that total cortisol (TotF) represents the sum free (F), CBG-bound (FC), and albumin-bound (FA) cortisol. The vertical box (compound dashed rectangle) indicates that total CBG (TotC) represents the sum of free CBG (C) and cortisol-bound CBG (FC). The dashed box indicates that total albumin (TotA) represents the sum of free albumin (A) and cortisol-bound albumin (FA). Feldman equations give a solution of free F as a root of a cubic polynomial [4]. Constraints: None.

Table 1.
Tutorial 1×2 matrix for cortisol binding equilibrium equations resulting in a cubic solution for free cortisol.

(equilibrium) concentration of albumin-bound cortisol (FA) *in vitro* at 37°C (dashed ellipse) is the product of (i) molar concentrations of the reactants, free cortisol (F) and free albumin (A), and (ii) the equilibrium association (affinity) constant for albumin-cortisol binding (K_{12}). Thus, inner cell entries for albumin-cortisol binding are in the form $K_{12} \cdot A \cdot F$. In **Table 1** and elsewhere, we designate the equilibrium affinity constant for CBG-cortisol binding as K_{11} and the equilibrium affinity constant for albumin-cortisol binding as K_{12} .

Although the equilibrium affinity (association) constants for CBG-cortisol (K_{11}) and albumin-cortisol (K_{12}) binding reactions are useful in the matrix notation, in other circumstances it may be preferable to consider the reciprocal, i.e. the equilibrium dissociation constant (K_d). We use the term K_{11}^{-1} , which is also equal to $1/K_{11}$, to indicate the equilibrium dissociation constant for CBG-cortisol binding. Similarly, we use the term K_{12}^{-1} , which is equal to $1/K_{12}$, to indicate the equilibrium dissociation constant for albumin-cortisol binding reaction. Note that equilibrium dissociation constants are expressed in more familiar units of concentration (nmol/L). Values abstracted from Coolens' quadratic equation reflect the high affinity of CBG-cortisol binding ($K_{11}^{-1} = 33$ nmol/L) and relatively low affinity ($K_{12}^{-1} = 330,000$ nmol/L) of albumin-cortisol binding (assuming 1:1 stoichiometry).

The principle of mass conservation is also illustrated in **Table 1**. For example, total concentrations of ligand (row sums, dotted rectangle) and BP (column sums, compound dash and dashed rectangles), are shown in right and bottom margins, respectively. Note that in the usual application of the equations, which is to obtain an analytic solution (i.e., a solution that can be obtained by algebraic formula) for X_F , total concentrations of ligand and BPs are typically measured (red), while equilibrium affinity constants, K_{11} and K_{12} for CBG- and albumin-cortisol binding, respectively, are taken from literature (yellow). In the example shown in **Table 1**, total cortisol, total CBG, and total albumin are measured (red); K_{11} and K_{12} are taken from the literature (yellow); and free cortisol concentration is solved (blue) by the cubic equation. As noted in Coolens et al. and elsewhere [3, 4, 25, 36, 37], the assumption that given value for K_{11} is broadly applicable across individuals, conditions, and clinical groups, may be inaccurate. For example, genome-wide association studies [36, 38] and the presence of recognized polymorphisms of CBG having reduced cortisol binding affinity in certain populations [25, 39] demonstrate that some individuals have normal concentrations of CBG, when measured by immunoassay, but reduced cortisol binding affinity. Individual differences in glycosylation of CBG may also influence its cortisol binding affinity, as do specific mutations associated with the syndrome of CBG deficiency [40–42].

3. Other models that treat cortisol as the sole ligand involved in protein binding in human plasma/serum (quadratic and quartic solutions)

In addition to the cubic equation described in **Table 1**, several variations on the basic cubic model have been suggested in the literature. Note that like the cubic equation, these variations also consider cortisol to be the sole ligand involved in protein-binding reactions. As a result, like the cubic equation, the corresponding solutions for X_F are polynomial equations that yield analytic solutions (quadratic solution for Coolens' equation and quartic solution for the model proposed by Nguyen et al. [3, 20]).

Matrix 1x2	Free C	Free A	
Free F	$K_{11} \cdot F \cdot C$	$N \cdot F$	Tot F
	Tot C		

Measured
 From literature
 To be solved

The solution for free cortisol proposed by Coolens et al. [3] is obtained under a constraint that F is small (see constraint listed below) [3, 7]. Coolens' constant N replaces $K_{12}A$ in the mass action formula to obtain the cell entry $N \cdot F$. Coolens' assumption listed under constraints below for the 1×2 matrix implies $A = \text{Tot}A$. The conservation of mass equation for $\text{Tot}F$ leads to Coolens quadratic solution for the free concentration F . Coolens solution gives $N = 1.74$, but other values are possible [3].

Constraints: Coolens assumption $K_{12}F \ll 1$; that is, $F \ll K_{12}^{-1} = K_D$, the equilibrium dissociation constant of cortisol-albumin binding.

Table 2.

1×2 matrix for cortisol binding equilibrium equations resulting in Coolens' quadratic solution.

Coolens' quadratic equation (**Table 2**) can still be represented as a 1×2 matrix. However, in Coolens' equation, the mass action term for X_{FA} in the cubic equation (dashed oval in **Table 1**) is re-parameterized such that $(K_{12}A \cdot F)$ is simplified to $(N \cdot F)$. In this formulation, $N = X_{FA}/X_F = K_{12} \cdot A \approx K_{12} \cdot X_{\text{Tot}A}$. Coolens' formula takes a value for equilibrium dissociation constant for albumin-cortisol binding from the literature ($= 330,000$ nmol/L) and assumes a normative value for serum albumin concentrations, yielding $N = 1.74$ [3]. The quadratic equation can be represented in matrix format as shown in **Table 2**. In Coolens' formulation, N is viewed as proportional to the concentration of total albumin concentration ($X_{\text{Tot}A}$), and in adaptations of Coolens' equation the value of N has been adjusted proportionately to measured $X_{\text{Tot}A}$ [3, 43]. The assumptions related to Coolens' equation and a general theorem to handle competition of multiple ligands for albumin-cortisol binding are further developed in Section 7 below.

Note that Coolens' simplification provides a simpler (quadratic) solution when compared to the cubic equation (**Table 1**). This is accomplished by combining $X_F + N \cdot X_F = (1 + N)X_F$ and deleting the column for X_A . This results in a 1×1 matrix table and a quadratic solution. For further discussion of the degree of polynomial equations, see Section 3 and Appendix 3.

3.1 Quartic solution

The quartic solution [20] adds a third column to the cubic solution for the additional binding protein, elastase-cleaved CBG (C_e), resulting in 1×3 matrix (see **Table 3**). Gudman-Hoyer and Ottesen further developed the quartic model to consider multiple ligands and dynamical rates of appearance and elimination of elastase-cleaved CBG [19]. However, the clinical relevance of the quartic model is uncertain, especially in view of reports by Hammond and co-workers that the identification of a putative low-affinity (elastase-cleaved) CBG using the 9G12 monoclonal antibody was related to experimental artifact [40]. Moreover, it appears that elastase-cleaved CBG

Matrix 1x3	C = Free CBG	A = Free Albumin	C _e = Free Cleaved CBG	
F = Free Cortisol	K ₁₁ F · C	K ₁₂ F · A	K ₁₃ F · C _e	Tot F
	Tot C	Tot A	Tot C _e	

Measured Otherwise Known To be solved

For this matrix, two forms of CBG having distinct cortisol binding affinities are proposed to exist: (i) full length CBG (C) and (ii) elastase-cleaved CBG (C_e). The four total concentrations are total cortisol (TotF), total CBG (TotC), total elastase-cleaved CBG (TotC_e), and total albumin (TotA) are measured (light red). The affinity constants for free cortisol binding to intact CBG (K₁₁), to elastase-cleaved CBG (K₁₃), and to albumin (K₁₂) are obtained from the literature or otherwise estimated (yellow) [19, 20]. The free cortisol concentration (F) is estimated as the root of a quartic polynomial as described in Nguyen et al. [20] (light blue).
Constraints: None, or in some cases that Tot C_e equals a fixed fraction of TotC.

Table 3.
1 × 3 matrix for equilibrium equations including elastase-cleaved CBG.

is rapidly cleared at local sites of inflammation, such that systemic serum concentrations of elastase-cleaved CBG are unmeasurably low [41].

Quartic solution including addition binding protein (α1-acidic glycoprotein, AAG) (1 × 3 matrix) (**Table 4**): In addition to CBG and albumin, α₁-acid glycoprotein (AAG), also known as *orosomucoid*, circulates in human plasma at a mean concentration of ≈24 μM and binds cortisol with an affinity (K_D = 62,000 nM) intermediate to CBG (K_D = 33 nM) and albumin (K_D = 330,000 nM) [18, 44]. **Table 4** shows a 1 × 3 matrix that includes AAG as an additional binding protein. The concentration of AAG-bound cortisol under physiologic conditions appears to be small [19]. However, depending on the concentration of AAG and other ligands that compete with cortisol for AAG-binding, it may contribute significantly to the pool of protein-bound cortisol. AAG may also represent an additional source of saturable cortisol-binding under

Matrix 1x3	C = Free CBG	A = Free Albumin	O = Free AAG Orosomucoid	
F = Free Cortisol	K ₁₁ F · C	K ₁₂ F · A	K ₁₃ F · O	Tot F
	Tot C	Tot A	Tot O	

Measured Otherwise Known To be solved

An alternative model includes orosomucoid (α – 1-acidic glycoprotein, AAG) as an additional cortisol-binding protein [44]. The four total concentrations are total cortisol (TotF), total CBG (TotC), total orosomucoid (TotO) and total albumin (TotA) are measured (light red). The affinity constants for CBG-cortisol (K₁₁), albumin-cortisol (K₁₂), and orosomucoid-cortisol (K₁₃) binding are obtained from the literature or otherwise estimated (yellow). The free cortisol concentration (F) is estimated as a root of a quartic polynomial (light blue).
Constraints: None.

Table 4.
1 × 3 matrix for equilibrium equations including orosomucoid (AAG).

conditions, such as CBG deficiency or low CBG concentrations [27]. As illustrated in **Table 4**, it is the concentration of free rather than total AAG that determines the concentration of AAG-bound cortisol. Considering the variety of other ligands that bind AAG, concentrations of free AAG (X_{AAG}) may be substantially reduced relative to total AAG (X_{TotAAG}), as discussed further in the general theorem (2×2 matrix) for albumin-cortisol binding (Section 7).

Degrees of characteristic polynomials: In the above examples (single ligand, multiple BPs), note that each additional column adds one additional order of complexity to the polynomial equations; by contrast, treatment of albumin-cortisol binding as a constant (N) reduces the order of the polynomial by one. The degree of characteristic polynomials is discussed further in Appendix 3.

Also note that all the models discussed thus far consider cortisol as the sole ligand; that is, there is only one row (for cortisol only) in the $n \times m$ matrix. Consequently, analytic solutions may be obtained by algebraic equations, such as the familiar quadratic, cubic, quartic solutions discussed above. However, when there are two or more ligands competing for protein binding, a more complex system of *coupled polynomial equations* obtains. These coupled polynomial equations do not yield simple analytic solutions; rather they require iterative procedures to obtain solutions [19, 45, 46]. For these problems, a more general approach taking advantage of mass action and mass conservation equations has been developed.

4. Competitive ligand-protein binding equilibrium equations (for two or more ligands, 2×2 matrix) require iterative rather than analytic solutions




Feldman's system of coupled equilibrium equations obtained from mass action and mass conservation equations is developed here in a matrix format for one or more ligands and one or more binding proteins [5, 6]. This will be done for n ligands and m binding proteins; however, the case $n = 2$ and $m = 2$, the 2×2 matrix, conveys the principles needed.

To simplify the discussion, consider the equilibrium of free cortisol concentration (F) binding to free CBG (C) and free albumin (A) as well as a known competitor (P) that also binds to CBG and albumin. This equilibrium can be represented in matrix format for a 2×2 matrix of affinities $[K_{ij}]$ extended to include the free concentration on the left and top margins and total concentrations on the right and bottom margins (**Table 5**). Note that it is the matrix of affinities (K_{ij}) that is 2×2 . Also note that the bounded concentrations X_{FC} , X_{FA} , X_{PC} , and X_{PA} have been replaced by mass action formula (assuming 1:1 stoichiometric binding). The four total concentrations give rise to four non-linear equations and, assuming total concentrations and all affinities K_{ij} are known, we have four equations for the four free concentrations: F (free cortisol), P (free competitor), C (free CBG), and A (free albumin).

This matrix is both a visual aid and a computation aid. The conservation of mass equations are derived as row sums of the free concentration on extreme left plus the cell entries to obtain the total concentration in the right margin:

$$\begin{aligned} Tot F &= F (1 + K_{11} C + K_{12} A) \\ Tot P &= P (1 + K_{21} C + K_{22} A); \text{ and as} \end{aligned} \tag{1}$$

Matrix 2x2	C = Free CBG	A = Free Albumin	
F = Free Cortisol	$K_{11} F \cdot C$	$K_{12} F \cdot A$	Tot F
P = Free Competitor	$K_{21} P \cdot C$	$K_{22} P \cdot A$	Tot P
	Tot C	Tot A	

 Measured  Otherwise Known  To be solved

This 2×2 matrix illustrates equilibrium with multiple ligands and multiple binding proteins. The four total concentrations (total cortisol (TotF), total competitor ligand (TotP), total CBG (TotC), and total albumin (TotA)) are measured (light red). The affinity constants for CBG-cortisol (K_{11}) and albumin-cortisol (K_{12}) binding are obtained from the literature or otherwise estimated (yellow). Assuming P is a specific ligand, the affinities (K_{21}) and (K_{22}) are also obtained from the literature (yellow). The free cortisol (F) and free competitor (P) concentrations are estimated by iteration of the equilibrium equations described by Feldman et al. [5] (light blue).
To explain: the solutions of free F and P are both a positive root of a cubic equation. However, the two cubic equations are coupled (the coefficients of one equation requires knowing the solution of the other), so F and P need to be solved simultaneously. There is no analytic solution by algebraic methods, but solutions can be obtained by iteration.
Constraints: None.

Table 5.
 2×2 matrix for competitive ligand binding equilibrium equations with two ligands (cortisol and competitor (P)) that both bind CBG (and albumin) (iterative solution).

column sums of the free concentration on extreme top plus the cell entries to obtain the total concentration in the bottom margin:

$$\begin{aligned} \text{Tot } C &= C (1 + K_{11} F + K_{21} P) \\ \text{Tot } A &= A (1 + K_{12} F + K_{22} P) \end{aligned} \tag{2}$$

The mass action equilibrium equations are represented as the cell entries in above matrix; for example, the CBG-bound cortisol concentration X_{FC} is entered as $K_{11} \cdot F \cdot C$ in the 1,1 (upper left-hand corner cell).

Note that these 1:1 stoichiometric mass action formulae allow the F to be factored out of the first row sum for Free F, with similar operations for all of the marginal sums giving a very convenient form for all four conservation of mass formulae above. For example, Feldman's 1972 iterative equations [5], for this case, are now easily derived from the systems of Eqs. (1) and (2) by cross dividing to obtain the system of iterative equations Eqs. (3) and (4):

$$\begin{aligned} F &= \frac{\text{TotF}}{(1 + K_{11} C + K_{12} A)} \\ P &= \frac{\text{TotP}}{(1 + K_{21} C + K_{22} A)} \end{aligned} \tag{3}$$

where

$$\begin{aligned} C &= \frac{TotC}{(1 + K_{11} F + K_{21} P)} \\ A &= \frac{TotA}{(1 + K_{12} F + K_{22} P)}. \end{aligned} \quad (4)$$

We call these iterative equations because guessing initial values for C and A, we can compute F and P (the first iteration); then with F and P we can compute C and A and then recompute F and P (the second iteration); and so on. A stopping rule can be defined as when F and P stop changing within specified limits.

Feldman et al. also continues this development by substituting the formulas for C and A into the equations for F and P [5] to obtain their Eq. (25). They are complicated equations but do show that the iterative equations can be written in terms of F and P alone. It will be somewhat simpler if we substitute the formulas for C and A into our original version of the F equation Eqs. (1) and (2) above, considering the P equation as a nuisance; that is, focusing on F and its equation. We have

$$Tot F = F \left(1 + \frac{K_{21} TotC}{(1 + K_{11} F + K_{21} P)} + \frac{K_{22} TotA}{(1 + K_{12} F + K_{22} P)} \right) \quad (5)$$

This suggests that the iterative solution might be computed as the roots. Roots refer to the solutions of the polynomial equations (polynomial set equal to zero). The characteristic polynomial is obtained by algebraically clearing fractions in Eq. (5).

To be clear about this, define the product

$$\Pi = (1 + K_{11} F + K_{21} P)(1 + K_{12} F + K_{22} P) = (K_{11} F + C_{21})(K_{12} F + C_{22}),$$

where $C_{21} = 1 + K_{21} P$ and $C_{22} = 1 + K_{22} P$, both > 1 .
and are constant with respect to F. Multiplying both sides of (5) by Π clears the fractions and gives

$$Tot F \cdot \Pi = F \cdot \Pi + K_{21} TotC \cdot (K_{12} F + C_{22}) + K_{22} TotA \cdot (K_{11} F + C_{21}) \quad (6)$$

So, Π is a quadratic polynomial and $F \cdot \Pi$ is a cubic polynomial and the other terms give linear polynomials or constants. This Eq. (6) is the cubic polynomial such as obtained in Dorin et al. [4] where there was no P and $C_{21} = C_{22} = 1$. The standard solution of the cubic equation given in [4] and given more generally here shows existence of a solution. Also, for plausible values of F and P, the standard solution of the cubic equation can show uniqueness of the solution.

Comments. We have focused on the equation for F, but we can repeat Eqs. (5) and (6) for P. We then have two polynomial equations. We should also mention an important duality; we could write equations like Eqs. (5) and (6) for free A and C and iterate to find the solutions for A and C first, then one step computations using Eq. (3) would give us F and P. Usually, we do not care about A and C, but you could solve for A and C first and then compute F.

The problem with this approach in the above comment is that the polynomials for F and P are *coupled*; that is, the coefficients of the F polynomial are functions of

P and the coefficients of the P polynomial are functions of F. For example, the 1×2 matrix results is a cubic polynomial for which we can compute the positive root since there is only one equation and no coupling. But for the 2×2 matrix there is coupling and we cannot solve the positive root because the coefficients are unknown since they are functions of the unknown P. Thus, we continue to need to find ligand-protein binding equilibrium solution values iteratively. Both Mazer [45] as well as Gudmand-Hoeyer and Ottesen [19] treat 2×2 cases but iterate to find solutions, as did and Rohatagi et al. for competition of prednisolone and cortisol for CBG binding [46].

None-the-less, we wish to save this duality theorem; it is true here and in general, so we will wait until the next section to write it down.

4.1 Generalization to $n \times m$ matrix representation of the equilibrium equations

The generalization of the equilibrium equations from the above case for 2×2 matrix to the $n \times m$ matrix is straightforward just with a cost of more notation. We use the notation system of Feldman et al. [5] where free hormones (ligands) were designated P_1, P_2, \dots, P_n and binding proteins were designated as Q_1, Q_2, \dots, Q_m and represent these equations in a matrix format, as shown in **Table 6**.

So, the conservation of mass equation for the concentration $[TotP_i]$ is the sum of the i th row:

$$TotP_i = P_i + P_iQ_1 + \dots + P_iQ_j + \dots + P_iQ_m = P_i + \sum_{j=1}^m P_iQ_j$$

Note that Feldman et al. [5] and we assume univalent (stoichiometric) binding for the ligand-protein binding reaction $P_i + Q_j \rightleftharpoons P_iQ_j$ in equilibrium. So, the mass action equilibrium gives $P_iQ_j = K_{ij} \cdot P_i \cdot Q_j$ where K_{ij} is the association constant (affinity) of this reaction.

Thus, the sum in the i th row becomes

Matrix $n \times m$	Q_1	...	Q_j	...	Q_m	
P_1	$K_{11}P_1Q_1$...	$K_{1j}P_1Q_j$...	$K_{1m}P_1Q_m$	$TotP_1$
...	
P_i	$K_{i1}P_iQ_1$...	$K_{ij}P_iQ_j$...	$K_{im}P_iQ_m$	$TotP_i$
...	
P_n	$K_{n1}P_nQ_1$...	$K_{nj}P_nQ_j$...	$K_{nm}P_nQ_m$	$TotP_n$
	$TotQ_1$...	$TotQ_j$...	$TotQ_m$	

The total concentrations $TotP_i$ and $TotQ_j$ are measured and the $n \times m$ matrix of association constants $K = [K_{ij}]$ are known. The concentrations of free ligands $P = [P_i]$ are to be estimated. The mass conservation equations for the n rows and m columns together with mass action formulae yield Feldman's iterative equations that solve for free ligand concentrations P in left margin column [5].

Table 6.
General $n \times m$ matrix.

$$TotP_i = P_i + \sum_{j=1}^m K_{ij} \cdot P_i \cdot Q_j = P_i \left(1 + \sum_{j=1}^m K_{ij} Q_j \right) \quad (7)$$

which generalizes Eq. (1) above and with similar expressions generalizing Eq. (2) yields the general Feldman's iterative equations

$$P_i = \frac{TotP_i}{\left(1 + \sum_{j=1}^m K_{ij} Q_j \right)} \quad (8)$$

with

$$Q_j = \frac{TotQ_j}{\left(1 + \sum_{i=1}^n K_{ij} P_i \right)}. \quad (9)$$

Though the Feldman equilibrium equations treated iteratively have been used to obtain equilibrium solutions of free ligand concentrations (P's) [5, 6, 19, 45], it would be helpful to consider existence and uniqueness of these solutions more generally. Thus, we continue the development. The generalization of Eq. (5) is

$$TotP_i = P_i \left(1 + \sum_{j=1}^m \frac{K_{ij} TotQ_j}{\left(1 + \sum_{i=1}^n K_{ij} P_i \right)} \right) \quad (10)$$

Before continuing this discussion, let us give the Duality theorem here.

4.2 Duality theorem for equilibrium matrix K

The transpose (reverse rows and columns) of the equilibrium table for the nxm matrix K gives an equivalent equilibrium table for the mxn matrix K^T . The solution(s) of the dual matrix (table) are the same as for the original matrix.

Proof. Instead of solving for P_i first as in Eq. (10), it is equally possible to write the analogous equations for Q_j , solve for the Q_j first and then solve for the P_i second using Eq. (8). In terms of the K matrix table we only need to reverse rows and columns, that is, use the matrix transpose K^T .

Continuing the discussion of Eq. (10), a relatively simple presentation of our system of coupled polynomials is obtained by clearing fractions where possible in Eq. (10). So, define

$$\Pi = \prod_{j=1}^m \left\{ 1 + \sum_{k=1}^n K_{kj} P_k \right\} = \prod_{j=1}^m \left\{ K_{ij} P_i + 1 + \sum_{k \neq i} K_{kj} P_k \right\} = \prod_{j=1}^m \{ K_{ij} P_i + C_{ij} \}$$

where $C_{ij} = 1 + \sum_{k \neq i} K_{kj} P_k > 1$ and is constant with respect to P_i .

Note that $\prod_{j=1}^m \{ K_{ij} P_i + C_{ij} \}$ could be expanded (analogous to the binomial theorem) as a sum of terms, which is a m-degree polynomial in P_i provided all $K_{ij} > 0$; and the constant term of this polynomial is $\prod_{j=1}^m C_{ij} > 1$.

So, clearing of fractions in Eq. (10) by multiplying both sides by Π yields

$$\Pi P_i + \sum_{j=1}^m K_{ij} TotQ_j P_i \prod_{v \neq j} \{ K_{iv} P_i + C_{iv} \} = (TotP_i) \Pi \quad (11)$$

Comment. Each Π in Eq. (11) is a polynomial where ΠP_i is a $m + 1$ degree polynomial and the $P_i \prod_{v \neq j}$ are m -degree polynomials; and the linear combination of polynomials is a polynomial. Thus Eq. (11) is a $(m + 1)$ degree polynomial equation in P_i , provided all $K_{ij} > 0$. (If a $K_{ij} = 0$, then the degree is reduced by 1, that is, the degree of the polynomial Eq. (11) equals the number of non-zero K_{ij} plus 1.)

4.3 Existence theorem for characteristic polynomial

Eq. (11) for P_i has at least one positive solution.

Proof. Eq. (11) for P_i as a $(m + 1)$ degree polynomial in each P_i can be written as $A_{m+1}P_i^{m+1} + A_mP_i^m + \dots + A_1P_i^1 + C = 0$, where $C = -(\text{Tot}P_i) \prod_{j=1}^m C_j < -\text{Tot}P_i < 0$ and $A_{m+1} = \prod_{i=1}^m K_{iu} > 0$.

Descartes' Rule of Signs for polynomials says the number of positive roots is related to the number of sign changes of the coefficients of the polynomial. For our $(m + 1)$ degree polynomial, there is at least one sign change regardless of whether coefficients $A_2 \dots A_{m+1}$ are positive or negative or zero. This implies there is at least one positive solution for P_i ; that is, existence of a solution is shown. Additional discussion of Descartes' Rule of Signs and analysis of the existence theorem is presented in Appendix 2.

4.4 Uniqueness theorem for characteristic polynomial

Eq. (11) for P_i has exactly one positive solution.

Proof. To show uniqueness of a positive root of the characteristic polynomial known to exist, we return to the way we obtained this characteristic polynomial. To clear fractions, we multiplied Eq. (10) by $\prod = \prod_{j=1}^m \{K_{ij}P_i + C_{ij}\}$. Since the characteristic polynomial is product of two functions, the roots of this polynomial are the sum (union) of the roots of each factor. Now the m roots of \prod are all negative. The second factor coming from Eq. (10) is

$$P_i \left(1 + \sum_{j=1}^m \frac{K_{ij} \text{Tot} Q_j}{(1 + \sum_{i=1}^n K_{ij} P_i)} \right) - \text{Tot} P_i. \text{ As developed above this becomes}$$

$$P_i \left(1 + \sum_{j=1}^m \frac{K_{ij} \text{Tot} Q_j}{(K_{ij} P_i + C_{ij})} \right) - \text{Tot} P_i = \sum_{j=1}^m \frac{\text{Tot} Q_j P_i}{(P_i + B_{ij})} - (\text{Tot} P_i - P_i) \text{ where } B_{ij} = \frac{C_{ij}}{K_{ij}}.$$

Next, P_i and $\frac{P_i}{(P_i + B_{ij})}$ are monotone increasing functions of P_i , so their sum (this factor) is also. Now free P_i satisfies $0 \leq P_i \leq \text{Tot} P_i$. So evaluating the second factor at each end point, we have at $P_i = 0$, factor = $-\text{Tot} P_i$ which is negative and at $P_i = \text{Tot} P_i$, factor = $\sum_{j=1}^m \frac{\text{Tot} Q_j \text{Tot} P_i}{(\text{Tot} P_i + B_{ij})}$ which is positive. This implies there is exactly one root (a positive root). Thus, the characteristic polynomial is the product of two factors and has m negative roots and exactly one positive root. This is a proof of uniqueness.

Comment. One might say the proof of existence given above is not needed, since the proof of uniqueness given here does both existence and uniqueness. Nonetheless,

we needed the detailed development of the characteristic polynomial and the expanded discussion of this was instructive (also see Appendix 2).

5. Clinical correlates of competition for CBG-cortisol binding

In discussing limitations of their proposed method of calculating free cortisol, Coolens et al. acknowledge that cortisol-binding affinity of CBG may vary between individuals [3], which has been confirmed in subsequent studies [36, 39, 47]. They also noted the potential role of other ligands that compete for CBG-cortisol binding: “The fact that only the interaction of cortisol with CBG is taken into consideration constitutes a second limitation. In some conditions, significant amounts of other steroids may interfere with this equilibrium. This will be the case during pregnancy and also for patients with congenital adrenal hyperplasia ... the proposed method cannot be applied to umbilical cord blood, and in congenital adrenal hyperplasia [3]”. Thus, although CBG binds cortisol with specificity, there are several other steroid compounds that bind CBG with significant affinity. If the free concentrations of these CBG-binding ligands are sufficiently high in the test tube, they can effectively compete with CBG-cortisol binding and raise the equilibrium concentration of X_F . CBG is also the transport globulin for progesterone, which binds CBG with 3-fold lower affinity than cortisol and at high concentrations of (free) progesterone can effectively compete in the CBG-cortisol binding reaction. For example, as described by Hodyl et al. very high progesterone concentrations in fetal cord blood are capable of elevating free cortisol concentrations through competition with cortisol at CBG’s hormone binding site. This competition raised X_F without CBG cleavage or altered CBG hormone-binding affinity [21]. Similar results demonstrating competition of CBG-cortisol binding by progesterone have been also reported elsewhere [48–51].

In addition to progesterone, other adrenal corticosteroids competitively interfere with CBG-cortisol binding. For example, Dunn et al. observed relatively high equilibrium association constants for CBG binding of 11-deoxycortisol, 21-deoxycortisol, and 17-hydroxyprogesterone, with lower but significant CBG-binding affinities of aldosterone, testosterone, and other compounds [14]. Although the clinical relevance of these precursors of cortisol biosynthesis is uncertain, their combined effects may be significant, especially when dynamic changes in their concentrations are coordinated by ACTH. These observations may explain the observation by Barlow et al. that Coolens’ equation significantly underestimated measured X_F after synacthen stimulation [52]. Similar results were reported by Vogeser et al. where underestimation of X_F by Coolens’ formula was especially notable in patients with pronounced acute phase response [53]. In addition, testosterone and aldosterone also bind CBG, albeit with relatively low binding affinities [14, 19, 54–56]. Pharmacologic compounds, such as prednisolone, progesterone, medroxyprogesterone, danazol, and others also bind CBG with significant affinity [57]. The effect of prednisolone competition for CBG-cortisol binding and resulting increased concentrations of free cortisol has been previously reported [22].

In vivo, cortisol is metabolized to cortisone by the 11-hydroxysteroid hydrogenase 2 (11-HSD2) enzyme expressed in kidney and other tissues. Cortisone binds CBG with intermediate affinity [14], raising the possibility that other metabolites of cortisol might also compete for CBG-cortisol binding. This hypothesis was further explored in an analysis comparing women on oral contraceptive pills (OC) and healthy volunteer

(HV) groups based on data of Perogramvros et al. [58, 59]. The data set was especially useful for modeling cortisol distribution *in vitro*, since multiple measurements of X_{TotF} , X_F , and free cortisone (X_E) were obtained in the same individual at multiple time points spanning a broad range of cortisol concentrations. Using measured concentrations of X_{TotF} and X_{TotCBG} to predict X_F based on Coolens' formula (represented in **Table 2**), we compared model-predicted vs. measured concentrations of X_F at each time point. As shown in **Figure 1**, the residual plots (measured X_F minus X_F estimated using Coolens' formula) demonstrate the following: (i) Coolens' formula provides a fair but inconsistent approximation to measured X_F in HV, (ii) in the OC group, X_F predicted by Coolens' formula significantly underestimates measured concentrations of X_F , with up to 100% percent error in calculated X_F , (iii) the pattern of residual error was time-varying in both groups, but was more prominent in OC, (iv) the pattern of residuals differed for per os (po) and iv modes of hydrocortisone administration, roughly paralleling measured concentrations of X_{TotF} and X_F . We hypothesized that

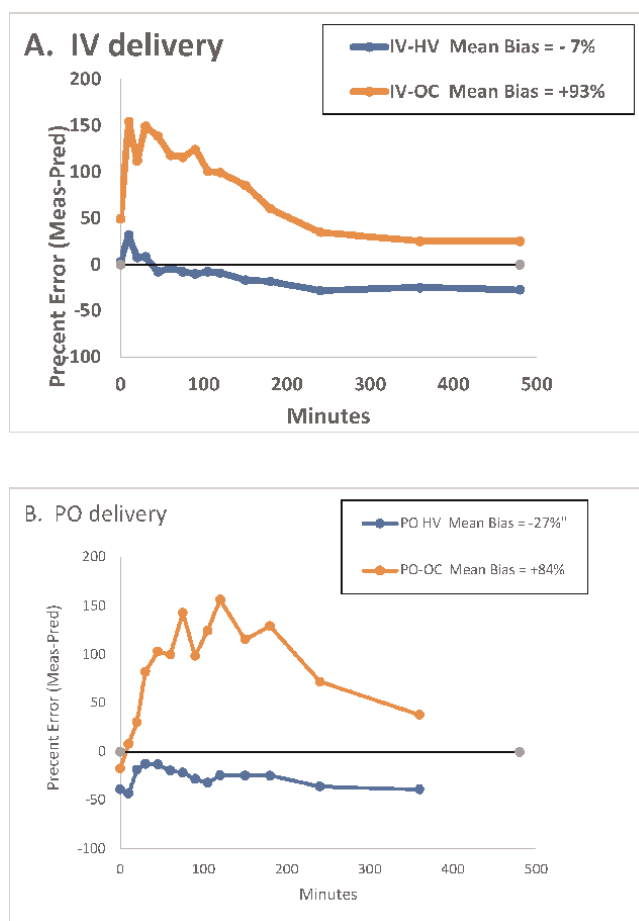


Figure 1. Percent error (bias) showing mean residuals (measured minus model-predicted free cortisol concentration) In healthy volunteers (HV, blue) vs. women on oral contraceptives (OC, red) following iv bolus (20 mg) (Panel A) and po hydrocortisone (20 mg) (Panel B). Model-predicted free cortisol concentrations (X_F) were obtained using K_{11} and N values taken from literature (Coolens' formula, see Matrix #2). X_F estimated by Coolens' formula significantly underestimated measured X_F in women on OC.

time-varying concentrations of competitor (P) resulted in higher concentrations of free cortisol than predicted by the Coolens' formula, which considers cortisol as the sole ligand involved in CBG binding (single row in **Table 2**).

In addition, we compared parameter solutions and residual plots for two alternative models. These parameter solutions represent the *inverse* matrix problem, as discussed also later in Section 6. That is, since X_F and X_{TotF} were measured at each time point, we used measured concentrations of X_{TotF} and X_F and assumed constancy of baseline X_{TotCBG} to iteratively solve for model-specific parameters of interest. In the minimal model, represented by **Table 2**, these parameters include K_{11} and N . In the competition model, represented by 2×2 **Table 5**, additional parameters, including affinity constant for competitor (P) binding to CBG [K_{21}], were obtained. Our finding that the competition model provided significantly better fit to experimental data as well as better residual plots compared to the minimal model provide additional support, albeit indirect, for the presence of ligands (P) that compete for CBG-cortisol binding [58]. The identity of the putative ligand(s) (P) remains speculative. However, since endogenous corticosteroid was suppressed in this study by antecedent administration of dexamethasone [59], these observations raise the possibility that other ligands, for example metabolites of cortisol (or progesterin in OC), might compete for CBG-cortisol binding. As free cortisone concentrations were also assayed at each time point and its CBG-binding affinity may be taken from the literature [14, 59], we were able to demonstrate that the transient increase in free cortisone concentrations observed after iv and po hydrocortisone bolus was not of sufficient magnitude to account for the observed difference between measured and model-predicted X_F (data not shown). However, it remains possible that other cortisol metabolites may increase in tandem with free cortisone with timing entrained by time-varying concentrations of X_F , the substrate for enzymes of cortisol metabolism. In the hypothetical example of multiple competing ligands, it may be possible to re-parameterize their integrated effects as a composite function represented by a harmonic mean (data not shown).

In summary, there are several validated examples of ligands that compete for CBG-cortisol binding; these include progesterone, adrenal steroid precursors of cortisol biosynthesis, synthetic compounds such as prednisolone, and metabolites of cortisol, such as cortisone.

At equilibrium in the test tube, the concentration of X_F is also affected by albumin-cortisol binding. As shown in **Table 2**, albumin-cortisol binding may be simplified [3] as a constant ratio (N) of albumin-bound to free cortisol ($X_{FA}/X_F = K_{12}^*A$). However, whether the simplification of using total (X_{TotA}) as a surrogate for free albumin (X_A) concentration is appropriate remains uncertain, as discussed in Section 7. Before addressing Coolens' assumption that $X_{TotA} \approx X_A$, let us first examine some useful data concerning the albumin-cortisol affinity constant (K_{12}). For this purpose we revisit albumin-cortisol binding data previously reported by Lewis et al. [27]. These experiments involve binding of 3H -labeled cortisol to a purified solution of human albumin and will assume 1:1 stoichiometry of albumin-cortisol binding. Consideration of multiple cortisol binding sites per albumin molecule is discussed in Appendix 4.

6. Albumin-cortisol binding in purified solution of human serum albumin using data of Lewis et al.

The experiment involves addition of a small mass of 3H -labeled cortisol (E), which is assumed to bind albumin with an affinity equal to that of endogenous (unlabeled)

cortisol (F), to solutions of varying concentrations of purified albumin [27]. Thus, the test tube consists of TotA and TotE, which at equilibrium also gives a free E and a free A. The 1×1 matrix for 1 ligand (E) and 1 binding protein (albumin) is shown in Table 7.

In the albumin-cortisol binding experiments of Lewis et al. [27], concentrations of free and albumin-bound E are measured and, using known values of X_{TotA} and the measured values of the percent free cortisol (R), the affinity constant (K_{12}) and corresponding equilibrium dissociation constant K_{12}^{-1} is estimated (blue). Conservation of mass laws give

$$\text{TotE} = E (1 + K_A A), \text{ or } E = \frac{\text{TotE}}{1 + K_A A}. \quad (12)$$

Rewriting Eq. (12) in terms of R = fraction that free E is of the total TotE, we have

$$\frac{1}{R} = 1 + K_A A. \quad (13)$$

The conservation of mass in the column gives

$$\text{TotA} = A (1 + K_A E), \text{ or } A = \frac{\text{TotA}}{1 + K_A E} \quad (14)$$

to be estimated.

Rewriting (14) in terms of dissociation constant $K_D = 1/K_A$, we have $A = \frac{K_D \text{TotA}}{K_D + E}$.

Matrix 1x1	Free A	
Free F	$K_{11} \cdot A \cdot F$	Tot F
	Tot A	

Measured Otherwise Known To be solved

For these in vitro studies reported by Lewis et al. ^3H -cortisol (F) is added to varying concentrations of purified albumin solution [27]. Added ^3H -cortisol is distributed between free (measured) and albumin-bound fractions at equilibrium, and here TotF is the amount of ^3H -cortisol added to the test tube. F is measured (light red), TotF and TotA are otherwise known (yellow). The affinity constant for albumin-cortisol binding is solved (blue) using varying concentrations of TotA, where the fraction $R = F/\text{TotF}$ and, according to (Feldman's) row eq. $1/R = 1 + K_{11} \cdot A$. Applying Coolens' assumption $K_{11} F < 1$ [3], then $A = \text{TotA}$. The plot of $1/R$ versus experimentally varied TotA provides a series of points which is nearly linear with slope = K_{11} . Goodness of fit of this model for the purified albumin assay can be judged by deviations from linearity. Note that this is an inverse problem in that the total and free concentrations are measured or experimentally known and the affinity constant K_{11} is to be estimated.
Constraints: $K_{11}F < 1$; note that in this experiment, $N = K_{11} A = K_{11} \text{TotA}$ and N varies in relation to experimentally varied TotA.

Table 7.
 1×1 matrix for equilibrium equations for experimental cortisol binding studies using purified albumin solution [27].

Now Coolens' approximation $E \ll K_D$ applies, in which case $A = \text{Tot}A$. Then $K_A A = K_A \text{Tot}A$, so that Eq. (12) becomes

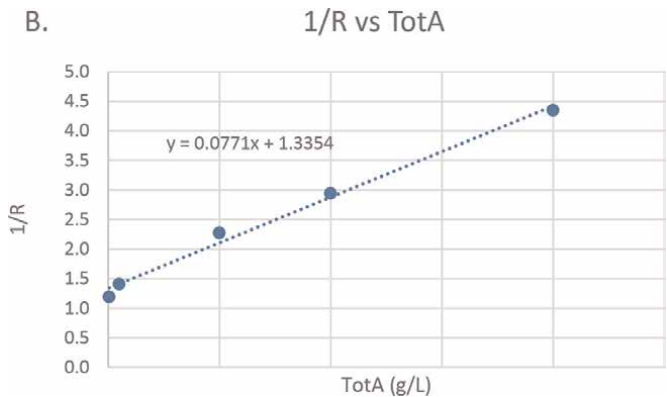
$$\frac{1}{R} = 1 + K_A \text{Tot}A \quad (15)$$

Note that we also use the notation $K_A \text{Tot}A = N$ to represent N in Coolens' formula, which in this formulation indicates that N is proportional to $X_{\text{Tot}A}$.

Assuming 1:1 stoichiometry of albumin-cortisol binding, a graphical estimate of K_A is obtained by plotting $1/R$ versus $\text{Tot}A$ and fitting the regression line where the slope is the estimate K_A . Data from Lewis et al. [27] are shown in **Table 8**, R represents the free ^3H -cortisol concentration expressed as a fraction of total ^3H -cortisol [$\text{free } ^3\text{H-cortisol} / [\text{albumin-bound } ^3\text{H-cortisol} + \text{free } ^3\text{H-cortisol}]$].

Plotting this data and fitting a regression line gives the graph shown in the plot associated with **Table 8**, which corresponds to $K_{12}^{-1} \approx 195,000 \text{ nmol/L}$. At median concentrations of serum albumin ($580,000 \text{ nmol/L}$), this $K_{12}^{-1} \approx 195,000 \text{ nmol/L}$ corresponds to $N = 3.0$. Lewis et al. addressed the issue of discrepant values for N in purified albumin solution (3.0) vs. the lower N (1.74) for plasma/serum samples used in Coolens' quadratic equation human serum [27]. They note that "in physiological

TotA (g/L)	R	1/R
A.		
0.1	0.84	1.19
1	0.71	1.41
10	0.44	2.27
20	0.34	2.94
40	0.23	4.35



A. Data from Lewis et al. purified albumin assay [27]. The experiment involves fixed concentration of labeled cortisol (F) added to solutions of varying concentrations of purified albumin, where the fraction $R = \text{free } F / \text{Tot}F$. B. Associated plot with slope $K_{11} = 0.0771 \text{ per g/L}$ according to eq. $1/R = 1 + K_{11} \cdot \text{Tot}A$, applying Coolens' assumption $K_{11} F \ll 1$, then $A = \text{Tot}A$). The conversion to units nmol/L gives $0.0771 / (15,047) = 5.124 \times 10^{-6} \text{ per nmol/L}$ and in terms of dissociation constant $K_D = 1 / 5.124 \times 10^{-6} = 195,200 \text{ nmol/L}$.

Table 8.
Data for free cortisol concentrations in binding studies of purified human albumin solution reported by Lewis et al. and associated plot of transformed free cortisol (F) vs. albumin concentration.

human albumin solutions 25% of ^3H -cortisol is in the free fraction ... This may suggest that the ratio of albumin-bound to unbound cortisol is 3.0, which is slightly higher than the value of 1.74 value used in the Coolens' calculation of free cortisol from total cortisol and CBG. Taken together we suggest that revision of the Coolens' value is probably not warranted" [27].

7. Toward a general theorem that includes competition for albumin-cortisol binding (2×2 matrix)

7.1 Coolens' simplification (re-parameterization of albumin-bound cortisol)

Coolens' assumption re-parameterizes the equation used to estimate the concentration of albumin-bound cortisol, which is represented by the inner cell indicated by dashed oval in **Table 1**. In the cubic solution, the mass action equation for albumin-bound cortisol (FA) is the product of $K_{12} \cdot F \cdot A$, where K_{12} is the equilibrium affinity constant for albumin-cortisol binding, F is the concentration of free cortisol, and A is the concentration of free albumin. Coolens' simplification of this equation transitions $K_{12} \cdot A$ to a single value (N). N is a constant, which makes the implicit assumption that both K_{12} and A are also constant. A related assumption is that $F < < K_{12}^{-1}$, which implies that F/K_{12}^{-1} is a very small number. In a simplified model that only considers one ligand (cortisol), these assumptions suggest that $\text{Tot}A = \text{free } A$ and that free A is unaffected by changes in F within the physiologic range of systemic cortisol concentrations.

To visualize the re-parameterization of albumin-bound cortisol in the matrix format, we refer to **Table 1** and focus on the column sum (compound box) showing that $\text{Tot}A = A(1 + K_{12}F)$. Given Coolens' assumption that $F < < K_{12}^{-1}$ and dividing through by K_{12}^{-1} , we obtain $K_{12} \cdot F < < 1$, so that in the column sum $\text{Tot}A = A(1 + K_{12}F) \cong A(1 + 0) = A$, which is a constant ($\text{Tot}A$). Now $K_{12}A \cong K_{12}\text{Tot}A = N$ is a constant. So we can replace $K_{12}FA$ in the matrix by NF , as shown in **Table 2**.

Coolens' Theorem. In the 1×2 matrix above, if $K_{12}F < < 1$, then

- i. $\frac{[FA]}{[F]} = N$ is a constant,
- ii. A is a constant and $K_{12}A = N$,
- iii. $A \cong \text{Tot}A$.

Comment. It is clear that the above theorem is intended for dynamic situations such as occur *in vivo* in human physiology. For example, statement (i) above means $\frac{[FA]}{[F]}$ is constant, as F (and FA) vary over time. Yet, the matrix above describes equilibrium situations such as occur *in vitro* (in a test tube) or as in a steady state condition in a dynamic system. The connection is often that the equilibrium *in vitro* is a representative (snapshot) in time of the dynamic process. In equilibrium in a test tube, dynamic variables become constants, as discussed in Section 1 above. This view might be considered accurate even *in vivo*, because binding takes place so quickly in time while other time-varying processes in the *in vivo* dynamic system develop relatively much more slowly.

Condition iii) is not absolutely necessary. See the general theorem below.

To introduce the general theorem, we consider Coolens' assumptions and Coolens' simplification to the context of competitive protein-ligand binding reactions where multiple ligands may compete with cortisol for albumin binding at one (or more) binding sites. These considerations may be generally applicable to BP's associated with non-specific binding reactions in which many ligands (multiple rows in nxm matrix) may be involved. As well, the theorem generally applies to BPs having high molar concentration in serum relative to molar concentration of the ligand(s) of interest. Because the concentrations of BPs, ligands, and competing ligands are constant in the test tube, the assumption of constancy of N as a means of simplifying numerical solutions for X_F may be most realistic *in vitro*. As addressed below, N may vary under different conditions that affect the ratio of X_{FA}/X_F *in vivo*, including supernumerary binding reactions that influence the concentration of free albumin (X_A) as a percent of total (X_{TotA}).

7.2 Theorem for generalization of Coolens' N

Without pre-condition and in all matrices and for every ligand P with the concentration [PA] and assuming 1:1 stoichiometric ligand P-albumin binding, we have

- i. $\frac{[PA]}{P} = N_P$ is a constant if and only if
- ii. A is a constant and then $N_P = K_P A$ and N_P is constant.
- iii. If A is constant then all mass action equations for A in the general matrix can be replaced by $N_P P$ for every ligand P.

Proof. By the mass action equation for cortisol-albumin binding $\frac{[PA]}{[P]} = K_P A$, so defining $N_P = \frac{[PA]}{[P]}$, we have N_P is constant if and only if A is constant.

For example, without loss of generality, considering 2×2 matrix where ligand P is a competitor to F in binding to A, we obtain the matrix shown in **Table 5**.

Writing $TotA = A (1 + K_{12}F + K_{22}P)$, a generalization of Coolen's condition might be $K_{12}F + K_{22}P \ll 1$, in which case $A \cong TotA$ is a constant. By the general theorem above, both $K_{12}A = N_F$ and $K_{22}P = N_P$ are constants. In the 2×2 matrix above the mass action equations for A can be replaced by $N_F F$ and $N_P P$ as shown by iii) in the general theorem. The resulting 2×2 matrix is shown in **Table 9**.

To take advantage of this simplification, this 2×2 matrix can be collapsed into a 2×1 matrix, which is useful for computation purposes, as shown in **Table 10**.

There is one more step that could be taken to explain that this equilibrium solution results in a cubic equation in terms of free C. Then using the solution for C, the Feldman equations result in solutions for free F and free P. That step is to use the Duality Theorem mentioned after the general equilibrium $n \times m$ matrix in **Table 6**, which transposes rows and columns. Thus, the 2×1 matrix (**Table 10**) becomes a 1×2 matrix, shown in **Table 11**, and the characteristic polynomial is of degree $m + 1 = 2 + 1 = 3$, a cubic equation in C. Once the value of C is obtained, the Feldman Eq. (12) give solutions for free F and free P (see caption of **Table 11**).

Corollary 1. In the 2×2 matrix above, if $K_{12}F \ll 1$ and P is constant then the following are true and equivalent:




Matrix 2x2	C = Free CBG	A = Free Albumin	
F = Free Cortisol	$K_{11} F \cdot C$	$N_{12} F$	Tot F
P = Free Competitor	$K_{21} P \cdot C$	$N_{22} P$	Tot P
	Tot C		

 Measured  Otherwise Known  To be solved

The three total concentrations: total cortisol (TotF), total competitor (TotP), and total CBG (TotC) are measured (light red). The affinity constants for CBG-cortisol (K_{11}) and albumin-cortisol (K_{12}) binding are obtained from the literature or otherwise estimated (yellow). Assuming P is a specific ligand, the Coolens constants for ligand-albumin binding (N_{21}) and (N_{22}) may be obtained from the literature (yellow). The free cortisol and free competitor concentrations (F and P) are estimated (light blue).
Constraints: General Coolens' assumption, $K_{12}F + K_{22}P \ll 1$.

Table 9.
 2×2 matrix for cortisol binding equilibrium equations with Coolens' approximation.

Matrix 2x1	C = Free CBG	
$(1 + N_{12}) F$	$K_{11} F \cdot C$	Tot F
$(1 + N_{22}) P$	$K_{21} P \cdot C$	Tot P
	Tot C	

 Measured  Otherwise Known  To be solved

By algebraic manipulation, one column from the 2×2 matrix (Table 9) can be combined with the marginal column of free concentrations; thus, one column from Table 9 is eliminated, resulting in Table 10, a 2×1 matrix.
Constraints: General Coolens' assumption, $K_{12}F + K_{22}P \ll 1$.

Table 10.
 2×1 matrix simplification by application of general Coolens' assumption.

- $\frac{[PA]}{P} = N_P$ is a constant if and only if
- A is a constant and $K_P A = N_P$,
- If A is constant then all mass action equations for A in the matrix can be replaced by $N_P P$ for every ligand P including F.

Matrix 1x2	$(1 + N_{12}) F$	$(1 + N_{22}) P$	
$C = \text{Free}$ CBG	$K_{11} F \cdot C$	$K_{21} P \cdot C$	$\text{Tot } C$
	$\text{Tot } F$	$\text{Tot } P$	

Measured
 Otherwise Known
 To be solved

This table illustrates the application of the Duality Theorem to change the 2×1 matrix (Table 10) into an equivalent 1×2 matrix (Table 11). Using this transformation, equilibrium equations can be solved first for free CBG concentration (C).

The conservation of mass equations are:

$$\text{Tot}C = C (1 + K_{11}F + K_{21}P)$$

$$\text{Tot}F = F (1 + N_{12} + K_{11}C) \text{ or } F = \text{Tot}F / (1 + N_{12} + K_{11}C)$$

$$\text{Tot}P = P (1 + N_{22} + K_{21}C) \text{ or } P = \text{Tot}P / (1 + N_{22} + K_{21}C.)$$

Now substituting F and P formulae into the first equation and clearing fractions gives a cubic Eq. (6) in C with all coefficients known.

Finally, this value of C can be substituted into the Feldman Eq. (12) for F and P above gives the values for free F and free P.

Constraints: General Coolens' assumption, $K_{12}F + K_{22}P \ll 1$.

Table 11.

1×2 matrix, the transpose of 2×1 matrix in Table 10, for cortisol binding equilibrium equations with Coolens' approximation.

Proof. Write $\text{Tot}A = A (1 + K_{12}F + K_{22}P) = A (1 + 0 + K_{22}P)$, so that

A is constant if and only if P is constant and the rest is true by the general theorem.

Comment 1. In general, if any $N_P = K_P A$ were not constant then A is not constant and then no other N_P is constant. These are an all-or-none result; every K_A in the A column can be replaced by constants N_P (they may be different constants) or none of them can be replaced by constants N_P .

Comment 2. In Corollary 1, for the 2×2 matrix, the fact that N is constant requires A to be constant, which if $A < \text{Tot}A$ requires P to be constant seems to be difficult to realize *in vivo*, but not *in vitro*.

Another problem may occur when $A < \text{Tot}A$ in that we may no longer know the value of $N_P = K_P A$.

Let us summarize comment 1 as corollary 2.

Corollary 2. In the general matrix, if any $N_P = K_P A$ were constant then all the other N_P are constants; and *in vivo*, if any $N_P = K_P A$ were not constant then all the other N_P are not constants.

Proof. Any $N_P = K_P A$ is constant if and only if A is constant, and A is constant if and only if all $N_P = K_P A$ are constant.

Corollary 3. In the 2×2 matrix above, if $K_{12}F \ll 1$ and $K_{22}P \ll 1$ then the following are true:

i. $A = \text{Tot}A$

ii. $\frac{[PA]}{P} = N_P$ and $\frac{[FA]}{F} = N_F$ are constant and

iii. $N_P = K_P \text{Tot}A$ and $N_F = K_F \text{Tot}A$.

Proof. Write $\text{Tot}A = A(1 + K_{12}F + K_{22}P)$. Then $\text{Tot}A = A(1 + 0 + 0) = A$,

Comment 3. In the above general theorem, we considered competition as one competitor, P. However, one may think of this P as a composite of many competitors P. A more formal analysis of this could be done using multiple competitors P as multiple additional rows in our matrix.

7.3 What if there are multiple cortisol binding sites on the albumin molecule?

The albumin-cortisol binding reaction is often simplified by assumption of (1:1) stoichiometry, whereby one molecule of albumin binds one molecule of cortisol. However, it is possible that albumin has more than one binding site for cortisol, as has been suggested for albumin binding of testosterone for example [60]. The matrix approach can still be usefully applied in the example of multiple binding sites, though care must be taken to distinguish 'per site' vs. 'per molecule' binding activities in the matrix. This is especially critical when dealing with conservation of mass equations for albumin in the multiple binding site model since an important operational objective of the matrix is to relate marginal totals to measured data. In the case of albumin, measured data is reported in molecular mass (g/L or mmol/L) rather than theoretical number of binding sites. A matrix approach to multiple cortisol binding sites on the albumin molecule is described in Appendix 4.

7.4 Current perspectives on albumin-cortisol binding

Competition probably affects albumin-cortisol binding and equilibrium concentrations of albumin-bound cortisol *in vitro*. The competitors having the greatest potential impact on free cortisol concentrations are ones that circulate at high concentrations and bind albumin with significant affinity, such as free fatty acids [60]. Our general theorem represented in **Table 9** suggests that the simplification for albumin-bound cortisol using a constant (N) is applicable if N can be reasonably estimated. A key element in this objective is ascertainment of free albumin (X_A) as a percent of total albumin ($X_{\text{Tot}A}$). By the same token, there is evidence that free A varies in relation to total A. Thus, it appears that free albumin concentrations (X_A), and consequently values for N, are reduced in hypoalbuminemic subjects [29, 61].

Given ease of measurement of serum total albumin concentrations, it may be useful to adjust N based on measured concentrations of $X_{\text{Tot}A}$. On the other hand, the impact of variation in N on free cortisol concentration is relatively small under conditions where most of the hormone is bound by CBG. Thus, in some formulations, such as Coolens' quadratic equation, normative rather than measured values for $X_{\text{Tot}A}$ are applied with minimal impact of free cortisol estimates; similar assumptions of normative values for $X_{\text{Tot}A}$ and N are made in formula used to estimate free testosterone and vitamin D concentrations [62, 63]. However, for conditions such as critical illness, septic shock, or CBG-deficiency in which bioavailable cortisol ($(X_F + X_{FA}) = F(1 + N)$) represents a more substantial fraction of $X_{\text{Tot}F}$, error associated with selection of an incorrect value for N has

a more significant impact on estimated X_F . Given these uncertainties concerning both the constancy and value for N , additional investigations concerning the use of Coolens' simplification to model albumin-bound cortisol concentrations are warranted.

8. Conclusions

We have introduced a matrix format for equilibrium (1) as a guide to writing down the Feldman equations, (2) to represent a given equilibrium problem/discussion *in vitro* or *in vivo* marking what is known and what is to be computed, (3) as an illustration of several formulations given in the literature, and (4) as an aid to computations/simplifications, as illustrated by Appendix 4. Although the present chapter has focused on cortisol, it may be understood that the matrix approach described herein is generalizable to analogous problems, including other corticosteroids of interest, sex steroids, thyroid hormones, vitamin D metabolites, and insulin-like growth factor 1. The approach is also generalizable to other ligand-protein binding problems, including substrate-enzyme and antigen-antibody reactions.

The topics treated with this matrix format include:

- i. Summary of contemporary models that consider cortisol as the sole ligand involved in BP interactions. A single ligand (cortisol) in $n \times m$ matrix yields analytic solutions using cubic (1×2), quartic (1×3), and quadratic (1×2 with re-parameterization of albumin-bound cortisol) equations.
- ii. Competition model for *specific* binding, by which multiple ligands compete for the specific serum transport BP (CBG in this case) characterized by high-affinity binding and limiting concentrations. In this example of specific binding, free CBG concentrations vary widely over the physiologic range of (free) cortisol concentrations. This results in saturable kinetics of CBG-cortisol binding. Other ligands may also compete with cortisol for limiting concentrations of free CBG. The competition model is represented by 2×2 matrix, which may be generalized to multiple ligands interacting with multiple BPs. Clinical examples of competition for CBG-cortisol binding, including analysis of women on OCP, were also developed using matrix notation. The coupled polynomial equations associated with the 2×2 matrix are not tractable to analytic solutions; rather, they require iterative solutions.
- iii. Competition model for *non-specific* binding, as exemplified by albumin-cortisol binding. In this situation, the equilibrium dissociation constant for albumin-cortisol binding (K_{12}^{-1}) greatly exceeds the concentration of free cortisol ($K_{12}^{-1} \gg X_F$); consequently, the free concentration of albumin (A) varies insignificantly over the physiologic range of free cortisol concentrations. The albumin-cortisol binding reaction was first addressed using a 1×1 matrix to represent the *in vitro* ^3H -cortisol binding experiments reported by Lewis et al. using purified albumin solutions [27].
- iv. The matrix for non-specific binding was subsequently expanded to a general, competitive (2×2) model and theorem for Coolens' simplification, which considers albumin-bound cortisol (X_{FC}) as a constant ratio (N) of albumin-bound to free cortisol concentrations. The generalized theorem raises the possibility that, given the multiplicity of ligands that bind albumin, the

concentration of free albumin (A) may be less than total albumin concentration ($A < \text{TotA}$).

- v. CBG binds cortisol with 1:1 stoichiometry, but there is a possibility of complex stoichiometry in the case of albumin-cortisol binding. Development of *per site* and *per molecule* matrix notation was useful for modeling the hypothetical example of multiple, independent cortisol-binding sites per albumin molecule. This approach was useful for multiple sites having different affinity constants for albumin-cortisol binding. However, in order to fulfill the objective of relating the matrix totals to measured totals (e.g., total albumin concentration in serum), it is important to account for sites per molecule when applying mass conservation equations.

The recognition that ligands other than cortisol that influence CBG-cortisol binding reactions closes a chapter on simple polynomial equations that consider cortisol as the sole binding ligand. The generalized system of Feldman equations, represented by the 2×2 matrix, involves coupled polynomial equations. In the presence of other competing ligands (P), estimation of free cortisol involves iterative rather than simple analytic solutions. In the case of albumin-cortisol binding, the multiplicity of ligands involved in non-specific binding challenge the assumption that free albumin is equal to total albumin and complicate accurate assessment of N. Thus, while N may be constant *in vitro*, N may vary between individuals and vary over time and condition within an individual subject. If N is not a constant and might vary within and between individual subjects, the simplicity of a constant N is no longer applicable. In that case, alternative measures to predict albumin-bound cortisol concentration or estimate N may be needed to accurately solve free cortisol concentrations. Since X_{TotA} is simply and routinely measured clinical laboratory, the challenge becomes determination of free albumin as a percent of X_{TotA} . With these (X_{TotA} and X_A) in hand, there may be an approach to solving for affinities or Coolens' N. Accurate assessment of N is more important in conditions, such as critical illness or exogenous hydrocortisone administration, where bioavailable cortisol represents a more substantial percentage of total cortisol.

In summary, the principles of mass action and conservation continue to govern the distribution of cortisol between free and protein-bound compartments *in vitro*. Alternative modeling approaches (and/or alternative measurements) may be needed to resolve the clinical problem of accurately estimating X_F without having to use laborious separation methods. We hope that this chapter provides a way forward on this important task.

Acknowledgements

The authors thank Frank K. Urban III, Professor of Electrical & Computer Engineering at Florida International University, Miami, FL for helpful discussion of the material. The research was supported by the Research Service of the New Mexico Veterans Administration Healthcare System in Albuquerque, NM. We wish to acknowledge Ilias Perogamvros, David Ray, Brian Keevil, Leon Aarons, Adrian Miller, and Peter Trainer at University of Manchester, UK, who generously provided the cortisol concentration data used in **Figure 1** and related modeling analysis [2, 58, 59].

Conflict of interest

The authors declare no conflict of interest.

Appendices

Appendix 1. A connection between dynamic model *in vitro* and equilibrium solutions *in vitro*:

The CBG-cortisol binding reaction in our four compartment model of *in vivo* cortisol distribution (2) applied to the *in vitro* experiment is represented by the differential equation $\frac{dFC(t)}{dt} = -\kappa_{-1}F(t)C(t) + \kappa_1C(t)F(t)$, where F is the free cortisol, C is the free CBG, and FC is CBG-bound cortisol; κ_1 and κ_{-1} are the on and off rates of this cortisol-CBG reaction. Rewriting this differential equation in a standard form: $\frac{dFC}{dt} + \kappa_{-1}FC = \kappa_1C \cdot F$, there is a well-known integral solution, and we get a convolution integral solution:

$$FC(t) = \frac{\kappa_1}{\kappa_{-1}} \int_0^t \exp(-\kappa_{-1}(t-\tau))C(\tau)F(\tau) d\tau, \text{ provided we start at } FC(0) = 0.$$

We recognize that the dynamic reaction of F binding to CBG to form the bound FC is proportional to a delayed version of the function $C \times F$ according to convolution integral solution. The half-life of the reaction $= \frac{\ln 2}{\kappa_{-1}}$ which equals $\frac{69}{.88/sec} = 0.8 \text{ seconds}$ for typically reported values of this off rate. The constant of proportionality is $\frac{\kappa_1}{\kappa_{-1}} = \frac{.027/nM-sec}{.88/sec} = .03/nM$, which engineers might call gain and biochemists call the affinity or association constant of the reaction; the reciprocal $= 33 \text{ nM}$ is the disassociation constant. We also recognize that FC, C, and F are constants at equilibrium, and that $\frac{dFC}{dt} = 0$ implies $FC = K_{11} C \times F$, which is the mass action equation for this reaction and is used in the equilibrium solution *in vitro*.

Next as an illustration of a general result, we show that the steady state solutions of the differential equations governing the dynamic behavior of three compartments (free, CBG-bound and albumin-bound cortisol) *in vitro*, in the test tube, are the same as the solutions of Feldman's iterative equations for that same test tube. The introductory sections entitled "Free, CBG-bound, and albumin-bound cortisol as a 3-compartment model" and "Cortisol in captivity" in the manuscript describe the *in vitro* situation represented in a test tube. The system of three differential equations for this 3-compartment model are

$$\begin{aligned} \frac{dF(t)}{dt} &= +\kappa_{-1}^C * FC(t) - \kappa_1^C C(t) * F(t) + \kappa_{-1}^A * FA(t) - \kappa_1^A A(t) * F(t) \\ \frac{dFC(t)}{dt} &= -\kappa_{-1}^C * FC(t) + \kappa_1^C C(t) * F(t) \\ \frac{dFA(t)}{dt} &= -\kappa_{-1}^A * FA(t) + \kappa_1^A A(t) * F(t) \end{aligned} \tag{16}$$

where $C(t) = TotCBG - FC(t)$ and $A(t) = TotA - FA(t)$.

The steady state solutions are these limits: $\lim_{t \rightarrow \infty} F(t) = F(\infty)$,

$\lim_{t \rightarrow \infty} FC(t) = FC(\infty)$, and $\lim_{t \rightarrow \infty} FA(t) = FA(\infty)$, The where clause in Eq. (4) in this chapter also implies the limits $\lim_{t \rightarrow \infty} C(t) = C(\infty)$, and $\lim_{t \rightarrow \infty} A(t) = A(\infty)$ exist.

On the other hand, the Feldman iterative equations are derived by schoolbook algebra from the conservation of mass and mass action system of equations

$$\begin{aligned} \text{Tot } F &= F (1 + K_{11} C + K_{12} A), \\ \text{Tot } C &= C (1 + K_{11} F) \\ \text{Tot } A &= A (1 + K_{12} F) \end{aligned} \quad (17)$$

The question is are iterative solutions for the equilibrium (F, C. and A) the same as the steady state solutions $F(\infty)$, $C(\infty)$, and $A(\infty)$?

We proceed using the convolution solution obtained above for $FC(t)$; thus under technical conditions satisfied here, we obtain

$$\begin{aligned} FC(\infty) &= \lim_{t \rightarrow \infty} FC(t) = \lim_{t \rightarrow \infty} K_{11} \int_0^t \kappa_{-1} \exp(-\kappa_{-1}(t - \tau)) C(\tau) F(t) d\tau \\ &= K_{11} C(\infty) F(\infty) \lim_{t \rightarrow \infty} \int_0^t \kappa_{-1} \exp(-\kappa_{-1}(t - \tau)) d\tau \end{aligned}$$

where $\int_0^t \kappa_{-1} \exp(-\kappa_{-1}(t - \tau)) d\tau = \exp(-\kappa_{-1}(t - \tau)) \Big|_0^t = 1 - e^{-\kappa_{-1}t}$

and $\lim_{t \rightarrow \infty} \{1 - e^{-\kappa_{-1}t}\} = 1$. Thus, the steady state solutions satisfy the mass

action eq. $FC(\infty) = K_{11}C(\infty)F(\infty)$. It is clear that the third equation of Eq. (16) results in a convolution solution for $FA(t)$ and that the steady state solutions satisfy the mass action eq. $FA(\infty) = K_{11}A(\infty)F(\infty)$.

It is now convenient to sum the 3 equations in the system of Eq. (16) to obtain

$$\frac{d(F(t) + FC(t) + FA(t))}{dt} = 0 \text{ for all } t \geq 0.$$

This implies $F(t) + FC(t) + FA(t) = \text{a constant for all } t$ and we recognize that the constant is $\text{Tot}F$. Taking the limit as $t \rightarrow \infty$ gives that the steady state solutions satisfy the conservation of mass equation $F(\infty) + FC(\infty) + FA(\infty) = \text{Tot}F$.

All this information implies that that the steady state solutions also satisfy the second and third equations of Eq. (16) above and the corresponding Feldman iteration equations and Feldman equilibrium solutions are the same as the steady state solutions.

Comment. The usual method of setting derivatives equal zero to obtain steady state solutions works here and works more quickly, but the above proof gives steady state solutions directly as limits, which is instructive.

Appendix 2. Descartes' Rule of Signs and existence and uniqueness of iterative solutions

Cartesian side bar: Descartes' Rule of Signs was published in 1637 by Rene Descartes in his work *La Geometrie*. The rule states that if the non-zero terms of a single-variable polynomial with real coefficients are ordered by descending variable exponent then the number of positive roots of the polynomial is either equal to the number of sign changes between consecutive (non-zero) coefficients or is less than it by an even number. A root of multiplicity k is counted as k roots. A corollary is that the

number of negative roots is the number of sign changes after multiplying the coefficients of odd power terms by -1 , or fewer than it by an even number. In 1828, Carl Friedrich Gauss improved the rule by providing the proof that when there are fewer roots of polynomials than there are variations of sign, the difference between the two is even.

End of side bar.

We have shown existence of positive solutions for each of the coupled characteristic polynomials by our Existence Theorem. We need to connect this with the iterative solutions and note that these solutions can exist simultaneously so that we have vector solutions for $P = (P_1, \dots, P_n)$.

Let vector P^ν be the iterations of Eq. (8) and Q^ν be the iterations of Eq. (9). Suppose that the limits $\lim_{\nu \rightarrow \infty} P^\nu = P$ and $\lim_{\nu \rightarrow \infty} Q^\nu = Q$ exist. Writing Feldman's iterative equations as the functions $P^\nu = f(Q^\nu)$ and $Q^\nu = g(P^{\nu-1})$, the composition is $P^\nu = f \circ g(P^{\nu-1})$ and taking limits we obtain $P = f \circ g(P)$, since f , g and $f \circ g$ are continuous functions. This last equation can be solved for P as a system of *coupled* polynomial equations. *Coupled* refers to the fact the coefficients of the polynomial in P_i depend on the other P_k , $k \neq i$. This shows the iterative solutions are the same as the polynomial roots. Note that the commonly used term "root" of a polynomial is a solution of the polynomial set equal to zero.

If we are concerned the limits P and Q may not exist, then we note that each P_i satisfies the inequalities, $0 \leq P_i \leq \text{Tot}P_i$ for $i = 1, \dots, n$, which is a closed (compact) box and the Heine-Borel theorem guarantees at least one limit point P in this box and a subsequence of P^ν 's converging to this P . The same argument as above guarantees that this P satisfies our system of coupled polynomials. In fact, for every limit point this is true. If all the limit points were equal, then the limit exists and is unique. Thus, the uniqueness of the iterative solutions is related to the uniqueness of the polynomial positive roots. So, the only question remaining is: Does the system of polynomial equations have one and only one positive solution? Negative and imaginary solutions of the polynomials are extraneous and not possible limits.

Comment. The existence and uniqueness of solutions of Feldman's iterative equations does not require that we obtain analytic solutions, that is, closed form formula. In fact, analytic solutions are readily available for the roots of polynomials of degree 4 or less, but it has been shown that the general 5th degree polynomials do not have analytic solutions. Most think solutions should be obtained by iterative numerical methods (or perhaps using differential equations). Fortunately, showing existence and uniqueness of solutions does not require analytic solutions.

It is possible to show uniqueness for all $n \times 1$ matrices. Each $m + 1$ degree polynomial is quadratic whose coefficients are in the pattern $(+, 0, -)$ that has precisely one sign change, and Descartes' Rule of Signs says the number of positive roots is one or less by 2 or more. Since having less is not possible, there is exactly one positive root, which is uniqueness. The duality of the iterative equations shows uniqueness for all $1 \times m$ matrices.

Summary. We have now shown that the Feldman iterative solutions are the same as the positive root(s) of the characteristic polynomial(s) and that Feldman iterative solutions are also the same as the steady state solutions of the corresponding differential equations (Appendix 1). We have three separate methods for computing equilibrium values in vitro; and we have established existence and uniqueness of these solutions.

Appendix 3. Degree of characteristic polynomials and singular value decomposition

The degree $(m + 1)$ of the polynomial (see Section 4) has been related to the number of binding proteins (Q_j); however, we can reverse the roles of ligands and BPs and obtain $(n + 1)$ degree polynomial. This points out a slight inaccuracy in the presentation above; the truth relates to the number of $K_{ii} > 0$, which is related to r equals rank of the matrix K ($r = \text{rank}(K)$).

Let us fix the inaccurate discussion above about the degree of the limiting polynomial; is it $(m + 1)$, $(n + 1)$, or $(r = \text{rank}(K))$? Since the rank of K must be less than or equal to $\min(m, n)$ and often is less, the number of positive K_{ii} 's may be less than $(m + 1)$ and $(n + 1)$. We note that the factors of the limiting polynomial for P_i involve the K_{iv} 's in the i^{th} row of K . For the product of linear factors $\prod_{v \neq i} \{K_{iv}P_i + C_{iv}\}$, if $K_{iv} = 0$, then this term becomes a positive constant, and the degree of the polynomial is reduced by one. This is true for every $K_{iv} = 0$ the i^{th} row of K . The result is that the degree of characteristic polynomial in P_i equals $1 + \text{number of positive } K_{iv} \text{ in the } i^{\text{th}} \text{ row of } K$.

For another view of the degree of the characteristic polynomial (in a different space), we will use a matrix version of the Feldman equations and the *singular value decomposition* of the matrix K . This decomposition says every $n \times m$ matrix K can be factored as $K = Q_1 \sum Q_2^T$ where $n \times n$ matrix Q_1 and $m \times m$ matrix Q_2 are each orthogonal ($Q_1^T Q_1 = I_n$ where $I_n = n \times n$ identity matrix I_n and

$Q_2^T Q_2 = I_m$); and where there are $r (= \text{rank}(K))$ positive singular values μ_i which form the diagonal of \sum such that $\sum = \begin{pmatrix} \text{diag}(\mu) & 0 \\ 0 & 0 \end{pmatrix}$. Another way of saying this is

$K = \sum_{i=1}^r \mu_i p_i q_i^T$ where p_i is a left singular $n \times 1$ vector corresponding to μ_i (column of Q_1) and q_i is a right singular $m \times 1$ vector corresponding to μ_i (column of Q_2).

We may need another matrix theory development for Feldman equations. In addition to matrix algebra, we will need the Hadamard (alternatively called Schur) product of two matrices of the same size defined as by elementwise products; that is, $A \odot B = [A_{ij} \cdot B_{ij}]$. Note that Hadamard products are commutative: $A \odot B = B \odot A$; whereas the usual matrix product of square matrices is not generally commutative. The Hadamard (Schur) product of two vectors of the same size is similarly defined as $\lambda \odot v = [\lambda_j \cdot v_j]$. The Schur product of a vector and a matrix follows quickly. We should also define Schur division of vectors $\lambda \oslash v = [\lambda_j / v_j]$ provided $v_j \neq 0$. The Schur product of vectors can be realized in the matrix algebra using square diagonal matrices like $\text{diag}(v)$ whose diagonal is made up of the elements of the vector v and off diagonal entries are all zero: $\lambda \odot v = \text{diag}(v) \lambda = \text{diag}(\lambda) v$. Also, $\text{diag}(v) \mathbf{1} = v$, where $\mathbf{1}$ is a vector with entries all equal to 1. Conversely, $\text{diag}(v)$ can be realized using a Schur product: $\text{diag}(v) = v \odot I = I \odot v$, where I is the usual matrix identity.

Comment. The important part of the Feldman equations in terms of matrix theory involves $\text{diag}(P) K \text{diag}(Q) = [K_{ij} P_i Q_j]$.

The pre-multiplication by $\text{diag}(P)$ can be represented by $P \odot K$, but the post-multiplication by $\text{diag}(Q)$ operates on the columns of K and is not easily represented by the Schur product \odot since the candidate expression of $K \odot Q$ operates on rows by commutativity and not on columns as required. Attempts at two other expressions give $K \text{diag}(Q) = K (Q \odot I)$. This requires a distributive law for computations, which is said not to exist; or alternatively $K \text{diag}(Q) = (Q \odot K^T)^T$, which is also difficult to use in computations.

Feldman Eqs. (1) and (2) with the $n \times m$ matrix K , $n \times 1$ vector $= [P_i]$, and $m \times 1$ vector $Q = [Q_j]$ can be written as

$$\text{diag}(P)\{1_n + K \text{diag}(Q)1_m\} = [\text{Tot}P_i] \quad (18)$$

and

$$\text{diag}(Q)\{1_m + K^T \text{diag}(P)1_n\} = [\text{Tot}Q_j]. \quad (19)$$

These equations look simpler in a vector form than in the matrix form.

$$P + (P \odot K)Q = \text{Tot}P \quad (20)$$

$$Q + (Q \odot K^T)P = \text{Tot}Q \quad (21)$$

But looks are deceiving. In future work, it may be possible to use matrix algebra augmented by Schur multiplication.

Appendix 4. Matrix application to hypothetical example of multiple cortisol binding sites per albumin molecule: reconciliation of mass conservation *per site* and *per molecule* with measured concentrations of total albumin.

Rather than assume simple 1:1 stoichiometry for albumin-cortisol binding, let us consider the more complex, hypothetical scenario where there are three independent cortisol-binding sites per albumin molecule. The per site equilibrium can be also analyzed using the proposed matrix notation. We parse the problem by first discussing per site equilibrium; once the per site equilibrium has been developed, we secondarily discuss per molecule equilibrium. The per site equilibrium is useful to determine the concentration of albumin-bound cortisol using mass action equations, while the per molecule equilibrium is also necessary for conservation of mass equations and relating the solution to clinical measurements in units of mass/volume (of total albumin). In this hypothetical example, let us suppose $\text{Tot}A$ is the concentration of albumin molecules and the 3 cortisol-binding sites per molecule are numbered 1, 2, and 3. Let each site have its own association (affinity) constant, K_{11} , K_{12} , K_{13} , respectively. Let total and free concentration per site be $\text{Tot}A_i$ and A_i , respectively. Relating concentrations to the number of molecules (or site #1) per unit volume justifies the concept of per site concentration. Note that each $\text{Tot}A_i = A_i$. Considering one ligand for this discussion, the 1×4 per site matrix can be drawn as (**Table A1**).

Theorem 1. The Feldman equations for the below matrix become

$$\text{Tot}F = F (1 + K_1C + K_{11}A_1 + K_{12}A_2 + K_{13}A_3)$$

$$\text{Tot}C = C (1 + K_1F)$$

$$\text{Tot}A = A_1(1 + K_{11}F)$$

$$\text{Tot}A = A_2(1 + K_{12}F)$$

$$\text{Tot}A = A_3(1 + K_{13}F)$$

Matrix 1×4 per site	C=CBG	A_1	A_2	A_3	
F	$K_1 C \cdot F$	$K_{11} A_1 \cdot F$	$K_{12} A_2 \cdot F$	$K_{13} A_3 \cdot F$	$TotF$
	$TotC$	$TotA$	$TotA$	$TotA$	

Free albumin concentrations for each site are labeled A_1 , A_2 , and A_3 concentrations, respectively. Here, free albumin concentration at a given site is the number of unbound said sites per unit volume. Note that there is no assumption in Table A1 that the three sites are identical with respect to their cortisol binding affinities (K_{11} , K_{12} , K_{13}). Constraints: Independent binding sites per molecule.

Table A1.
 1×4 matrix per site for 3 independent binding sites on albumin.

Comment 1. We now know that the equation for TotF has 4 columns and that the characteristic polynomial is 5th degree, so there probably is no analytic solution; that is, with formulas that can be evaluated. The general solution for this problem can be obtained by iteration

Comment 2. One might think of using duality because then the 4 equations for 1 TotC and the 3 TotA lead to quadratic polynomials which can be written down. However, the 4 quadratics are coupled with the coefficients depending on unknowns. So, we still need to iterate to find numerical solutions.

Comment 3. Note that according to these Feldman equations, the *per site* free A_i are different if and only if the *per site* affinities K_{1j} are different.

Comment 4. If the 3 sites were identical, then all of the affinities K_{1j} are the same, the A_i are the same and $= F (1 + K_1 C + K_{11} S)$, where $S = 3A_1$ and K_{11} is *per site*. Note also the converse: if K_{1j} are equal then the sites can be considered to be identical. This equation for TotF leads to a cubic solution.

We have shown

Corollary 1. If the sites are identical (with respect to affinities) and independent, then

- i. the affinities for F binding to the 3 sites of Albumin are equal (to K_{11}),
- ii. the three free A_i are equal and define $S = A_1 + A_2 + A_3 = 3A_1$,
- iii. the Feldman equations collapse and with $S = 3 A_1$ and $TotA$ replaced by 3 TotA is represented by the 1×2 matrix (Table A2)

Matrix 1×2 (cubic)	C=CBG	S	
F	$K_1 C \cdot F$	$K_{11} S \cdot F$	$TotF$
	$TotC$	$3 TotA$	

Table A1 is simplified by the summation $S = A_1 + A_2 + A_3$. The identical, independent site assumption implies $S = 3A_1$. This simplification reduces the 1×4 matrix (Table A1) to this 1×2 matrix. Constraints: Independent binding sites and identical binding sites ($K_{11} = K_{12} = K_{13}$).

Table A2.
 1×2 matrix for 3 identical, independent sites simplified by summing the per site free albumin concentrations in Table A1.

- iv. the resulting characteristic polynomial is the cubic equation reported in [4] with TotA replaced by 3TotA.

Proof. Statement ii) is based on algebra and the rest is a matter of recognition.

Corollary 2. If Coolens' assumptions apply, each $K_{1j}F \ll 1$, then each $A_i = \text{Tot}A_i = \text{Tot}A$ and

- i. each $\frac{FA_i}{F} = N_i$ is constant, and
 ii. each $N_j = K_{1j}\text{Tot}A$; and in this case,

the polynomial for the row F becomes Coolen's quadratic equation, which can be solved, provided *Coolens' N* is replaced by $N_1 + N_2 + N_3$.

Proof. Statement i) is based on the Feldman equations $\text{Tot}A = A_i(1 + K_{1j}F) = A_i(1 + 0)$, under Coolen's assumptions. Statement ii) and iii) follow from $\frac{FA_i}{F} = K_{1j}A_i = K_{1j}\text{Tot}A = N_j$.

It is instructive to draw the 1×4 per site matrix for this corollary (**Table A3**) which can be collapsed to a 1×2 matrix (**Table A4**) with the $N = N_1 + N_2 + N_3$. This leads to Coolen's quadratic equation and solution. End of Proof.

Matrix 1×4	C=CBG	A_1	A_2	A_3	
F	$K_1C \cdot F$	$N_1 \cdot F$	$N_2 \cdot F$	$N_3 \cdot F$	TotF
TotC					

The 1×4 matrix per site (Table A1) is simplified by Coolens' approximation to obtain this Table A3. Note that the 3 independent sites are not required to be identical here.

Constraints: Independent binding sites and Coolens' approximations ($K_{1i}A_i \ll 1$, for $i = 1, 2, 3$).

Table A3.

1×4 matrix per site for cortisol binding equilibrium equations with Coolens' approximations.

Matrix 1×2 (quadratic)	C=CBG	S	
F	$K_1C \cdot F$	$N \cdot F$	TotF
TotC			

Applying Coolens' approximations to Table A1 results in three Coolens' N s, i.e. N_1 , N_2 , and N_3 . Thus, without assuming identical sites (and/or identical affinities) Coolens' approximations simplify Table A1 to Table A4 by $S = A_1 + A_2 + A_3$ and $N = N_1 + N_2 + N_3$.

Constraints: Independent binding sites and Coolens' approximations ($K_{1i}A_i \ll 1$, for $i = 1, 2, 3$).

Table A4.

1×2 matrix simplification by summing free albumin's A_1 , A_2 , and A_3 and by summing Coolens' N_1 , N_2 , and N_3 .

We can generalize Corollary 2 to the situation where the multiple sites are different as long as the sites remain independent and Coolens' assumption applies. It is clear from the Feldman equations (Theorem 1) that the per site free albumin $A_i = \text{Tot}A/(1 + K_{1i}F)$ are different and that the Coolens' $N_i = K_{1i}A_i$ are different, all since the affinities K_{1i} are different

Theorem 2. If the albumin molecules have ν independent, possibly non-identical, sites and the Coolens' assumption $\sum_{i=1}^{\nu} K_{1i}F \ll 1$ applies, then

- i. each $A_i = \text{TotA}$ and
- ii. each $\frac{FA_i}{F} = N_i$ is constant, and $N_i = K_{1i} \text{TotA}$
- iii. the per site $1 \times (\nu + 1)$ per site equilibrium matrix (analogous to the above 1×4 matrix) collapses to a 1×2 matrix (as above) where

$$N = \sum_{i=1}^{\nu} N_i = \sum_{i=1}^{\nu} K_{1i} \text{TotA}$$

Proof. If $\sum_{i=1}^{\nu} K_{1i} F \ll 1$ then each $K_{1i} F \ll 1$ and i) is true and $N_i = K_{1i} \text{TotA}$. The Feldman equation for TotF becomes $\text{TotF} = F (1 + K_1 C + N)$.

Probabilistic approach to ligand-protein binding for multisite binding proteins using Boolean logic: Note that the quantity $S = A_1 + A_2 + A_3 = 3A_1$ is not the same as free Albumin (X_A). X_A could be defined as the concentration of albumin molecules for which none of the three cortisol-binding sites of the albumin molecule are occupied (bound). Nonetheless, the cubic solution that results from the above 1×2 matrix is correct. To explain S, we need a further development. A given site is occupied or not, which is a binary outcome. This means concentrations of specific configurations of occupancy of multiple sites are like Boolean subsets and that Boolean algebra applies. Relative concentrations (specific concentration divided by a total concentration) are like probabilities, which means probability theory applies. The Boolean subsets are called events and independence of the sites imply $P(A \cap B) = P(A)P(B)$, though some care is required because probabilities are somewhat site-specific. However, this development is beyond the scope of the present chapter.

Author details


Richard I. Dorin^{1*} and Clifford R. Qualls²

1 New Mexico Veterans Administration Healthcare System, and Departments of Medicine and Biochemistry and Molecular Biology, University of New Mexico, Albuquerque, NM, USA

2 New Mexico Veterans Administration Healthcare System, and Department of Mathematics and Statistics, University of New Mexico, Albuquerque, NM, USA

*Address all correspondence to: rdorin@salud.unm.edu

IntechOpen

© 2024 The Author(s). Licensee IntechOpen. This chapter is distributed under the terms of the Creative Commons Attribution License (<http://creativecommons.org/licenses/by/3.0>), which permits unrestricted use, distribution, and reproduction in any medium, provided the original work is properly cited. 

References

- [1] Bikle D, Bouillon R, Thadhani R, Schoenmakers I. Vitamin D metabolites in captivity? Should we measure free or total 25(OH)D to assess vitamin D status? The Journal of Steroid Biochemistry and Molecular Biology. 2017;**173**:105-116
- [2] Dorin RI, Urban FK 3rd, Perogramvros I, Qualls CR. Four-compartment diffusion model of cortisol disposition: Comparison with 3 alternative models in current clinical use. Journal of the Endocrine Society. 2022; 7(2):bvac173
- [3] Coolens JL, Van Baelen H, Heyns W. Clinical use of unbound plasma cortisol as calculated from total cortisol and corticosteroid-binding globulin. Journal of Steroid Biochemistry. 1987;**26**(2): 197-202
- [4] Dorin RI, Pai HK, Ho JT, Lewis JG, Torpy DJ, Urban FK III, et al. Validation of a simple method of estimating plasma free cortisol: Role of cortisol binding to albumin. Clinical Biochemistry. 2009;**42** (1–2):64-71
- [5] Feldman H, Rodbard D, Levine D. Mathematical theory of cross-reactive radioimmunoassay and ligand-binding systems of equilibrium. Analytical Biochemistry. 1972;**45**(2):530-556
- [6] Feldman HA. Mathematical theory of complex ligand-binding systems of equilibrium: Some methods for parameter fitting. Analytical Biochemistry. 1972;**48**(2):317-338
- [7] Tait JF, Burstein S. *In vivo* studies of steroid dynamics in man. In: Pincus G, Thimann KV, Astwood EB, editors. The Hormones: Physiology, Chemistry and Applications. Vol. V. NY: Academic Press; 1964. pp. 441-557
- [8] Bikle DD. The free hormone hypothesis: When, why, and how to measure the free hormone levels to assess vitamin D, thyroid, sex hormone, and cortisol status. JBMR Plus. 2021;**5**(1): e10418
- [9] Cameron A, Henley D, Carrell R, Zhou A, Clarke A, Lightman S. Temperature-responsive release of cortisol from its binding globulin: A protein thermocouple. The Journal of Clinical Endocrinology and Metabolism. 2010;**95**(10):4689-4695
- [10] Chan WL, Carrell RW, Zhou A, Read RJ. How changes in affinity of corticosteroid-binding globulin modulate free cortisol concentration. The Journal of Clinical Endocrinology and Metabolism. 2013;**98**(8):3315-3322
- [11] Meyer EJ, Nenke MA, Rankin W, Lewis JG, Torpy DJ. Corticosteroid-binding globulin: A review of basic and clinical advances. Hormone and Metabolic Research. 2016;**48**(6):359-371
- [12] Nenke MA, Nielsen ST, Lehrskov LL, Lewis JG, Rankin W, Moller K, et al. Pyrexia's effect on the CBG-cortisol thermocouple, rather than CBG cleavage, elevates the acute free cortisol response to TNF-alpha in humans. Stress. 2017;**20**(2):183-188
- [13] Vogeser M, Briegel J. Effect of temperature on protein binding of cortisol. Clinical Biochemistry. 2007;**40** (9–10):724-727
- [14] Dunn JF, Nisula BC, Rodbard D. Transport of steroid hormones: Binding of 21 endogenous steroids to both testosterone-binding globulin and corticosteroid-binding globulin in human plasma. The Journal of Clinical

Endocrinology and Metabolism. 1981;
53(1):58-68

[15] Stroupe SD, Gray RD, Westphal U. Steroid-protein interactions. Kinetics of binding of cortisol and progesterone to human corticosteroid-binding globulin. *FEBS Letters*. 1978;**86**(1): 61-64

[16] Stroupe SD, Harding GB, Forsthoefel MW, Westphal U. Kinetic and equilibrium studies on steroid interaction with human corticosteroid-binding globulin. *Biochemistry*. 1978;
17(1):177-182

[17] Westphal U. Steroid-Protein Interactions. In: *Monographs on Endocrinology*. II, Vol. 27. New York, NY: Springer-Verlag; 1971

[18] Colombo S, Buclin T, Decosterd LA, Telenti A, Furrer H, Lee BL, et al. Orosomucoid (alpha1-acid glycoprotein) plasma concentration and genetic variants: Effects on human immunodeficiency virus protease inhibitor clearance and cellular accumulation. *Clinical Pharmacology and Therapeutics*. 2006;**80**(4):307-318

[19] Gudmand-Hoeyer J, Ottesen JT. Analysis and validation of a new extended method for estimating plasma free cortisol including neutrophil elastase and competition from other steroids. *The Journal of Steroid Biochemistry and Molecular Biology*. 2018;**181**:109-124

[20] Nguyen PT, Lewis JG, Sneyd J, Lee RS, Torpy DJ, Shorten PR. Development of a formula for estimating plasma free cortisol concentration from a measured total cortisol concentration when elastase-cleaved and intact corticosteroid binding globulin coexist. *The Journal of Steroid Biochemistry and Molecular Biology*. 2014;**141**:16-25

[21] Hodyl NA, Stark MJ, Meyer EJ, Lewis JG, Torpy DJ, Nenke MA. High binding site occupancy of corticosteroid-binding globulin by progesterone increases fetal free cortisol concentrations. *European Journal of Obstetrics, Gynecology, and Reproductive Biology*. 2020;**251**:129-135

[22] Rohatagi S, Barth J, Mollmann H, Hochhaus G, Soldner A, Mollmann C, et al. Pharmacokinetics of methylprednisolone and prednisolone after single and multiple oral administration. *Journal of Clinical Pharmacology*. 1997;**37**(10):916-925

[23] Gardill BR, Vogl MR, Lin HY, Hammond GL, Muller YA. Corticosteroid-binding globulin: Structure-function implications from species differences. *PLoS One*. 2012;
7(12):e52759

[24] Klieber MA, Underhill C, Hammond GL, Muller YA. Corticosteroid-binding globulin, a structural basis for steroid transport and proteinase-triggered release. *The Journal of Biological Chemistry*. 2007;**282**(40): 29594-29603

[25] Simard M, Hill LA, Lewis JG, Hammond GL. Naturally occurring mutations of human corticosteroid-binding globulin. *The Journal of Clinical Endocrinology and Metabolism*. 2015;
100(1):E129-E139

[26] Simard M, Underhill C, Hammond GL. Functional implications of corticosteroid-binding globulin N-glycosylation. *Journal of Molecular Endocrinology*. 2018;**60**(2):71-84

[27] Lewis JG, Bagley CJ, Elder PA, Bachmann AW, Torpy DJ. Plasma free cortisol fraction reflects levels of functioning corticosteroid-binding

globulin. *Clinica Chimica Acta*. 2005;**359** (1–2):189-194

[28] Westphal U, Firschein HE, Pearce EM. Binding of hydrocortisone-4-C14 and progesterone-4-C14 to serum albumin, demonstrated by paper electrophoresis. *Science*. 1955;**121**(3147): 601-602

[29] Yamamoto M, Ariyoshi Y, Matsui N. The serum concentrations of unbound, transcortin bound and albumin bound cortisol in patients with dysproteinemia. *Endocrinologia Japonica*. 1982;**29**(5): 639-646

[30] Zheng X, Bi C, Brooks M, Hage DS. Analysis of hormone-protein binding in solution by ultrafast affinity extraction: Interactions of testosterone with human serum albumin and sex hormone binding globulin. *Analytical Chemistry*. 2015; **87**(22):11187-11194

[31] Mendel CM. The free hormone hypothesis: A physiologically based mathematical model. *Endocrine Reviews*. 1989;**10**(3):232-274

[32] Mendel CM. The free hormone hypothesis. Distinction from the free hormone transport hypothesis. *Journal of Andrology*. 1992;**13**(2):107-116

[33] Mendel CM, Miller MB, Siiteri PK, Murai JT. Rates of dissociation of steroid and thyroid hormones from human serum albumin. *The Journal of Steroid Biochemistry and Molecular Biology*. 1990;**37**(2):245-250

[34] Pardridge WM. Transport of protein-bound hormones into tissues *in vivo*. *Endocrine Reviews*. 1981;**2**(1): 103-123

[35] Bikle DD, Gee E. Free, and not total, 1,25-dihydroxyvitamin D regulates 25-hydroxyvitamin D metabolism by

keratinocytes. *Endocrinology*. 1989; **124**(2):649-654

[36] Bolton JL, Hayward C, Direk N, Lewis JG, Hammond GL, Hill LA, et al. Genome wide association identifies common variants at the SERPINA6/SERPINA1 locus influencing plasma cortisol and corticosteroid binding globulin. *PLoS Genetics*. 2014;**10**(7): e1004474

[37] Lee JH, Meyer EJ, Nenke MA, Falhammar H, Torpy DJ. Corticosteroid-binding globulin (CBG): Spatiotemporal distribution of cortisol in sepsis. *Trends in Endocrinology and Metabolism*. Mar 2023;**34**(3):181-190

[38] Crawford AA, Bankier S, Altmaier E, Barnes CLK, Clark DW, Ermel R, et al. Variation in the SERPINA6/SERPINA1 locus alters morning plasma cortisol, hepatic corticosteroid binding globulin expression, gene expression in peripheral tissues, and risk of cardiovascular disease. *Journal of Human Genetics*. 2021;**66**(6):625-636

[39] Lin HY, Underhill C, Lei JH, Helander-Claesson A, Lee HY, Gardill BR, et al. High frequency of SERPINA6 polymorphisms that reduce plasma corticosteroid-binding globulin activity in Chinese subjects. *The Journal of Clinical Endocrinology and Metabolism*. 2012;**97**(4):E678-E686

[40] Hill LA, Sumer-Bayraktar Z, Lewis JG, Morava E, Thaysen-Andersen M, Hammond GL. N-glycosylation influences human corticosteroid-binding globulin measurements. *Endocrine Connections*. 2019;**8**(8):1136-1148

[41] Hill LA, Vassiliadi DA, Dimopoulou I, Anderson AJ, Boyle LD, Kilgour AHM, et al. Neutrophil elastase-cleaved corticosteroid-binding globulin

is absent in human plasma. *The Journal of Endocrinology*. 2019;**240**(1):27-39

[42] Perogamvros I, Underhill C, Henley DE, Hadfield KD, Newman WG, Ray DW, et al. Novel corticosteroid-binding globulin variant that lacks steroid binding activity. *The Journal of Clinical Endocrinology and Metabolism*. 2010;**95**(10):E142-EE50

[43] Boonen E, Meersseman P, Vervenne H, Meyfroidt G, Guiza F, Wouters PJ, et al. Reduced nocturnal ACTH-driven cortisol secretion during critical illness. *American Journal of Physiology. Endocrinology and Metabolism*. 2014;**306**(8):E883-EE92

[44] Kerkay J, Westphal U. Steroid-protein interactions. XIX. Complex formation between alpha 1-acid glycoprotein and steroid hormones. *Biochimica et Biophysica Acta*. 1968;**170**(2):324-333

[45] Mazer NA. A novel spreadsheet method for calculating the free serum concentrations of testosterone, dihydrotestosterone, estradiol, estrone and cortisol: With illustrative examples from male and female populations. *Steroids*. 2009;**74**(6):512-519

[46] Rohatagi S, Hochhaus G, Mollmann H, Barth J, Derendorf H. Pharmacokinetic interaction between endogenous cortisol and exogenous corticosteroids. *Die Pharmazie*. 1995;**50**(9):610-613

[47] Emptoz-Bonneton A, Cousin P, Seguchi K, Avvakumov GV, Bully C, Hammond GL, et al. Novel human corticosteroid-binding globulin variant with low cortisol-binding affinity. *The Journal of Clinical Endocrinology and Metabolism*. 2000;**85**(1):361-367

[48] Rosenthal HE, Slaunwhite WR Jr, Sandberg AA. Transcortin: A

corticosteroid-binding protein of plasma. X. Cortisol and progesterone interplay and unbound levels of these steroids in pregnancy. *The Journal of Clinical Endocrinology and Metabolism*. 1969;**29**(3):352-367

[49] Dorr HG, Heller A, Versmold HT, Sippell WG, Herrmann M, Bidlingmaier F, et al. Longitudinal study of progestins, mineralocorticoids, and glucocorticoids throughout human pregnancy. *The Journal of Clinical Endocrinology and Metabolism*. 1989;**68**(5):863-868

[50] Abou-Samra AB, Pugeat M, Dechaud H, Nachury L, Bouchareb B, Fevre-Montange M, et al. Increased plasma concentration of N-terminal beta-lipotrophin and unbound cortisol during pregnancy. *Clinical Endocrinology*. 1984;**20**(2):221-228

[51] Doe RP, Dickinson P, Zinneman HH, Seal US. Elevated nonprotein-bound cortisol (NPC) in pregnancy, during estrogen administration and in carcinoma of the prostate. *The Journal of Clinical Endocrinology and Metabolism*. 1969;**29**(6):757-766

[52] Barlow NL, Holme J, Stockley RA, Clark PM. An evaluation of measured and calculated serum free cortisol in a group of patients with known adrenal suppression. *Annals of Clinical Biochemistry*. 2010;**47**(Pt 3):200-204

[53] Vogeser M, Mohnle P, Briegel J. Free serum cortisol: Quantification applying equilibrium dialysis or ultrafiltration and an automated immunoassay system. *Clinical Chemistry and Laboratory Medicine*. 2007;**45**(4):521-525

[54] Dorin R, Urban III FK, Qualls C. Influence of cortisol concentration on the relationship between aldosterone

secretion rate and aldosterone concentration: Modeling and simulation. In: Endocrine Reviews. Vol. 38, No. 3 (Supplement). Oxford, UK: Oxford University Press; Jun 2017. p. 600

[55] Zager G, Burtis WJ, Luetscher JA, Dowdy AJ, Sood S. Increased plasma protein binding and lower metabolic clearance rate of aldosterone in plasma of low cortisol concentration. The Journal of Clinical Endocrinology and Metabolism. 1976;**42**(2):207-214

[56] Zipser RD, Speckart PF, Zia PK, Edmiston WA, Lau FY, Horton R. The effect of ACTH and cortisol on aldosterone and cortisol clearance and distribution in plasma and whole blood. The Journal of Clinical Endocrinology and Metabolism. 1976;**43**(5):1101-1109

[57] Pugeat MM, Dunn JF, Nisula BC. Transport of steroid hormones: Interaction of 70 drugs with testosterone-binding globulin and corticosteroid-binding globulin in human plasma. The Journal of Clinical Endocrinology and Metabolism. 1981; **53**(1):69-75

[58] Dorin RI, Perogamvros I, Qualls C. Distribution of cortisol in human serum *in vitro*: Role of competitive ligand-protein interactions in women on oral contraceptives. In: Journal of the Endocrine Society. Vol. 7, No. Supplement_1. Oxford, UK: Oxford University Press; Oct-Nov 2023. p. A76

[59] Perogamvros I, Aarons L, Miller AG, Trainer PJ, Ray DW. Corticosteroid-binding globulin regulates cortisol pharmacokinetics. Clinical Endocrinology. 2011;**74**(1):30-36

[60] Jayaraj A, Schwanz HA, Spencer DJ, Bhasin S, Hamilton JA, Jayaram B, et al. Allosterically coupled multisite binding

of testosterone to human serum albumin. Endocrinology. 2021;**162**(2):bqaa199

[61] Matsui N, Yamamoto M, Seo H, Niinomi M, Ariyoshi Y. Determination of serum cortisol fractions by isocolloidismolar equilibrium dialysis. Changes during pregnancy. Endocrinologia Japonica. 1979;**26**(2): 263-273

[62] Vermeulen A, Verdonck L, Kaufman JM. A critical evaluation of simple methods for the estimation of free testosterone in serum. The Journal of Clinical Endocrinology and Metabolism. 1999;**84**(10):3666-3672

[63] Bouillon R, Schuit F, Antonio L, Rastinejad F. Vitamin D binding protein: A historic overview. Frontiers in Endocrinology (Lausanne). 2019;**10**:910

Glucocorticoid Ablation Restores Glycemic and Thermogenic Parameters in Obesity

Orien L. Tulp

Abstract

Glucocorticoid ablation following adrenalectomy resulted in restoration of the impaired non-shivering thermogenesis and impaired glucose tolerance and insulin resistance in obese LA/Ntvl//*-cp* rats. This is a congenic rat strain where the only difference between the lean and obese phenotypes was the presence of the epigenetic expression of obesity in an NIDDM-free animal model. Groups of young adult obese animals were adrenalectomized, followed by thermogenesis and glycemic assessment thereafter. In an additional subgroup, animals were administered insulin daily in an attempt to maintain the insulin resistance state. Adrenalectomy resulted in a complete restoration of normal resting and norepinephrine stimulated thermogenesis and an amelioration of the glycemic parameters of insulin resistance.

Keywords: obesity, insulin resistance, metabolomics, overnutrition, congenic rat, adrenalectomy

1. Introduction

The development of overweight and obese conditions is commonly associated with insulin resistance in man and animals along with multiple associated pathophysiologic comorbidities. Among the comorbidities, the insulin resistance of obesity and overweight conditions is strongly associated with numerous common pathophysiologic sequelae including but not limited to non-insulin dependent diabetes (NIDDM), hypertension (HTN), stroke, renal complications, certain cancers, musculoskeletal, and cardiovascular disorders to cite just a few of the possible complications that may develop over time. The prevalence of obesity and overweight conditions is increasing at an alarming rate in Westernized populations, with the onset now beginning at earlier ages than in past generations [1–3].

The LA/Ntvl//*-cp* rat model is a unique congenic animal model of epigenetic obesity. The initial expression of the obese stigmata typically begins by 5 to 6 weeks of age, where the affected offspring begin to express the stigmata, including an altered gait and outward more rounded appearance [4, 5]. The only obvious genetic difference between the lean and obese phenotypes is the autosomal recessive expression of the obesity (*-cp*) trait in one quarter of the offspring of heterozygous breeding pairs. Therefore all other inherited characteristics being equal, this rat strain is an excellent

animal model to investigate the metabolic processes contributing to the development of an obese state and its pathophysiologic complications [4, 6]. The obese phenotype typically develop hyperinsulinemia and insulin resistance, elevations in plasma amylin, and disordered glycemic response to carbohydrate loading by early adulthood in both sexes, but have been found to remain free of diabetes of either type throughout most or all of their projected lifespan [4, 5, 7, 8]. Dysregulation of glucocorticoid actions have also been found in obesity and overweight conditions, where they provide further impairments in the regulation of glucose uptake and glycemic status, and contribute to the magnitude of glucose intolerance and impaired thermogenesis, which like other aspects of glucose oxidation is dependent on efficient glucose uptake in brown adipose tissue for expression of BAT-mediated elements of nonshivering thermogenesis [2–16]. The closely related SHR/Ntul//*-cp* strain share the same genetic trait for obesity (the *-cp* trait) but unlike the LA/Ntul//*-cp* strain, the SHR/Ntul//*-cp* strain also develops symptoms of moderate to severe NIDDM in both sexes by early adulthood. In both strains the obesity trait was obtained from the Koletsky rat and purified via multiple rounds of back-crossing to attain the congenic status, whereby the only known apparent surviving trait from the Koletsky origin was the evidence of the expression of the autosomal recessive obesity (*-cp*) trait [10–19]. To date, the obese of both *-cp* strains have not been observed to reproduce due to unknown endocrinologic or other factors, similar to that which has been observed in other autosomal recessive obese rodent strains although the histologic presence of spermatozoa in obese LA/Ntul//*-cp* rats has been reported [20]. In addition, the obese phenotype of the LA/Ntul//*-cp* rats also exhibit an impaired thermogenic response to caloric overnutrition induced by the cafeteria diet and other thermogenic regimens, and which has been observed to persist throughout most if not all of the projected lifespan in the obese phenotype of this strain [4, 6, 8, 14–16].

While the specific biochemical mechanisms that contribute to the impaired capacity for non shivering thermogenesis and caloric expenditure in the obese phenotype remain unclear, the thermogenic defect is presumed to contribute to their enhanced caloric efficiency and contribute at least in part to their propensity for excess fat accretion and storage in adipose tissue depots. Dysregulation of glucocorticoid actions involving the insulin-dependent GLUT4 transporters and insulin insensitivity in addition to impaired thyroidal and sympathetic actions have been reported in the obese of several strains, and likely contribute a role in this animal model as well [9–12, 20–23]. Regardless of the energy mechanisms involved, the LA/Ntul//*-cp* rat strain ranks among the longest surviving obese rat strains known due to the longevity-prone Lister/Albany/NIH background, with the lean phenotype often surviving to 4 years or more and the obese littermates to 2.5 to 3 years under standard laboratory conditions [16–19]. The current investigation was designed to further elucidate the mechanisms of carbohydrate intolerance and its association with impaired nonshivering thermogenesis, and to determine if the metabolic derangements were associated with the expression of the obese trait in this rat strain. Rats were studied from the earliest visible onset of the expression of the obese trait throughout postweaning development and early adulthood. Rats typically become of reproductive age in the lean phenotype by early adulthood, but reproductive activity has not been observed in the obese phenotype. These physiologic developments occur at an age at which the onset of metabolic evidence of insulin resistance in the obese phenotype will have developed [20]. Michaelis et al. have demonstrated that the obese phenotype of this strain demonstrate little if any glycosuria throughout much of their normal lifespan despite the carbohydrate source in the diet being fed [7, 24].

In human populations, familial syndromes of obesity and NIDDM often occur together, suggesting a possible genetic predisposition in their development, and consistent with an implication of a receptor defect in insulin actions, including possible dysregulation of the GLUT4 transporter system. However, the magnitude of the expression of the obesity and NIDDM parameters may differ in their molecular mechanisms in the two disorders. The -cp trait for obesity was originally derived from the Koletsky rat, and bred into the NIH colony of the SHR rat, followed by 12 or more cycles of backcrossing, whereby the resulting obese offspring exhibit NIDDM by early adulthood. The metabolic basis for the development of NIDDM has been presumed to occur due to a combination of a receptor and postreceptor linked activity in carbohydrate metabolism implicating the insulin receptor. In contrast, when the same -cp trait was bred into the LA/N strain, the obese offspring developed moderate insulin resistance but not NIDDM, suggesting that the impairment in insulin action in that substrain survived as a receptor mediated effect only [6, 7, 17, 19, 25]. In the current investigation, the experimental design was developed in an attempt to further elucidate key parameters resulting in the epigenetic expression of obesity, to include the potential impact of the counterregulatory effects of adrenal glucocorticoid hormones on thermogenic and glycemic parameters.

2. Methods and materials

The rats for this investigation were obtained from Drexel University at 6 weeks of age. Rats were designated as lean or pre-obese on the basis of visible observation of emerging obese stigmata. The animals consisted of normally reared lean and obese male animals as biological littermates (1 lean plus 1 obese, $n = 6$ rats/treatment group). The preobese rats were selected based on physical characteristics, including typical indicators of changes in gait, stance, and palpable subcutaneous fat combined with lower resting VO_2 measures than occurred in their lean littermates [6]. The animals that were selected from the above criterion were placed in shoebox cages lined with one inch of fresh pine shavings, changed periodically 3 times a week, and housed under standard laboratory conditions from 6 until 12 weeks of age. Room temperatures were maintained at 22–24°C with controlled humidity of 50 to 60% relative humidity. All animals received free access to Purina Chow #5012 and house water throughout, beginning at weaning (21 days of age) and continuously throughout the remainder of the study. Purina chow formula # 5012 manufacturers certificate of analysis reported an energy density of 3.34 kcal/gram. The detailed composition lacked refined carbohydrates and was indicative of a low glycemic index. When animals were 9 to 12 weeks of age during the final 3 weeks of the study they were offered the highly palatable cafeteria (Café) diet thereafter in addition to the Purina chow diet. The Café regimen consisted of a rotation of four tasty items each day out of 20 total Café food items. The quantities of all foods consumed were carefully recorded after correction for spillage and uneaten residuals. The twenty different Café foods that were provided in the daily master menu included at least one reliable nutritive protein source.

The daily caloric intakes were determined periodically during the 6-week study. Each animal was placed in an individual metabolic cage for 3 days, during which time all total food that had been consumed was tabulated, measured by weight, corrected for spillage, and resulting caloric intake during the final 2 days, while the data obtained during the first day discarded, thus enabling the individually housed

animals to acclimate to the change in environment of the metabolic cages. The Purina chow was ground in a homogenizer for ease in determining the accuracy of measurement throughout the duration of the study. The groups of animals were also offered the highly palatable cafeteria (Café) diet in addition to the Purina chow during weeks 9 through 12. The Café diet included numerous typical ‘finger foods’ such as snack items that included Oreo and peanut butter cookies, assorted sweets and sugary confections, hot dogs, white bread, popcorn, etc., and totals consumed corrected to account for wastage and uneaten residues each day. The net caloric intake was determined from the manufacturer’s published nutritional information for each individual food item consumed. Thus, the caloric intake reported includes the total Purina Chow plus the Café food items consumed after correction for spillage and uneaten remnants.

Determination of the Resting Metabolic Rates (RMR). Measurement of the RMR of lean and obese rats were determined in the fasted state. Measures of RMR were obtained with a Collins Small Animal Spirometer apparatus (WE Collins, Braintree MA, USA) fitted with a locally manufactured closed circuit 1 cubic foot volume watertight Plexiglas animal chamber [6, 8, 26–28]. All measures of VO₂ were conducted at thermal neutrality (30°C) by immersing the sealed canister in a constant temperature water bath, allowed to equilibrate for up to 15 min, and the temperature was kept constant by immersing the animal chamber in the temperature controlled circulating water bath. The data was corrected for conditions of local altitude and relative humidity, and expressed per kg of body weight^{0.75} power to correct for potential differences in body composition and surface area [6, 8, 26–28]. Typically, with this procedure, animals were observed to explore their new surroundings for 2 to 3 min upon initial placement in the submersible chamber, after which time they were observed to be resting comfortably during equilibration of the system and for the remainder of their occupation and measurement of RMR in the chamber. Reliable measures were typically obtained within 15 min of observation and continued for an additional 15 min segment. Animals were familiarized with the procedure prior to obtaining measure of record to minimize the effects of stress or training issues on the final results. Significant differences in body weights and this metabolizing tissues were observed in the two phenotypes due to the drastic differences in actual body composition due to the obesity [6].

Adrenalectomy. A partial (hemi-) or complete adrenalectomy (Hemi-ADX/ADX) was performed in groups (n = 6 rats/group) of pre-obese rats as described by Marchington et al. In this procedure rats were subjected to pentobarbital anesthesia (5.5 mg/kg BW, intraperitoneally) when 6 weeks of age [29]. Briefly, the surgical procedure consisted of a single 1 to 1.5 cm mid-posterior incision, and the adrenals located by palpation and inspection followed by surgical removal *in toto*. The animals warmed on an electronic heating pad during and after the surgical procedure to prevent anesthesia-induced post-surgical hypothermia. Animals were given a 0.9% NaCl solution supplement *ad libitum* in addition to house water following adrenal surgery. An additional group received a hemi-adrenalectomy and were treated exactly the same as the obese and bilateral adrenalectomy groups were treated. A final subgroup (n = 4) of adrenalectomized rats received a daily Lente insulin injection, starting at 1 U / day and ramping up to a max of 8 u/day on the final day of the study in an attempt to continue the magnitude of insulin resistance in the absence of the adrenal secretions. Animals were closely monitored daily, and were observed to survive the surgical procedure without difficulty. During the final dissection, the completeness of the adrenalectomy procedure was determined by inspection to confirm the presence

of one or no remaining adrenal tissue remnants. All groups had 6 rats / group at the onset, but in the Obese+ADX + Ins group only 4 rats remained at 12 weeks of age, as some animals inadvertently succumbed due to apparent hypoglycemia during fasting and thus their data was not included in the final data computations.

Measures of glycemic status. Measures of glycemic status included a) an oral glucose tolerance (OGT), plasma insulin (I), glucose (G) and the computing the I:G ratio of rats. In addition, the area under the OGT curve (AUC) was computed as previously described [7, 30]. The measures of oral glucose tolerance (OGT) were performed in 8-h fasted animals as outlined by Tulp et al. [30]. The glucose challenge consisted a measured quantity based on body weight of a 50% glucose solution (25 mg glucose/kg BW) administered slowly via gavage over a 1-min duration in fasting animals via oral gavage. Periodic bloods were obtained for measurement of blood glucose concentration from the tail vein in heparinized capillary tubes initially and at the 30-, 60-, 90 and 120-min post gavage. The bloods were subjected to plasma glucose determination with a glucose oxidase method, and recorded as mg/dl [30]. The AUC for the glucose curve from 0 to 120 min was calculated as described previously [30]. Upon sacrifice, truncal blood were collected for measures of fasting glucose and insulin. Insulin concentrations were determined via solid phase radioimmunoassay. Data were analyzed via standard descriptive statistics, ANOVA, and Students unpaired t tests [31]. This study was reviewed and approved by Institutional IACUC (Institutional Animal Care and Use Committee prior to the investigation.

3. Results

The initial and final body weights of rats are depicted in **Figure 1** at each age studied. These data show that the body weights of all groups were similar upon assignment to the respective treatment groups. In contrast, at 12 weeks of age, the obese and adrenalectomized obese rats were observed to be significantly greater than those of their unoperated lean littermates. Since all groups had the same genetic background the same diets and were housed under identical laboratory conditions with

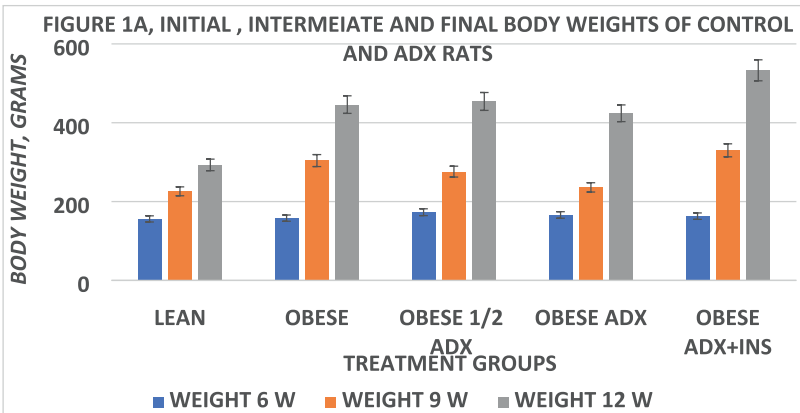


Figure 1. Body weights of rats at 6, 9 and 12 weeks of age. Data are mean \pm 1 SEM, n=4-6 rats/treatment group. $P < 0.05$ obese vs. lean at each age studied. All groups were observed to gain weight with age ($p < 0.05$, students T test for paired comparisons).

the exception of the autosomal recessive expression of the *-cp* trait, the differences in final body weights and weight gain following ADX are considered significant.

When adrenalectomized obese rats were 9 weeks of age midpoint and prior to the addition of the Café diet however, their body weights were still similar to those of their lean littermates. Upon introduction of the Café diet regimen however, the obese adrenalectomized rats exhibited significant hyperphagia. The hyperphagia was followed by additional weight gain that was equal to or greater than their unoperated obese littermates by the culmination of the study at 12 weeks of age. The final data point for body weights is indicated in **Figures 2–4** in **Figure 5**, the mean weight gain between 6 and 9 weeks of age is depicted and indicates that weight gain in both lean and obese-ADX rats was similar, averaging 70 grams per rat. However as noted, when the obese+adx group consumed the Café regimen, their weight gain during the final 3 weeks of the study significantly exceeded that of their lean littermates by a factor of 2.75. This rate of weight

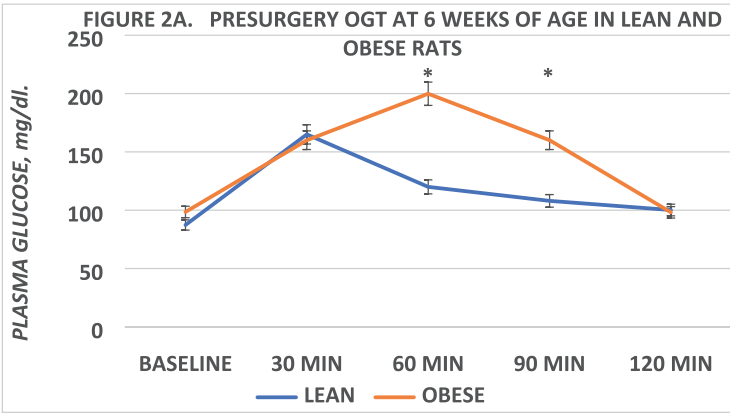


Figure 2.
*Oral Glucose tolerance Test in lean and obese rats at 6 weeks of age. Data are mean \pm 1 SEM. * = $P < 0.05$ (Lean Vs Obese) at 60 and 90 min. $P = n.s.$ at baseline, 30 and 120 min. *Comparisons by unpaired Student's *t* test.*

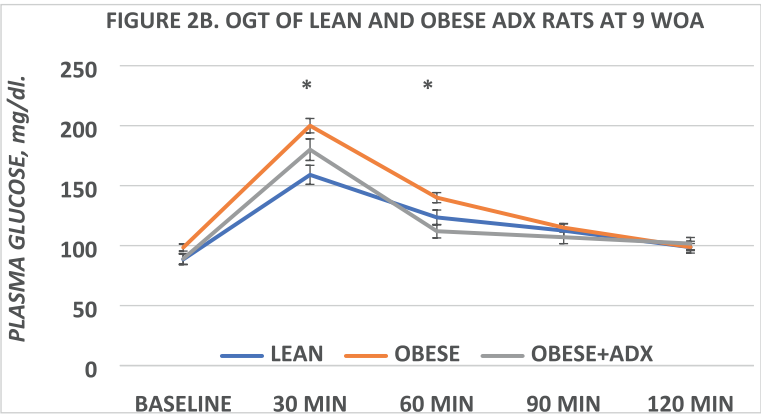


Figure 3.
*The effect of ADX on glycemic responses at 9 weeks of age. The data are mean \pm 1 SEM, $n = 6$ rats/group. The plasma glucose and postprandial absorptive phase of obese rats were significantly greater than the other groups at +30 and + 60 min ($p < 0.05$; students unpaired *t* test). WOA = weeks of age.*

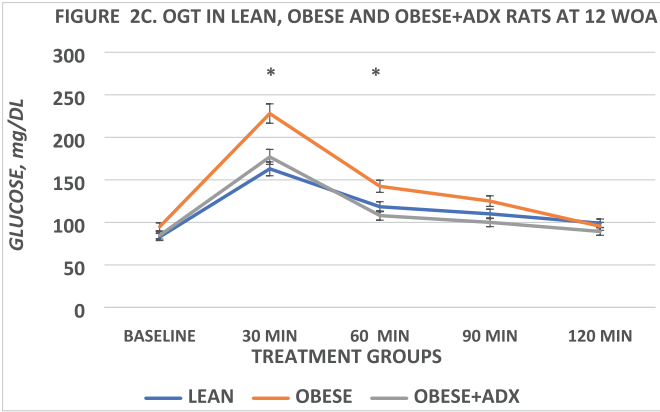


Figure 4. Effect of ADX and diet on glycemic excursions at 12 weeks of age. Data are mean \pm 1 SEM, $n = 6$ rats/group. The glycemic responses of the obese rats were significantly greater than the other groups at +30 and +60 min ($p = < 0.05$; students unpaired t test). WOA = weeks of age. OGT obtained after 3 weeks of the Caf \acute{e} diet regimen. Note the difference in the vertical axis in **Figure 4** vs. **Figures 2 or 3** (0 to 300 in 4 vs. 0 to 250 mg/dl in 2 and 3).

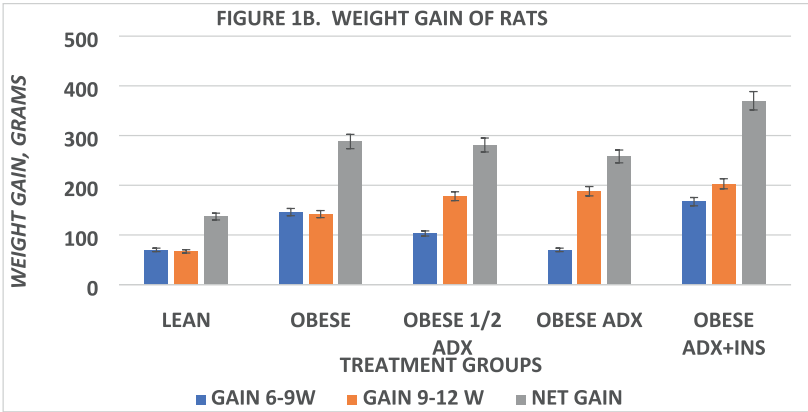
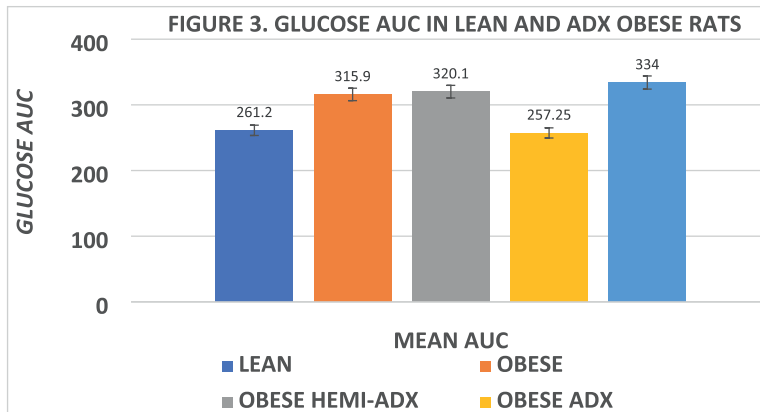


Figure 5. Weight gain of rats at 6, 9 and 12 weeks of age. Data are mean \pm 1 SEM, 4–6 rats/group. $P = < 0.05$ (lean vs. obese, Student's unpaired t test) at each age studied. In addition, all groups gained weight between 6 and 12 weeks of age ($p = < 0.05$, students paired comparisons t test).

gain was similar to a 2.7-fold greater rate of weight gain in the unoperated obese group. Thus, those rats attained a final rate of weight gain that measured equal to or greater than that which was observed among the other experimental groups.

The measures of Oral Glucose tolerance are depicted in **Figures 2–4** and the and the glucose area under the glucose curves (the AUC_{glucose}) is depicted in **Figure 6**. These data are consistent with a prolonged glycemic response in the obese phenotype that also included a greater magnitude of glycemic excursion at the highest glucose concentrations observed than occurred in their similarly treated lean littermates. These observations are suggestive of a prolonged absorptive phase in the obese phenotype. When 9 weeks of age, the glycemic responses and the AUC_{glc} in the obese+ADX rats were now similar to their unoperated lean littermates, while only the untreated obese remained elevated. At 12 weeks of age, as depicted in **Figure 4**, the glycemic excursions in the lean

**Figure 6.**

Mean glucose AUC from 4-point OGT at 12 weeks of age. Data are the mean \pm 1 SEM, N = 4–6 RATS/GROUP. Bars computed from of plasma glucose values depicted in **Figure 4** above. Obese, obese + hemi-ADX and obese + ADX+ insulin is similar (n.s) while glucose AUC of lean and obese + ADX are similar. Presurgical AUCglc at 6 weeks of age from **Figure 2** was 264 vs. obese 312. Numerical values above each bar above are the mean AUC at 12 weeks of age.

and adrenalectomized obese rats remained of similar magnitude. The unoperated obese continued to demonstrate a deranged glycemic response at 12 weeks of age, consistent with a prolonged absorptive phase, but glycosuria was absent, as was diagnostic criterion indicative of NIDDM.

The data reflecting ADX of obese rats at 12 weeks of age is shown in **Figure 4** above. The glycemic responses in the unoperated lean and in the obese+ADX groups are similar, reflecting a normalization of the glycemic responses in the obese animals following the ADX procedure. In contrast, the glycemic responses in the unoperated obese animals continue to indicate modest glucose dysregulation, with peak glucose concentrations exceeding 200 mg/dl at the 30-min data point but returning to pre-glucose administration plasma concentrations at the 120-min time point in all groups including the unoperated obese, Café fed animals.

The final glycemic parameters including plasma glucose, plasma insulin, and the Insulin to glucose ratio as an estimate of insulin resistance are shown in **Table 1** and indicate that fasting plasma glucose concentrations were similar in all groups, with a trend toward elevations in plasma glucose in the Obese+ADX + Insulin group. The greater value in the insulin groups is reflective of their non-fasting state, as fasting in that group resulted in premature hypoglycemic deaths of some animals. Plasma insulin concentrations were markedly elevated in the obese phenotype but were similar to those of lean animals following complete adrenalectomy. In contrast, hemi-adrenalectomy resulted in plasma insulin concentrations that were similar to unoperated obese rats, while administration of exogenous insulin resulted in yet still greater plasma insulin concentrations and insulin to glucose ratios, indicative of insulin resistance in those animals.

The mean AUCglc of the different groups at 12 weeks of age is shown in **Figure 6**, in addition to the numerical mean above each bar. Note that the AUCglc of the unoperated lean and the obese+ADX AUCglc are virtually identical (261.2 vs. 257.25, respectively), indicating the ADX procedure resulted in a virtual normalization in the glycemic responses. In contrast, the final AUCglc in the obese, Obese+hemiADX and the Obese+ADX + Insulin are similar, (315.9, 320.1 and 334.0 respectively), and consistent with insulin resistance of similar magnitude in the 3 groups.

Group	n	Glucose	Insulin	I:G ratio
Lean	6	144.0 ± 9.0 ^a	253 ± 20 ^a	1.43 ± 0.16 ^a
Obese	6	145.5 ± 15.7 ^a	874 ± 30 ^b	6.01 ± 1.40 ^b
Obese Hemi-ADX	4	141.0 ± 27.0 ^a	1060 ± 41 ^b	7.52 ± 1.5 ^b
Obese-ADX	6	126.3 ± 4.9 ^a	299.5 ± 71.5 ^a	2.40 ± 1.08 ^a
Obese ADx + INS	3	223.0 ± 21.0 ^b	1941 ± 110 ^{c#}	8.70 ± 1.8 ^{b#}
ANOVA		ns [#]	p = <0.05	p = <0.05

Effects of ADX and diet on glycemic parameters of lean and obese rats at 12 weeks of age. All data are reported as the mean ± 1 SEM (n = 6 rats/group). Truncal bloods were collected in heparin at 12 weeks of age. Rats in a semi-fasted (2–4 h) state. Different subscript letters denote distinct statistical subgroups via Student-Neuman-Keuls application for identification of significance in different subgroups. # = non-fasting.

Table 1.
Glycemic parameters in lean and obese LA/Ntvl/-cp rats.

The effects of adrenalectomy on parameters of adiposity at 12 weeks of age are shown in **Table 2** and indicate that the combined fat pad mass and percent adiposity of the obese animals was markedly greater than was observed in their lean littermates. Adrenalectomy resulted in a partial normalization in fat accretion, while fat pad mass and percent adiposity of the hemi-adrenalectomized rats were similar to those of unoperated obese rats. When adrenalectomized rats were administered supraphysiologic doses of insulin however, fat pad mass and the percent adiposity exceeded that of the unoperated obese littermates. The insulin administration resulted in a return of parameters of insulin resistance, and combined with the greater overall caloric intake, resulted in yet greater fat accretion as predicted. The caloric efficiency in column 4 of the data table is consistent with a greater caloric efficiency in the obese, obese-hemi adrenalectomy and insulinized animals.

The levels of relative adiposity of the 5 groups are indicated in **Table 2**. The grams of the 3 fat pad depots are presented in the far-left column and the percent adiposity in the adjacent column. Comparing the relative adiposity with the Insulin to glucose ratio as an indicator of insulin resistance in **Table 1**, the relative adiposity corresponds with the magnitude of insulin resistance in each group, where the Obese+ADX is

Group	n	AT Mass, g.	% Adiposity	Net CE_6-9W	CE 9-12W
Lean	6	5.54 ± 0.11 ^a	1.87 ± 0.04e-2 ^a	0.08 ± 0.01 ^a	0.05 ± 0.01 ^a
Obese	6	21.18 ± 2.10 ^c	4.74 ± 0.47e-2 ^c	0.09 ± 0.01 ^b	0.06 ± 0.01 ^b
Obese Hemi-ADX	4	22.04 ± 1.90 ^c	4.85 ± 0.25e-2 ^c	0.10 ± 0.01 ^b	0.06 ± 0.00 ^b
Obese-ADX	6	12.81 ± 2.30 ^b	3.02 ± 0.54e-2 ^b	0.08 ± 0.01 ^a	0.05 ± 0.01 ^a
Obese ADx + INS	4	28.2 ± 2.50 ^c	5.29 ± 0.25e-2 ^c	0.10 ± 0.01 ^b	0.06 ± 0.01 ^b
ANOVA		ns	p = <0.05	p = <0.05	p = <0.05

Data are mean ± 1 SEM, n = 4–6 rats/group. The mass of adipose tissue was computed as the sum of the Dorsal, Retroperitoneal and Epididymal fat pad depots as dissected at 12 weeks of age; The percent adiposity data in column two reflects the combined mass of the three depots expressed as g / g. BW × 100. CE = caloric efficiency from 6 to 9 weeks and 9 to 12 weeks of study. The groups with different superscripts indicate statistically different subgroups at p = < 0.05 via Student Neuman Keuls analysis.

Table 2.
Effects of adrenalectomy on adipose parameters in lean and obese LA/Ntvl/-cp rats.

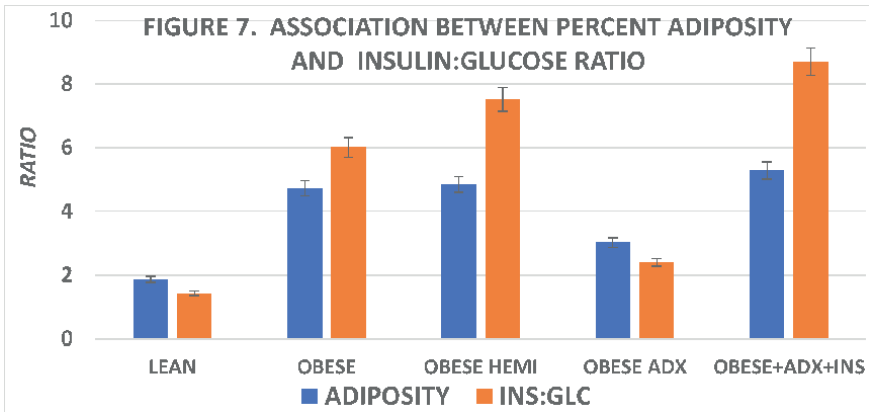


Figure 7.
Association between percent adiposity and insulin to glucose ratio. Data are mean \pm 1 SEM, N = 4–6 rats/group.

similar to the similarly fed unoperated lean controls (**Figure 7**), while all other treatment groups remain similarly elevated by comparison. The net caloric intake during weeks 6 to 9 is reflected in column 3 of **Table 2** and indicates that caloric intake in the obese+ADX is similar to unoperated lean animals, while the caloric intake of all other groups was similar. The caloric efficiency indicated in the far-right column corresponds with the caloric intake data, consistent with the magnitude of insulin resistance and adiposity observed.

Rhus, the results of this investigation indicate that bot unoperated obese and obese-adrenalectomized developing a greater magnitude of adiposity than occurred in their lean littermates, indicative a = of a phenotype effect on weight gain and the expression of obesity. The significant differences in weight gain between the phenotypes occurs despite their having the same genetic origins and being reared under the same environment and dietary conditions. The coexistence of insulin resistance is evident in the obese phenotype, as reflected by greeter plasma insulin concentrations in addition to an exaggerated insulin to glucose ratio in the obese. The obese phenotype exhibited hyperphagia and an improved efficiency of weight gain following hemi-adrenalectomy or adrenalectomy plus insulin replacement in an attempt to maintain a state of insulin resistance in the absense of adrenal secretions. In contrast, adrenalectomized obese animals exhibited glycemic and thermogenic parameters that were similar to those of their unoperated lean littermates, consistent with the impression that the counterregulatory effects between insulin and adrenal glucocorticoid hormones are key contributory factors in the insulin resistance and in parameters reflecting insulin sensitivity.

The Interscapular Brown adipose tissue (IBAT) depots were excised in their entirety after sacrifice and are depicted in **Figure 8**. The data indicates that the IBAT mass of obese rats and the proportion of IBAT mass to body weight were significantly greater in the obese phenotype. Neither partial or complete adrenalectomy was effective in restoring iBAT mass to normal, likely because increases in the IBAT mass associate with hyperphagia beginning soon after postweaning development, via processes of hypertrophy and hyperplasia [4, 13]. The IBAT to BW ratio was however only partially corrected since the final body weights of the adrenalectomized animals were intermediate between those of the lean and obese phenotype while the IBAT mass was similar n both groups.

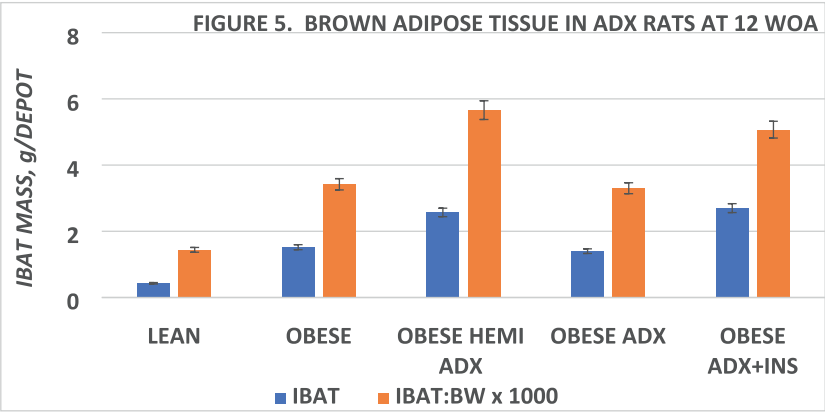


Figure 8.
Brown adipose tissue mass of lean and obese rats at 12 weeks of age. Data are mean \pm 1 SEM, $n = 4-6$ rats/group. $P = < 0.05$ obese vs. lean for IBAT mass and IBAT: Body weight (Students unpaired t test). WOA = weeks of age.

The effect of ADX on RMR is depicted in **Figure 9**. Measures on RMR in the lean, obese, and obese-adrenalectomized rats are depicted in **Figure 9**, and indicate that in lean animals, the RMR increased with age, in contrast, the RMR of obese rats decreased with advancing age. The RMR of the adrenalectomized obese rats however, attained levels similar to those of unoperated lean littermates by 12 weeks of age, reflective of the improvements in insulin sensitivity in those animals.

Measures of RMR at in all 5 treatment groups are depicted in **Figure 10** and indicate that RMR of the lean animals remained similar at all 3 ages studies. In contrast, the RMR of the obese rats were lower at the onset at 6 weeks and increased only modestly with age and dietary treatment. The effects of partial and complete adrenalectomy were similar at 6 and 9 weeks of age, and increased when fed the cafeteria diet supplement at 12 weeks of age only in fully adrenalectomized animals. RMR increased in magnitude in the insulinized adrenalectomized obese animals to

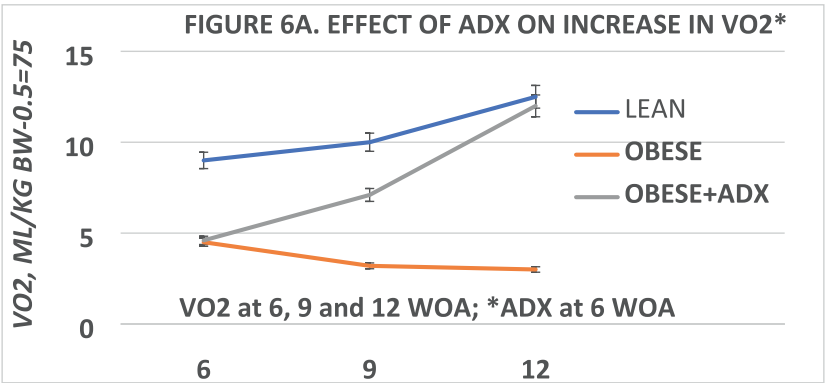


Figure 9.
The effect of adrenalectomy on resting VO₂ in LA/Ntvl/-cp rats. Data are expressed as the mean \pm 1 SEM ($n = 6$ rats/treatment group). Significance was determined with a $p = < 0.05$ via students unpaired t test comparing lean vs. obese, and obese+ADX vs. obese. Final VO₂ of adrenalectomized obese rats at 12 weeks of age was similar to lean littermates ($p = n.s.$).

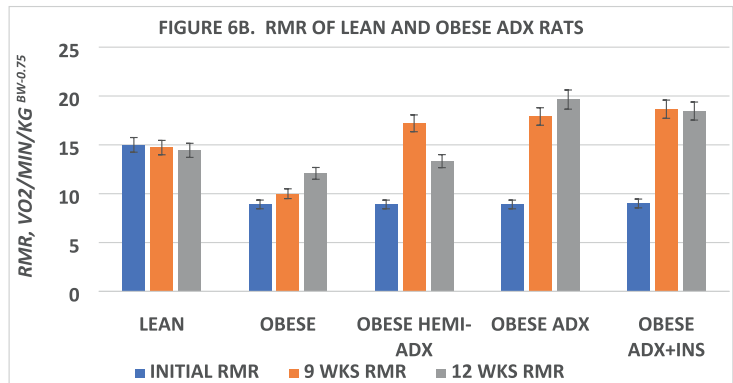


Figure 10. Effect of treatment groups on RMR at 12 weeks of age. Data are mean \pm 1 SEM, $n = 4-6$ rats/group except group obese + ADX + INS, where $n = 4$ due to fasting induced premature deaths in 2 animals.

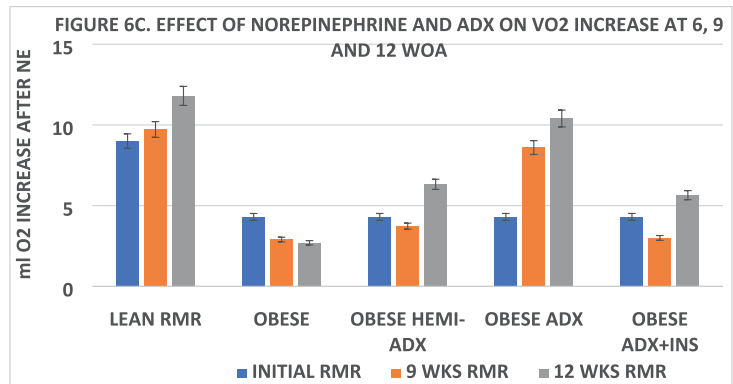


Figure 11. Effect of treatment groups on NE increase in RMR at 12 weeks of age. Data are mean \pm 1 SEM, $n = 6$ rats/group except group obese + ADX + INS, $n = 4$ due to fasting induced premature deaths of 2 animals. $0 < p < 0.05$ (lean vs. obese, obese hemi ADX and obese ADX + INS; $p = n.s.$ (lean vs. obese ADX at 9 and 12 WOA; WOA = weeks of age).

levels similar to obese adrenalectomized at the 12-week time point, after 3 weeks of the cafeteria diet supplement, during which time they also gained excessive weight and greater fat accretion.

The effects of norepinephrine administration on VO₂ in the various treatment groups is depicted in **Figure 11**. The data shown are the increase in VO₂ over the RM, taken 15 min after administering the NE (100 μ g/kg BW, s.c. in the interscapular region). In lean rats, the NE induced increase was greater at each age studied. In contrast, in the obese phenotype, NE had only a modest effect, initially about one half of the response of lean animals, and which response decreased at each subsequent time point. Adrenalectomy in obese animal restored the NE response to that of their lean littermates, while partial adrenalectomy and adrenalectomy followed by inulin treatment were ineffective in restoring the thermic response to NE.

4. Discussion

The contributions of glucocorticoid actions on insulin-stimulated formation and cytoplasmic translocation of GLUT4 transporters has been well documented [9, 32–34]. When the regulation of the transporters become disrupted due to glucocorticoids or other factors, the typical physiologic response is an increase in insulin secretion in an apparent attempt to overcome the glucose transporter impediment. The cascade of metabolic events which follow contributes to the progressive development of insulin resistance along with its pathophysiologic sequelae. In humans and likely rats as well, as the level of excess glucocorticoid stimulation continues, the elevations in cortisol contribute to preadipocyte differentiation and additional lipid accretion. Thus, pathophysiologic influences on adipose tissue depots may further exaggerate the impact of hyperinsulinemia and insulin resistance which may extend to additional tissues including skeletal muscle, brain and others that are also dependent on molecular glucose for oxidative metabolism [32–34]. Therefore, pharmacologic or surgical ablation of adrenal glucocorticoid inhibitory activity would seem to be an effective strategy to restore GLUT4 transporter functions, permit the restoration of endoplasmic reticulum synthesis and intracellular translocation to the plasma membranes, improve cellular glucose uptake and oxidation, and thus diminish the overall magnitude of insulin resistance in the various tissues of the obese phenotype of this and other genetically obese rat strains. Insulin is known to impact multiple aspects of energy metabolism and storage, including lipogenesis, activation of preadipocytes, and substrate oxidative processes, all of which may serve as primary or secondary factors that contribute to excess energy storage in adipocytes and other tissues, including hepatic fatty acid and glycogen synthesis and storage [35–37].

Evidence of the onset of insulin resistance were already apparent in the obese phenotype by 6 weeks of age, as demonstrated by the delayed glycemic excursions during the oral glucose tolerance challenge. Moreover, the disordered glycemic responses became more exaggerated by 12 weeks of age in the same obese animals, consistent with a progression of the insulin resistance state. In contrast, the magnitude of disordered glycemic responses following bilateral adrenalectomy became normalized to those of their lean littermates by 12 weeks of age, consistent with a restoration of normal glycemic parameters following adrenal ablation. However, when a subgroup of the obese adrenalectomized animals were subjected to the hyperphagia inducing Café diet regimen plus daily insulin injections in an attempt to re-establish insulin resistance in the absence of adrenal glucocorticoid secretions, adiposity progressed at an accelerated rate and with a similar magnitude of insulin resistance. These observations are consistent with adrenal mediated contributions to the process leading to insulin resistance and adiposity.

Insulin resistance also is known to impede the metabolic process of non-shivering thermogenesis in brown adipose tissue [38–42]. Insulin resistance also contributes to dysregulation of lipid metabolism in both brown and white adipose tissues, where it impacts on activity of lipoprotein lipase, essential for the mobilization and release of stored triglyceride [10–14]. Brown adipose tissue is recognized as a major contributor to the process of non-shivering thermogenesis, and has been attributed to play a role in energy balance during periods of over- and under nutrition [38–42]. Brown adipose tissue mass increases during early prepubertal life via the processes of hyperplasia, and via hypertrophy of brown adipocytes beyond adolescence and during periods of

metabolically- or pharmacologically-mediated decreases in thermogenic activity [38, 39, 42, 43]. Thus, the presence of insulin resistance has been shown to impair cellular glucose uptake in isolated brown adipocytes, and to generate decreases in resting and pharmacologically-stimulated alterations in thermogenic activity in isolated cells and *in vivo* responses to nutritional and pharmacologic stimuli [10–12, 43]. In other studies, the presence of chronic insulin resistance was associated with the ‘unbowning’ of brown adipose tissue, as the numerous small lipid locules normally active during thermogenic activity accumulated additional lipid during their decreased periods of thermogenic activity, giving way to a less intense brown coloration of the tissue [41]. In the present study, ablation of glucocorticoid influences via bilateral adrenalectomy resulted in a recovery of normal thermogenic responses by 12 weeks of age, consistent with adrenal glucocorticoid-induced contributions to insulin resistance and impaired nonshivering thermogenesis, *in vivo*.

Insulin resistance impedes the process of non-shivering thermogenesis, in addition to contributing to dysregulation of lipid metabolism in both brown and white adipose tissues [10–14]. Brown adipose tissue is recognized as a major contributor to the process of non-shivering thermogenesis, and to play a role in energy balance during periods of over- and under nutrition [38–42]. Brown adipose tissue mass increases via the processes of hyperplasia during early life, and via hypertrophy of brown adipocytes beyond adolescence, and during periods of metabolically- or pharmacologically-mediated decreases in thermogenic activity [38, 39, 42, 43]. The presence of insulin resistance impaired cellular glucose uptake in isolated brown adipocytes, and in decreases in resting and pharmacologically-stimulated alterations in thermogenic activity [10–12, 43]. In other studies, the presence of chronic insulin resistance was associated with the ‘unbowning’ of brown adipose tissue, as the numerous small lipid locules normally active during thermogenic activity accumulated additional lipid during their decreased periods of thermogenic activity, giving way to a less intense brown coloration of the tissue [41]. In addition, the thermic increases following the Café diet regimen are manifested by a combination of short-term neurosympathetic and longer-term thyroidal actions, both of which hormonal systems interact with the lipogenic activities that modulate energy metabolism and expenditure [36]. Thus, the roles of insulin and glucocorticoid hormones cannot be viewed independently with respect to parameters of the integrated complex regulation of energy balance in man and animals.

Acknowledgements

The author thanks the University of Science Arts and Technology, Montserrat for the provision of institutional resources to develop this manuscript.

Author details


Orien L. Tulp^{1,2}

1 Colleges of Medicine and Graduate Studies, University of Science Arts and Technology, Montserrat, BWI, USA

2 The Einstein Medical Institute, Florida, USA

*Address all correspondence to: o.tulp@usat.edu

IntechOpen

© 2023 The Author(s). Licensee IntechOpen. This chapter is distributed under the terms of the Creative Commons Attribution License (<http://creativecommons.org/licenses/by/3.0>), which permits unrestricted use, distribution, and reproduction in any medium, provided the original work is properly cited. 

References

- [1] Jacks DG, Kerna NA. A comprehensive analysis of obesity part I. Overview of obesity. *Journal of Obesity Nutrition Disorders*: JOND-130. 2018;1-6. DOI: 10.29011/2577-2244. 100030
- [2] Poku-Mensah C, Einstein GP, Tulp OL. Insulin sensitivity is a significant influential risk factor in the development of cardiovascular disease in diabetes mellitus. *The FASEB Journal*. 2021;35:461A. DOI: 10.1096/fasebj.2021.35.S1.05024
- [3] Stierman B, Afful J, Carroll MD. National Health and Nutrition Examination Survey 2017–March 2020 Prepandemic Data Files Development of Files and Prevalence Estimates for Selected Health Outcomes. Series NHSR 158. 2021. pp. 1-21. DOI: 10.15620/cdc:106273
- [4] Tulp OL. Effects of aging, phenotype, and carbohydrate feeding on caloric efficiency and adiposity in the LA/Ntvl//*-cp* rat. *Advanced Obesity Weight Management Control*. 2021;11(1):5-11. DOI: 10.15406/aowmc.2021.11.00329
- [5] Huang HJ, Young AA, Koda JE, et al. Hyperamylinemia, hyperinsulinemia, and insulin resistance in genetically obese LA/N-*cp* rats. *Hypertension*. 1992;19(1 Suppl):101-109
- [6] Tulp OL. Characteristics of thermogenesis, obesity, and longevity in the LA/N-*cp* rat. *ILAR News Journal*. 1990;32(3):33-139
- [7] Michaelis OEIV. New Models of Genetically Obese Rats for Studies in Diabetes, Heart Disease, and Complications of Obesity, Veterinary Resources Branch, Division of Research Services. Bethesda, MD: NIH Publication; 1988. pp. 13-15
- [8] Tulp OL, Einstein GP. Thermogenesis, aging and obesity in the LA/Ntvl//*-cp* (corpulent) rat. *Advanced Obesity Weight Management Control*. 2021;11(2):37-43. DOI: 10.15406/aowmc.2021.11.00333
- [9] Kahn CR. Role of insulin receptors in insulin-resistant states. *Metabolism*. 1980;29(5):455-466
- [10] Bukowiecki LJ, Deshaies Y, Collet AJ, Tulp O. Major thermogenic defect associated with insulin resistance in brown adipose tissue of obese-diabetic SHR/N-*cp* rats. *American Journal of Physiology*. 1991;261:E204-E213
- [11] Marette A, Tulp OL, Bukowiecki LJ. Mechanism linking insulin resistance to defective thermogenesis in brown adipose tissue of obese diabetic SHR/N-*cp* rats. *International Journal of Obese*. 1991;15:23-831
- [12] Atgie C, Marette A, Desautels M, Tulp O, Bukowiecki LJ. Specific decrease in mitochondrial thermogenic capacity in brown adipose tissue of obese SHR/N-*cp* rats. *American Journal of Physiology*. 1993;265:1674-1680
- [13] Tulp OL. The effects of experimental over nutrition on non-shivering thermogenesis and obesity in LA/N-*cp* rats. *Computer Bloch Physiology*. 1991;98A:567-574
- [14] Tulp OL, DeBolt SP. Aging and obesity in the corpulent rat. In: *Nestle Nutrition Series, Research and Practice in MNA and Aging*. Basel: Nestle Publications; 1999. pp. 149-155
- [15] DeBolt SP. Effects of Aging and Obesity on Adaptive Thermogenesis and Energy Metabolism in LA/N-Corpulent Rats [PhD thesis]. Philadelphia: Drexel University Publishers; 1992. p. 314

- [16] Tulp OL, Shields SJ. Thermogenesis in cafeteria-fed LA/N-cp (corpulent) rats. *Nutrition Research*. 1984;**4**:325-332
- [17] Hansen CT. The development of the SHR/N- and LA/N-cp (corpulent) congenic rat strains. In: *New Models of Genetically Obese Rats for Studies in Diabetes, Heart Disease, and Complications of Obesity*. Bethesda, MD: NIH Publication, Division of Research Services, Veterinary Resources Branch, National Institutes of Health; 1988. pp. 7-10
- [18] Koletsky S. Obese spontaneously hypertensive rats-A model for the study of atherosclerosis. *Experimental Biology and Pathology*. 1990;**19**:53-60
- [19] Greenhouse DD, Hansen CT, Michaelis OE IV. Development of fatty and corpulent rat strains. *ILAR News Journal*. 1990;**32**(3):2-4
- [20] Sasner JM, Jones CT, Marco GD, Champlin AK, Tulp OL. Morphometric features of protein-restricted LA/N-cp (corpulent) rats. In: *Proceedings, Colby-Bates-Bowdoin Research Symposium*. Boudoin Maine; 1983. p. 6A
- [21] Wolpert SI, Bye RM, Tulp OL. Effect of α -methylparatyrosine on thermogenesis in cafeteria fed rats. *Clinical Research*. 1983;**31**(3):677A
- [22] Wolpert SI, Bye RM, Tulp OL. Effect of α -methylparatyrosine on thermogenesis before and after cafeteria feeding in rats. *Federation Proceedings*. 1984;**43**(5):701A
- [23] Tulp OL. Nonshivering thermogenesis revisited: Sympathetic and non-sympathetic contributions. *Advanced Obesity Weight Management Control*. 2023;**13**(1):25-28. DOI: 10.15406/aowmc.2023.13.00387
- [24] Michaelis OE, Ellwood KC, Tulp OL, Greenwood MRC. Effect of feeding ¹sucrose or starch diets on parameters of glucose tolerance in the LA/N-corpulent rat. *Nutrition Research*. 1986;**6**(2):95-99
- [25] Michaelis OEIV. *New Models of Genetically Obese Rats for Studies Diabetes, Heart Disease, and Complications of Obesity*. Bethesda, MD, USA: NIH, Division of Research Services, Veterinary Resources Branch, Government Printing Office; 1988. pp. 13-15
- [26] Young NL, Tulp OL. The effects of norepinephrine and nutritional status on resting metabolic rates in LA/N-cp rats. *Computer Biochemical Physiology*. 1989;**94**(4):597-602
- [27] Kleiber M. *The Fire of Life: An Introduction to Animal Energetics*. New York: Wiley Publishers; 1961:
- [28] Wang ZM, Zhang J, Ying Z, Heymsfield SB. Organ-tissue level model of resting energy expenditure across mammals: New insights into Kleiber's Law. *International Scholarly Research Network*. 2012;**2012**:673050. DOI: 10.5402/2012/673050
- [29] Marchington D, Rothwell NJ, Stock MJ, York DA. Energy balance, diet induced thermogenesis and brown adipose tissue in obese (fa/fa) Zucker rats after adrenalectomy. *Journal of Nutrition*; **113**:1395-1400
- [30] Tulp OL, Brown T. Effect of a fructan-chromium complex on glycemic responses of congenic obese LA/Ntul/-cp rats. *Journal of Nutrition Health Food Engineering*. 2016;**5**(2):594-598. DOI: 10.15406/jnhfe.2016.05.00167
- [31] Ott L. Multiple comparisons. In: *Introduction to Statistical Methods and Data Analysis*. 3rd ed. Boston MA: PWS-Kent; 1988. pp. 437-466
- [32] Dimitriadis G, Leighton B, Parry-Billings M, Sasson S, Young M,

- Krause U, et al. Effects of glucocorticoid excess on the sensitivity of glucose transport and metabolism to insulin in rat skeletal muscle. *The Biochemical Journal*. 1997;**321**:707-712. DOI: 10.1042/bj3210707
- [33] Gathercole LL, Morgan SA, Bujalska IJ, Hauton D, Stewart PM, Tomlinson JW. Regulation of lipogenesis by glucocorticoids and insulin in human adipose tissue. *PLoS One*. 2011;**6**:e26223. DOI: 10.1371/journal.pone.0026223
- [34] Hauner H, Schmidt P, Pfeiffer EF. Glucocorticoids and insulin promote the differentiation of human adipocyte precursor cells into fat cells. *The Journal of Clinical Endocrinology and Metabolism*. 1987;**64**:832-835. DOI: 10.1210/jcem-64-4-832
- [35] Tulp OL, Awan AR, Einstein GP. Treatment with α -methylparatyrosine inhibits sympathetic but not thyroidal responses to diet-induced thermogenesis in lean cafeteria-overfed rats. *Current Trends in Toxicology and Pharmacology Research*. 2022;**2**(1):1-6. DOI: 10.53902/CTTR.2022.02.000504
- [36] Tulp OL. Estimation of the sympathetic and thyroidal partitions to diet induced thermogenesis in the rat Chapter 6. *New Advances in Medicine and Medical Science*. 2023;**3**:53-66. DOI: 10.9734/bpi/namms/v3/5729E
- [37] Tulp OL. The development of brown adipose tissue during experimental over-nutrition in rats. *International Journal of Obesity*. 1981;**5**(6):579-591 and *The Adipose Tissue Issue*, John Libbey & Company, London, pp. 579-591, (1981) ed
- [38] Tulp OL, Frink R, Danforth E Jr. Effect of cafeteria-feeding on brown and white adipose tissue cellularity, thermogenesis, and body composition in rats. *The Journal of Nutrition*. 1982;**112**(12):2250-2260
- [39] Tulp OL, Gregory MH, Danforth E Jr. Characteristics of diet-induced brown adipose tissue growth and thermogenesis in rats. *Life Sciences*. 1982;**30**(18):1525-1530
- [40] Tulp OL. Does insulin resistance contribute to the ‘unbrowning’ or beigeing of brown adipose tissue in obese and obese diabetic rats. *Academia Biology*. 2023;**1**(1):001-004
- [41] Tulp OL. Effects of acute starvation on brown adipose tissue status in the rat. *Nutrition Report International*. 1983;**28**(2):227-233
- [42] Tulp OL, Root D, Frink R. The effect of anti-hypertensive drug treatment on brown adipocyte diameter and locule distribution in rats. *Comparative Biochemistry and Physiology*. 1984;**79C**(2):317-320
- [43] Tulp OL, Awan AR, Einstein GP. Adrenalectomy improves glycemic parameters in congenic LA/Nt μ l μ -cp rats. *Endocrinology & metabolism. International Journal*. 2021;**9**(3):61-67. DOI: 10.10154/emij.2021.09.00310 Published 20 Dec 2021

Steroidogenesis of Corticosteroids, Genetic Mutation, and Endocrine Disruption Leading to Adrenal Insufficiency

Ying Su, Ren-Shan Ge and Hong Xie

Abstract

Steroidogenesis, the process by which steroids are synthesized, involves a complex cascade of enzymatic reactions that ultimately produce hormones, such as cortisol and aldosterone. Cortisol is a steroid hormone that plays a critical role in the regulation of various physiological processes, including metabolism, immune response, and stress response. Aldosterone is responsible for blood pressure and water balance. The biosynthesis of cortisol and aldosterone occurs primarily in the adrenal cortex and is processed by a series of enzymatic reactions that convert cholesterol into cortisol and aldosterone. Enzymes include CYP11A1, 3 β -hydroxysteroid dehydrogenase 2, CYP11B1, CYP11B2, CYP17A1, and 21-hydroxylase. Mutations or defects in these enzymes can lead to impaired cortisol and aldosterone biosynthesis, thereby resulting in various disorders such as congenital adrenal hyperplasia, adrenal hypoplasia congenita, and familial glucocorticoid deficiency. Endocrine disruptors, such as phthalates, bisphenols, and pesticides, affect adrenal cortex development or steroidogenesis, thereby causing adrenal cortex dysfunction. Understanding the complex process of steroidogenesis involved in cortisol and aldosterone biosynthesis can provide crucial insights into the pathophysiology of adrenal disorders and inform the development of targeted therapies to alleviate the associated symptoms.

Keywords: cortisol, aldosterone, adrenal cortex dysfunction, steroidogenesis, endocrine disruptors

1. Introduction

Corticosteroids are a class of steroid hormones that play critical roles in various physiological processes in the body. They are synthesized through a complex process known as steroidogenesis. Corticosteroids belong to two main subclasses: glucocorticoids and mineralocorticoids, each with distinct functions and regulation. Glucocorticoids primarily regulate metabolism, immune responses, and stress responses, while mineralocorticoids are mainly involved in maintaining electrolyte

balance and fluid homeostasis. In this chapter, we will focus on the steroidogenesis of corticosteroids, with an emphasis on glucocorticoid and mineralocorticoid biosynthesis.

2. Adrenal corticosteroid biosynthesis and regulation

2.1 Adrenal cortex anatomy

The adrenal gland is essentially divided into two endocrine glands, composed of two structures of different embryonic origin and function, namely the outer cortex and inner medulla (**Figure 1**). The adrenal medulla is an extension of the sympathetic nervous system and consists of irregularly arranged chromaffin cells. The adrenal medulla is not the subject of the current chapter. The adult adrenal cortex is histologically and functionally divided into three distinct zones, each controlled by unique hormonal signals. The outer zona glomerulosa (zG) synthesizes aldosterone, a mineralocorticoid hormone that regulates sodium retention and blood vessel volume, thereby controlling blood pressure. The middle zona fasciculata (zF) synthesizes glucocorticoids (cortisol in humans or corticosterone in rodents), which play a key role in glucose metabolism, immune responses, and stress responses. The innermost zona reticularis (zR) is responsible for the biosynthesis and secretion of androgens [1]. The adrenal is covered by a layer of capsule. Controversy has sometimes surrounded the existence of mouse and rat zR zones, but its presence can be clearly documented based on morphological criteria. However, it is worth noting that the thickness of this zone can vary significantly among different mouse strains [2].

According to immunohistochemistry, some researchers have described the presence of an intermediate zone or undifferentiated zone between zG and zF in rats and mice. This zone does not express corticosteroid-specific enzymes such as

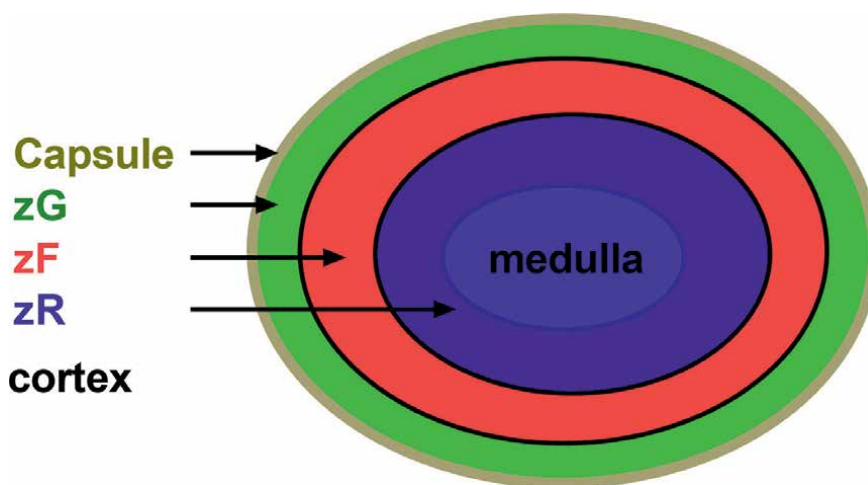


Figure 1. Illustration of adrenal glands. The adrenal gland comprises an inner medulla and an outer adrenal cortex. The cortex is covered by a thin cellular capsule. The adrenal cortex has three classical zones, the zG (zona glomerulosa) which is under capsule, zF (zona fasciculata) which exists between zG and zR (zona reticularis), and zR which is innermost of the adrenal cortex, showing distinct morphology.

cytochrome P450 aldosterone synthase (CYP11B2) in the zG and cytochrome P450 11 β -hydroxylase (CYP11B1) in the zF [3–5].

The foetal human adrenal gland primarily consists of a specialized foetal zone that synthesizes precursor steroids, which can be converted to oestrogen by the placenta. This foetal zone is surrounded by definitive tissue. After birth, the foetal zone rapidly “involutates” or disappears and is replaced by the expanding definitive zone [6]. Recent evidence suggests that the developing mouse adrenal cortex may mainly comprise a foetal zone. The residue of this zone forms the so-called X zone around day 10 postpartum, following its replacement by definitive tissue around birth [7]. Cells of the mouse X zone appear highly basophilic [7].

This book chapter primarily focuses on zG and zF zones, dealing with the biosynthesis of corticosteroids, including cortisol/corticosterone and aldosterone.

2.2 Adrenal development

The development of the adrenal gland is a complex and fascinating process that begins during early embryonic development. The adrenal gland is a unique endocrine organ located on top of the kidneys and plays a key role in regulating various physiological processes in the body. During early embryonic development, the adrenal gland arises from two distinct regions: the adrenal cortex and the adrenal medulla. These two regions have different embryological origins and functions. The adrenal cortex originates from the mesoderm [8], while the adrenal medulla develops from neural crest cells (see review [9]). This book chapter focuses on adrenal cortex development. The development of the adrenal gland can be divided into several stages, each characterized by specific cellular and molecular events. The first stage is known as the specification stage, during which the precursor cells are specified to become adrenal cortex, called the anlage of the adrenal cortex, which is first identified at 3–4 weeks of gestation in humans, due to a condensation of the coelomic epithelium. The next stage is the proliferation and differentiation stage, where the precursor cells undergo rapid proliferation and begin to differentiate into the specific cell types of the adrenal gland and migrate to the superior end of the mesonephros, and the adrenal gland is first recognizable at 4–6 weeks of gestation in humans. In the adrenal cortex, different zones start to form (called foetal zone and definitive zone) at 8–10 weeks of gestation. By late gestation, the foetal adrenal gland starts to develop into the early form of the adult adrenal cortex and the morphology of zG and zF appears. Then, the foetal zone declines and disappears during the first three postnatal months. Finally, the final adult zonal pattern is established and stabilized between 10 and 20 years of age [8].

Although there may be variations in developmental milestones and timing between different species, the overall processes of adrenocortical development in rats and mice are similar to those in humans [4, 10]. Several researchers have reported that the precursors of steroidogenic tissues first appear in mouse and rat embryos as transcription factor steroidogenic factor 1 (SF-1, also called nuclear receptor family 5 member A1, NR5A1)-positive adrenogenital primordium at approximately E8.5–E9.5 in mice and E11.5 in rats [4, 10, 11]. This adrenogenital primordium separates into distinct adrenal and gonadal primordia around E10.5–E11.5 in mice and E12.5 to E14.5 in rats. Medullary precursor cells migrate into the adrenal primordium around E12.5 in mice and E15 in rats. Subsequently, the adrenal gland becomes encapsulated around E14.5 in mice and E16.5 in rats [4, 10, 11].

In rats and mice, zonation of the adrenal cortex begins in late gestation [4, 10, 11]. Besides, the mouse adrenal cortex also has an X zone [4, 10, 11], which exists in the innermost region of the cortex surrounding the medulla. The X zone first appears around 10 days after birth and reaches its maximum volume in males during the weaning period. It degenerates during puberty in males under the action of androgens. However, in female mice, the X zone reaches its maximum size at around 3 months of age and gradually degenerates with age or rapidly during the first pregnancy under the influence of oestrogens [7, 12, 13]. The function of the X zone remains unclear, but it is believed to be equivalent to the foetal zone found in human adrenal glands [14].

As the adrenal gland continues to develop, it undergoes morphological changes and establishes functional connections with other organs. One significant interaction occurs between the adrenal cortex and the placenta during foetal development [12]. The foetal adrenal cortex produces precursor steroids that can be converted into oestrogens by enzymes in the placenta, contributing to the hormonal balance in the developing foetus [12].

The final stage of adrenal gland development is the maturation stage, during which the adrenal gland acquires its final structure and function. This process involves the refinement of hormone production, establishment of innervation, and vascularization of the organ. Additionally, the adrenal gland undergoes changes in response to various physiological and pathological stimuli throughout life.

2.3 Steroidogenesis of corticosteroids

Due to the specific structures of adrenal cortex, each adrenal cortex zone secretes distinct steroid hormones, including corticosteroids. **Figure 2** provides an illustration of the steroidogenic pathway within each zone of the human adrenal cortex.

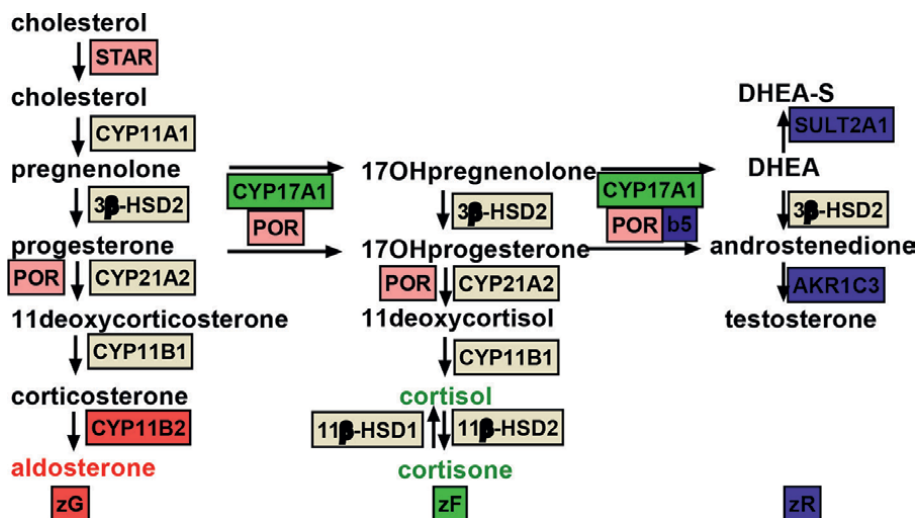


Figure 2.

Pathways of steroidogenesis in the adrenal cortex. Cholesterol is shuttled into inner membrane of the mitochondrion, when it is processed variously to produce different steroidogenic products including glucocorticoids (cortisol in humans), mineralocorticoids (aldosterone) and adrenal androgens. zG, zona glomerulosa; zF, zona fasciculata; zR, zona reticularis; DHEA, dehydroepiandrosterone; DHEA-S, dehydroepiandrosterone sulfate. Red color represents aldosterone synthesis; green color represents cortisol or corticosterone synthesis; blue color represents adrenal androgen synthesis.

These pathways have distinct proteins (or enzymes) for the stepwise conversion from precursor cholesterol into aldosterone (mineralocorticoid) in the zG, cortisol (glucocorticoid) in the zF, and androgens in the zR.

The synthesis of corticosteroids starts with cholesterol, a precursor molecule that serves as the backbone for steroid hormone biosynthesis. In the adrenal cortex cells, cholesterol is present in free form or in esterified form [15]. Cholesterol in adrenal cortex cells is obtained from both dietary intake via several receptors and transporters, including scavenger receptor member B 1 (SCARB1), also called high-density lipoprotein receptor [16, 17] and low-density lipoprotein receptor (LDLR), and de novo synthesis within the body [13].

Once inside the adrenal cortex cells, cholesterol undergoes a series of enzymatic reactions to convert it into corticosteroids. These reactions take place in different cellular compartments, including the mitochondria and the smooth endoplasmic reticulum. Each step of corticosteroid biosynthesis is catalyzed by specific enzymes expressed in a tissue-specific manner.

The first step in the biosynthesis of corticosteroids is the conversion of cholesterol to pregnenolone. This reaction is catalyzed by the enzyme cytochrome P450 cholesterol side-chain cleavage (CYP11A1). It occurs in the inner mitochondrial membrane and involves the cleavage of the side chain of cholesterol. Transportation of cholesterol to the inner mitochondrial membrane is the initial and limiting step for the biosynthesis of all corticosteroids [15]. Although the underlying mechanisms responsible for the transportation remain unclear, it is thought that the steroidogenic acute regulatory protein (STAR) plays a critical role in this cholesterol transport [18]. When cholesterol reaches CYP11A1, it carries out several steps of hydroxylation and side-chain cleavage of cholesterol to form pregnenolone, which is assisted by cofactors adrenodoxin and the enzyme adrenodoxin reductase [19].

Pregnenolone serves as the precursor for the biosynthesis of both glucocorticoids and mineralocorticoids. Because different zone cells contain distinct other steroidogenic enzymes, they biosynthesize distinct corticosteroids.

In the zG cells, the conversion of pregnenolone to progesterone is mediated by enzymes 3β -hydroxysteroid dehydrogenase/ Δ^{5-4} isomerase 2 (3β -HSD2), and then progesterone is further into 11-deoxycorticosterone and corticosterone after enzymatic reactions catalyzed by cytochrome P450 21-hydroxylase (CYP21A2) and CYP11B1, respectively. In the last step, CYP11B2 catalyzes aldosterone biosynthesis [20].

In the zF cells, the smooth endoplasmic reticulum contains cytochrome P450 17α -hydroxylase/ $17-20$ -lyase (CYP17A1), which converts pregnenolone into 17α -hydroxypregnenolone. CYP17A1 catalyzes two steps of reaction, including 17α -hydroxylation, which requires coenzyme cytochrome P450 reductase (POR), and $17-20$ -lysis, which requires cytochrome b5 (b5). The 17α -hydroxypregnenolone is converted to 17α -hydroxyprogesterone by 3β -HSD2. After that, 17α -hydroxyprogesterone is further converted to 11-deoxycortisol and cortisol after the catalysis of CYP21A2 and CYP11B1. Interestingly, the rat and mouse adrenal cortex do not express CYP17A1, therefore, only glucocorticoid corticosterone is formed.

The next crucial step in cortisol level control is cortisol metabolism. This process is regulated by two enzymes, 11β -hydroxysteroid dehydrogenase 1 (11β -HSD1) and 11β -hydroxysteroid dehydrogenase 2 (11β -HSD2). Both enzymes are expressed in the adrenal cortex [1, 21, 22]. 11β -HSD1 is responsible for the activation of biologically inert cortisone to active cortisol [23], while 11β -HSD2 does the opposite reaction, catalyzing the conversion of cortisol to cortisone [22, 24]. 11β -HSD2 selectively

oxidizes the 11 β -hydroxy group of cortisol/corticosterone to a ketone, resulting in cortisol inactivation. This step plays a significant role in maintaining the appropriate balance between cortisol and its inactive form, cortisone, as it prevents the excessive buildup of cortisol in tissues with high expression of 11 β -HSD2.

Once biosynthesized, mineralocorticoids like aldosterone and glucocorticoids like cortisol are released into the bloodstream. Cortisol binds to corticosteroid-binding globulin (CBG) or albumin that circulates it throughout the body. Cortisol can then reach its target tissues, where it exerts its effects by binding to the intracellular glucocorticoid receptor (NR3C1) and thereby modulating target gene expression.

2.4 Regulation of aldosterone synthesis

The biosynthesis of aldosterone is tightly regulated to maintain electrolyte balance and fluid homeostasis in the body. Several factors, including hormonal, enzymatic, and physiological mechanisms, contribute to the regulation of aldosterone biosynthesis. The renin-angiotensin-aldosterone system (RAAS) is a key hormonal pathway that regulates aldosterone biosynthesis. When blood pressure decreases or sodium levels are low, the juxtaglomerular cells in the kidneys release an enzyme called renin into the bloodstream. Renin acts on its substrate angiotensinogen, which is produced by the liver, to convert it into angiotensin I. Angiotensin I is then converted into angiotensin II by the action of an enzyme called angiotensin-converting enzyme, predominantly found in the lungs. Angiotensin II acts as a potent stimulator of aldosterone biosynthesis by binding to the angiotensin II type 1 receptor (AT1 receptor) on the cells of the adrenal cortex. Activation of the AT1 receptor triggers a series of intracellular signaling events that lead to increased aldosterone production. The key enzyme of aldosterone biosynthesis within the adrenal cortex is the enzyme CYP11B2.

In addition to the RAAS, other hormonal systems can also influence aldosterone biosynthesis. For example, plasma potassium levels directly stimulate aldosterone release. Hyperkalaemia (high potassium levels) stimulates aldosterone biosynthesis and secretion, while hypokalaemia (low potassium levels) inhibits it. Potassium exerts its effect through depolarization of the zG cells, leading to increased calcium influx and subsequent activation of various signaling pathways involved in aldosterone production.

Atrial natriuretic peptide and brain natriuretic peptide, which are released by specialized cells in the heart, also play a role in regulating aldosterone biosynthesis. Atrial natriuretic peptide and brain natriuretic peptide act as inhibitors of the RAAS, opposing the effects of angiotensin II. They promote diuresis and natriuresis, lowering blood pressure, and counteracting the stimulatory effects of angiotensin II on aldosterone release.

The physiological state of the body also influences aldosterone biosynthesis. Physical factors such as blood volume, blood pressure, and body position can affect aldosterone production. For instance, in conditions of low blood volume or blood pressure, baroreceptors detect these changes and stimulate the release of aldosterone to promote sodium and water retention, thereby increasing blood volume and pressure.

Various genetic and molecular mechanisms also contribute to aldosterone biosynthesis regulation. The expression of key enzymes involved in aldosterone biosynthesis, such as CYP11B2, is regulated by different transcription factors and signaling pathways, such as calcium/calmodulin-dependent protein kinase pathway after the

rapid intracellular elevation of calcium [25]. Mutations or alterations in these regulatory mechanisms can lead to dysregulation of aldosterone biosynthesis and result in disorders such as primary aldosteronism.

2.5 Regulation of cortisol/corticosterone biosynthesis

The biosynthesis and release of cortisol/corticosterone are tightly regulated by various mechanisms to maintain physiological homeostasis. Several factors, including hormonal, neural, and physiological mechanisms, contribute to the regulation of cortisol biosynthesis. The hypothalamic-pituitary-adrenal (HPA) axis plays a central role in the regulation of cortisol biosynthesis. The hypothalamus releases corticotropin-releasing hormone (CRH) in response to various internal and external stressors. CRH stimulates the anterior pituitary gland to release adrenocorticotrophic hormone (ACTH) into the bloodstream. ACTH then acts on the adrenal cortex, specifically the zF, to stimulate the biosynthesis and secretion of cortisol. ACTH binds to melanocortin two receptors (MC2R) on the zF cells, initiating a signaling cascade that leads to increases in intracellular cyclic adenosine monophosphate (cAMP) levels. This, in turn, activates several enzymes involved in cortisol biosynthesis, such as CYP11A1. The release of CRH from the hypothalamus and ACTH from the pituitary gland is subject to a complex feedback system to regulate cortisol production. High levels of cortisol inhibit the release of CRH and ACTH, thereby reducing further cortisol biosynthesis. Conversely, low cortisol levels stimulate the release of CRH and ACTH, leading to increased cortisol production. The negative feedback regulation of cortisol is also influenced by other factors, such as the circadian rhythm. Cortisol levels follow a diurnal pattern, with the highest levels occurring in the early morning and the lowest levels during sleep. The regulation of this circadian rhythm involves the interaction between the suprachiasmatic nucleus in the brain, the pineal gland, and the HPA axis.

Another important regulator of cortisol biosynthesis is the NR3C1. Once synthesized, cortisol binds to NR3C1 in target tissues, resulting in negative feedback on the HPA axis. The binding of cortisol to NR3C1 inhibits the release of CRH and ACTH, thereby reducing cortisol biosynthesis and secretion.

Apart from the hormonal regulation, other factors influence cortisol biosynthesis. Stress, both physical and psychological, can trigger an increase in cortisol production. Stress-related signals, such as pain, injury, or emotional distress, activate the HPA axis [26–28] and lead to the release of cortisol to help the body cope with the stressor.

Cortisol biosynthesis is also influenced by various physiological factors. Blood glucose levels, for example, can impact cortisol production. Low blood glucose levels stimulate the release of CRH and ACTH, leading to increased cortisol biosynthesis and release. The immune system and inflammation can also influence cortisol levels, as cytokines and other inflammatory mediators can regulate HPA axis activity.

Overall, the biosynthesis and release of cortisol are tightly regulated by a complex interplay of hormonal, neural, and physiological mechanisms. Various factors, including the HPA axis, circadian rhythm, stress, and immune system function, contribute to maintaining appropriate cortisol levels and ensuring proper physiological responses to stress and metabolic demands. The biosynthesis of corticosteroids, especially glucocorticoids, is tightly regulated through complex feedback mechanisms involving the HPA axis. The HPA axis acts as a central control system, controlling the release of hormones involved in corticosteroid biosynthesis and regulating the body's response to stress.

3. Adrenal cortex diseases related with gene mutations

3.1 Congenital adrenal hyperplasia (CAH)

CAH (**Table 1**) is a group of autosomal recessive genetic disorders characterized by the enzymatic defects in the biosynthesis of cortisol, a vital hormone produced by the adrenal glands [29–31]. This condition affects the adrenal cortex, leading to impaired production of cortisol, along with other hormones such as aldosterone and adrenal androgens, because the resulting ACTH excess stimulates adrenal cortex growth through adrenocortical cell proliferation [32]. CAH is primarily caused by mutations in genes involved in steroid hormone biosynthesis, particularly the *CYP21A2* gene [32], referred as 21-hydroxylase deficiency [33].

The *CYP21A2* gene provides instructions for producing an enzyme known as cytochrome 21-hydroxylase, which plays a crucial role in the biosynthesis of cortisol and aldosterone [34]. In CAH, mutations in this gene result in reduced or absent 21-hydroxylase activity, leading to a block in cortisol biosynthesis. As a compensatory mechanism, the pituitary gland produces increased amounts of ACTH to stimulate the adrenal glands to produce cortisol precursors. However, due to the enzymatic deficiency, these precursors accumulate and are diverted to the production of androgens, resulting in excessive adrenal androgen release [35–38].

Empty cell	Disorder	Gene	OMIM
Defects of corticosteroid steroidogenesis (congenital adrenal hyperplasia, CAH)	Congenital lipoid adrenal hyperplasia (LCAH)	<i>STAR</i>	201710
	P450 side chain cleavage syndrome (CAH)	<i>CYP11A1</i>	118485
	3 β -hydroxysteroid dehydrogenase deficiency (CAH)	<i>HSD3B2</i>	201810
	21-hydroxylase deficiency (CAH)	<i>CYP21A2</i>	201910
	11 β -hydroxylase deficiency (CAH)	<i>CYP11B1</i>	202010
	17-hydroxylase deficiency (CAH)	<i>CYP17A1</i>	202110
	P450 oxidoreductase deficiency (CAH)	<i>POR</i>	613571
	Steroidogenic factor 1 deficiency	<i>NR5A1</i>	184757
	Corticosterone methyl oxidase type II deficiency	<i>CYP11B2</i>	124080
Adrenal hypoplasia congenita (AHC)	X-linked adrenal hypoplasia congenita (AHC)	<i>NR0B1</i>	300200
	Steroidogenic factor 1 deficiency	<i>NR5A1</i>	184757
Familial glucocorticoid deficiency (FGD)	Familial glucocorticoid deficiency (FGD)	<i>MC2R</i>	202200
		<i>MRAP</i>	607398

Table 1.
Reported monogenetic causes of primary adrenal insufficiency and associated phenotype in humans.

The severity of CAH can vary depending on the specific mutation in the *CYP21A2* gene. The classic form of CAH is the most severe and is further classified into two types: salt-wasting CAH and non-salt-wasting CAH. Salt-wasting CAH, accounting for around 75% of cases, is characterized by a deficiency of both cortisol and aldosterone, leading to electrolyte imbalances and potentially life-threatening salt loss. Non-salt-wasting CAH involves only cortisol deficiency, with aldosterone levels remaining normal, leading to milder symptoms [32].

In addition to the *CYP21A2* gene variants, there are other rare forms of CAH caused by mutations in genes such as *CYP11B1* [39, 40], referred as 11 β -hydroxylase deficiency [41, 42], and *HSD3B2* [32, 43, 44], referred as 3 β -hydroxysteroid dehydrogenase deficiency, which encode other enzymes involved in steroid biosynthesis. These forms of CAH are associated with different enzyme deficiencies and result in distinct clinical presentations.

CYP11B1 mutation refers to a genetic alteration in the *CYP11B1* gene [39, 40] which encodes the enzyme 11 β -hydroxylase [41, 42]. This enzyme is crucial for the biosynthesis of cortisol and aldosterone, two important adrenal steroid hormones. Mutations in the *CYP11B1* gene can reduce or completely abolish the activity of 11 β -hydroxylase, resulting in disrupted cortisol and aldosterone biosynthesis. As a result, there is an accumulation of precursor molecules, such as 17-hydroxyprogesterone and progesterone, which can be converted into adrenal androgens. The symptoms and severity of 11 β -hydroxylase deficiency can vary depending on the specific mutation and the residual enzyme activity. Common symptoms include excessive production of adrenal androgens, leading to varying degrees of genital ambiguity in females, early-onset pubic hair growth in both males and females, and menstrual irregularities [41, 42, 45–49].

HSD3B2 mutation refers to a genetic alteration in the *HSD3B2* gene, which encodes the enzyme 3 β -HSD2 [43]. This enzyme plays a crucial role in the conversion of pregnenolone to progesterone in the adrenal cortex. Mutations in the *HSD3B2* gene can lead to reduced or absent activity of the 3 β -HSD2, resulting in impaired production of cortisol and aldosterone. This deficiency can cause an imbalance in the adrenal hormone pathway, leading to elevated levels of precursor hormones such as pregnenolone and progesterone [32, 43, 44]. The symptoms and severity of 3 β -HSD2 deficiency can vary depending on the specific mutation and the residual enzyme activity. Individuals with this form of CAH may experience symptoms such as salt-wasting, ambiguous genitalia in females, adrenal crises, and abnormal growth.

CYP11B2 mutation refers to a genetic alteration in the *CYP11B2* gene, which encodes an enzyme called aldosterone synthase [50]. This enzyme is responsible for the final step in the biosynthesis of aldosterone, a mineralocorticoid hormone produced in the adrenal cortex. Mutations in the *CYP11B2* gene can lead to aldosterone synthase deficiency, which is a rare form of CAH known as corticosterone methyl oxidase type II deficiency (CMO-II) [50–52]. This deficiency affects the production of aldosterone, resulting in insufficient levels of this hormone. Aldosterone is important for regulating sodium and potassium balance in the body, as well as maintaining blood pressure. Consequently, individuals with CMO-II may experience symptoms associated with mineralocorticoid deficiency, such as salt-wasting and electrolyte imbalances. Additionally, reduced aldosterone levels may lead to excess production of precursor hormones, leading to an imbalance in the adrenal hormone pathway.

One specific form of CAH is known as STAR deficiency. STAR deficiency is a rare autosomal recessive disorder caused by mutations in the *STAR* gene [44, 53]. This gene provides instructions for producing the STAR, which plays a crucial role in

transporting cholesterol into the mitochondria of adrenal cells. Cholesterol is a key precursor in the biosynthesis of cortisol and other steroid hormones. In individuals with STAR deficiency, the impaired function of the STAR protein prevents cholesterol from being transported effectively into the mitochondria. As a result, cortisol production is severely reduced or absent. The adrenal glands attempt to compensate by increasing ACTH secretion, leading to adrenal hyperplasia as they try to produce more cortisol precursors, leading to the accumulation of lipid droplets, which is also referred as congenital lipoid adrenal hyperplasia (CLAH). However, since the precursors cannot be converted into cortisol, they are eventually diverted towards the production of adrenal androgens, which can lead to symptoms such as early puberty and virilization in females. The clinical presentation of STAR deficiency varies depending on the severity of the mutation. Severe forms typically present in infancy with life-threatening adrenal crisis and salt-wasting due to the deficiency of aldosterone, in addition to cortisol deficiency. Milder forms may present later in childhood or even adulthood, and may not have significant salt-wasting or adrenal crisis [54–58].

CYP11A1 deficiency (also referred as P450 side chain cleavage syndrome) is a rare genetic disorder that falls under the umbrella term of CAH. Unlike most forms of CAH, which are caused by specific enzyme deficiencies in the adrenal steroidogenic pathway, CYP11A1 deficiency results in a defect in the first and rate-limiting step of steroid hormone biosynthesis. Defects in the *CYP11A1* gene disrupt this conversion, leading to impaired production of cortisol, aldosterone, and other adrenal steroid hormones [15, 59]. The clinical presentation of CYP11A1 deficiency can vary widely depending on the severity of the mutation and the residual activity of the enzyme. In some cases, individuals with CYP11A1 deficiency can present with ambiguous genitalia at birth, similar to other forms of CAH [15, 59]. However, unlike other forms of CAH, the deficiency in CYP11A1 affects the entire adrenal steroidogenesis pathway, resulting in low levels of cortisol, aldosterone, and adrenal androgens. This can cause salt-wasting, adrenal crises, and potentially life-threatening complications in infancy [15, 59].

CYP17A1 is an enzyme that plays a key role in the steroid hormone synthesis pathway. Mutations or variants in the *CYP17A1* gene can result in various forms of CAH, also known as 17 α -hydroxylase deficiency [53, 60, 61]. This condition affects the adrenal glands' ability to produce cortisol and adrenal androgens, leading to a disruption in the biosynthesis of these hormones [53, 60, 61]. The severity of 17 α -hydroxylase deficiency can vary depending on the nature of the mutation. In some cases, individuals with this condition may have ambiguous genitalia at birth due to impaired production of adrenal androgens. This can affect sexual development, causing individuals assigned female at birth to undergo masculinization during puberty. In addition, the reduction in cortisol production may result in adrenal insufficiency, leading to symptoms such as fatigue, weakness, and electrolyte imbalances [53, 60, 61]. In individuals with 17 α -hydroxylase deficiency, the lack of cortisol feedback to the pituitary gland causes an increase in ACTH production. This stimulates the adrenal glands to produce more precursor hormones that are subsequently shunted to the production of mineralocorticoids, specifically aldosterone. The elevated levels of aldosterone can lead to hypertension and contribute to potassium wasting and low renin levels [53, 60, 61].

POR (P450 oxidoreductase) is an enzyme that plays a crucial role in the function of several other enzymes (CYP17A1 and CYP21A2) involved in steroid hormone biosynthesis, including those responsible for cortisol and aldosterone production. Mutations in the *POR* gene can lead to a specific form of CAH known as P450 oxidoreductase deficiency [43, 62]. P450 oxidoreductase deficiency affects multiple enzymatic reactions related to

steroid hormone synthesis. The POR gene mutations can impair the activity and stability of the P450 oxidoreductase enzyme, leading to disruptions in various steps of the adrenal steroidogenesis pathway. Patients with P450 oxidoreductase deficiency may present with a wide range of symptoms and varying degrees of hormone deficiencies. The clinical presentation can include symptoms of cortisol deficiency such as fatigue, low blood sugar, and poor growth. Additionally, some individuals may exhibit mineralocorticoid deficiency symptoms such as salt-wasting, hyponatraemia (low sodium levels), and hyperkalaemia. One distinctive feature of P450 oxidoreductase deficiency is that it affects both the adrenal cortex and the gonads, leading to abnormalities in reproductive development. In males, this can manifest as undervirilization or ambiguous genitalia at birth, while in females, it can lead to primary amenorrhea or incomplete sexual development during puberty [63]. These features distinguish P450 oxidoreductase deficiency from other forms of CAH.

Management of CAH involves lifelong hormone replacement therapy to replace cortisol and potentially aldosterone, balancing hormone levels and preventing adrenal crises. Additional treatments may be required to manage the physical and hormonal aspects of the condition, particularly in individuals with the classic form of CAH. Close monitoring by a multidisciplinary medical team is essential to optimize treatment and quality of life for individuals with CAH.

3.2 Adrenal hypoplasia congenita (AHC)

AHC (**Table 1**) is a rare genetic disorder characterized by hypoplasia or absence of the adrenal glands. This condition affects the production of cortisol and, in some cases, aldosterone, leading to adrenal insufficiency. AHC can be classified into two main types: X-linked AHC (also known as AHC type 1) and autosomal recessive AHC (AHC type 2). AHC type 1 is caused by mutations in the *NR0B1* (nuclear receptor family 0 member b1) gene (also called *DAX1*, dosage-sensitive sex reversal, adrenal hypoplasia critical region, on chromosome X, gene 1) [32], while AHC type 2 is caused by mutations in the *SF-1* gene (also known as *NR5A1*) [64]. These genes play essential roles in the development and function of the adrenal glands.

The presentation and severity of AHC can vary among individuals depending on the specific gene mutation and its impact on adrenal development [65]. Males with X-linked AHC usually have more severe symptoms, including dehydration, vomiting, low blood sugar, and adrenal crises in infancy [66–68]. In contrast, females may have milder symptoms due to random X-inactivation and can present with primary amenorrhea and delayed sexual development during puberty [66–68].

In autosomal recessive AHC, both males and females can be affected, and the severity of symptoms can vary. Symptoms typically include adrenal insufficiency-related manifestations such as fatigue, weakness, poor weight gain, and low blood pressure.

Therefore, AHC is a rare genetic disorder characterized by underdeveloped or absent adrenal glands, resulting in cortisol and possibly aldosterone deficiency. The two main types, X-linked AHC and autosomal recessive AHC are caused by mutations in specific genes involved in adrenal gland development and function.

3.3 Familial glucocorticoid deficiency (FGD)

FGD, also known as primary glucocorticoid resistance or autosomal recessive pseudohyperaldosteronism, is a rare genetic disorder characterized by the inability of

the body to respond properly to cortisol, resulting in adrenal insufficiency [69]. FGD is typically caused by mutations in MC2R. Mutations in the MC2R gene can disrupt the normal functioning of the MC2R protein, resulting in an impaired response to ACTH and subsequent cortisol deficiency [70–72]. FGD is also caused by mutations in the *MRAP* (melanocortin 2 receptor accessory protein) gene [73, 74], which is required for proper function and transport of the MC2R protein to the cell membrane location [32]. *Mrap*^{-/-} knockout mice have been found to mimic the human FGD phenotype [73, 75]. Individuals with FGD typically present with symptoms of adrenal insufficiency, including fatigue, weakness, hypoglycaemia, poor weight gain, and potentially life-threatening adrenal crises [32]. In some cases, mineralocorticoid deficiency may also occur, leading to electrolyte imbalances and salt-wasting.

Diagnosis of FGD involves hormone testing to evaluate cortisol and ACTH levels. Genetic testing can confirm the presence of mutations in the MC2R gene or other relevant genes associated with ACTH signaling.

4. Corticosteroid-disrupting endocrine disruptors

Many endocrine disruptors, including perfluoroalkylated and polyfluoroalkylated substances (PFAS), phthalates, polybrominated diphenyl ethers (PBDEs), and insecticides, interfere with the adrenal cortex endocrine system.

4.1 Polyfluoroalkylated substances (PFAS)

PFAS are a group of synthetic chemicals that are characterized by the presence of fluorinated carbon chains [76, 77]. These compounds have gained significant attention due to their widespread use in various industrial and consumer products, as well as their persistence in the environment and potential adverse health effects [76, 77]. PFAS have unique properties, including water and oil repelling, heat resistance, and chemical stability, which make them useful in a wide range of applications. They have been used in the production of non-stick cookware, water-resistant textiles, firefighting foams, paper and packaging materials, and many other products [76, 77]. One of the concerning aspects of PFAS is their persistence in the environment [76, 77]. These compounds do not readily break down and can remain in the environment for long periods of time. As a result, they have been detected in various environmental compartments, including air, soil, water, and wildlife. Studies have highlighted potential health impacts associated with PFAS exposure [76, 77]. Using human adrenocortical carcinoma cells HAC15, it was found that two most widely used PFAS, perfluorooctanoic acid (PFOA, C8) and perfluorooctane sulfonate (PFOS, C8S), can significantly upregulated *CYP11B2* expression by several times and increased aldosterone secretion via stimulating reactive oxygen species production [78]. Oral PFOS exposure to adult Sprague-Dawley male rats for 28 days downregulated the expression of corticotropin-releasing factor 1 receptor (*Crf1r*) in the pituitary gland and *Nr3c1* in the pituitary gland, thereby leading to the reduction of corticosterone biosynthesis [79]. Using human adrenocortical carcinoma cells H295R cells, it was found that PFOS at 200 μ M can significantly upregulate *MC2R*, *CYP11B1* and *CYP11B2* expression, thereby increasing cortisol and aldosterone secretion [80]. Some PFAS are potent inhibitors of human 11 β -HSD2. The inhibitory potency of PFAS depends on the carbon chain length and sulfur atoms. PFAS significantly inhibited human 11 β -HSD2 with a potency as C10 (half-maximal inhibitory concentration, IC₅₀,

9.19 μM) > C11 (15.09 μM) > C12 (18.43 μM) > C9 (20.93 μM) > C13 (124 μM) > C14 (147.3 μM) > other C4–C7 carboxylic acids and C8S > C7S = C10S > other sulphonic acids [81, 82]. PFOS and PFOA also inhibit human 11 β -HSD1 activity with IC₅₀ values of 7.56 μM and 37.61 μM , respectively, while perfluorobutanesulfonic acid and perfluorohexanesulfonic acid do not inhibit the enzyme activity at 250 μM [83].

4.2 Phthalates

Phthalates, also known as phthalate esters, are a group of industrial chemicals primarily used as plasticizers [84]. They are commonly added to plastics to make them more flexible, durable, and transparent. Phthalates can be found in various products such as vinyl flooring, adhesives, coatings, medical devices, toys, cosmetics, and personal care products. Phthalates are not chemically bound to the plastics they are added to, which means they can easily leach out over time and be released into the environment or come into contact with humans through product use. As a result, there has been growing concern about their potential health effects. Studies have suggested that certain phthalates may have endocrine-disrupting properties, meaning they can interfere with the normal function of hormones in the body. One of their targets is the adrenal cortex. They have been shown to have adverse effects on the development and function of the adrenal cortex, which produces glucocorticoids and mineralocorticoids. Studies have demonstrated that exposure to phthalates during critical periods of adrenal gland development can lead to alterations in adrenal structure and function.

Phthalates have been implicated in disturbances of mineralocorticoid biosynthesis. Animal studies have demonstrated that exposure to certain phthalates, such as the most widely used phthalate di-(2-ethylhexyl) phthalate (DEHP), can affect the RAAS, resulting in changes in aldosterone levels and electrolyte balance [85]. Rat studies have shown that prenatal exposure to certain phthalates, such as the most widely used phthalate DEHP can disrupt adrenal development, leading to changes in adrenal size and reduction of aldosterone in adult offspring [86]. A second exposure in the adult rat male offspring when they are exposed in utero to low levels of DEHP can markedly reduce serum aldosterone levels, possibly via downregulation for the expression of potassium channel *Kcnk5* and the retinoid-X receptors *Rxra* and *Rxrb* [87]. This could be due to the epigenetic regulation of genes related to adrenal cortex steroidogenesis [88]. Although in utero exposure to DEHP at the highest dose (750 mg/kg) does not affect corticosterone levels of adult male offspring [86], other more potent phthalates such as di-pentyl phthalate can reduce aldosterone and corticosterone and ACTH levels after in utero exposure, although aldosterone is most sensitive to DPeP exposure (at 10 mg/kg) [89]. Di-pentyl phthalate disrupts corticosteroid biosynthesis mostly by downregulating the expression of *Agtr1a*, *Mc2r*, *Scarb1*, *Cyp11a1*, *Hsd3b1*, *Cyp21*, *Cyp11b1*, *Cyp11b2*, *Nr5a1*, and *Nr4a2*, possibly via inducing reactive oxygen species production [89].

The effects of phthalates on glucocorticoids and mineralocorticoid biosynthesis in puberty and adults may depend on doses and phthalate types. Rat studies have reported decreased levels of corticosterone, following di-butyl phthalate and DEHP exposure, suggesting a disruption in the function of the HPA axis [90]. Bis (2-butoxyethyl) phthalate exposure to male rats in puberty (from day 35 to 56 postpartum) also reduces serum corticosterone and aldosterone level without affecting ACTH, possibly via downregulating the expression of steroidogenesis-related genes (*Scarb1*, *Star*, *Cyp11a1*,

Cyp21, *Cyp11b1*, *Cyp11b2*, *Nr5a1*, *Nr4a1*, and *Nr4a2*) by inducing reactive oxygen species [91]. In contrast, other studies have shown increased glucocorticoid and ACTH levels after exposure to DEHP in rats at 20 and 40 days of age, indicating an activation of the stress response [92]. These effects on glucocorticoid levels may be linked to alterations in the expression and activity of enzymes involved in glucocorticoid metabolism, such as 11 β -HSD2 [93, 94]. Some phthalates with di-propyl phthalate, dibutyl phthalate, and di-cyclohexyl phthalate also weakly inhibit human 11 β -HSD2 activity [94]. Although DEHP does not inhibit human 11 β -HSD2 while its metabolite mono-diethylhexyl phthalate can moderately inhibit this enzyme activity [93, 94].

It is important to note that the specific effects of phthalates on adrenal cortex development and function may vary depending on the type of phthalate, exposure levels, timing, and duration of exposure. Furthermore, these effects may differ between animal models and humans. Studies in human populations regarding the associations between phthalate exposure and adrenal cortex function are limited and often rely on indirect measurements of hormone levels or urinary metabolites. The Hokkaido Study with 202 mother-infant pairs showed that maternal urinary DEHP metabolites were negatively correlated with cord serum cortisol and cortisone levels, indicating that corticosteroid synthesis in the adrenal cortex of infants is reduced [95]. Overall, evidence suggests that phthalate exposure can disrupt adrenal cortex development and function, affecting both glucocorticoid and mineralocorticoid hormone systems.

4.3 Polybrominated diphenyl ethers (PBDEs)

PBDEs are a class of flame retardants that have been widely used in various consumer products, including electronics, textiles, plastics, and furniture. PBDEs can persist in the environment and bioaccumulate in organisms. Some studies suggest that certain PBDEs may contribute to disruptions in adrenal cortex steroidogenesis. 4-Bromodiphenyl ether (BDE3), the PBDE's photodegraded metabolite increases serum aldosterone and corticosterone levels at 200 mg/kg without affecting adrenocorticotrophic hormone level after male rats are exposed to this chemical from the age of day 35 to 56. The mechanism possibly is related with the upregulation of *Cyp11b1*, *Scarb1*, *Star*, *Cyp11b2*, *Cyp21*, and *Nr5a1* expression by decreasing the phosphorylation of AMP-activated protein kinase and increasing peroxisome proliferator-activated receptor-gamma coactivator (PGC)-1 α (PGC-1 α) and phosphorylated cyclic AMP-responsive element-binding protein [96]. Two PBDEs, 2-OH-BDE85 and 2-OH-BDE47 at a micromolar concentration induce transcriptional changes associated with endoplasmic reticulum stress and the unfolded protein response, which possibly impairs the adrenocortical secretory function in human H295R cells [97]. However, the exact mechanisms through which PBDEs may interfere with adrenal cortex steroidogenesis are still being investigated. Furthermore, the specific effects may vary depending on the type of PBDE compound, the dose and duration of exposure, and individual factors such as age and overall health. Some PBDEs also inhibit 11 β -HSD2. BDE-47 and BDE-153 potently inhibit human 11 β -HSD2, with IC₅₀ values of 11.97, and 4.41 μ M, respectively, while BDE-3 and BDE-47 inhibit rat 11 β -HSD2 with IC₅₀ values of 12.42 and 5.95 μ M [98]. However, all these PBDEs do not affect human and rat 11 β -HSD1 activity [98].

4.4 Bisphenols

Bisphenols are a group of chemical compounds used in the production of various consumer products, including plastics and epoxy resins. One of the most well-known

bisphenols is bisphenol A (BPA) [99]. The potential effects of bisphenols on adrenal cortex steroidogenesis, which is the synthesis of steroid hormones in the adrenal glands, have raised concerns due to their classification as endocrine disruptors. Bisphenols, including BPA, have been shown to interfere with hormonal signaling pathways and affect the function of hormone receptors. Adrenal cortex steroidogenesis can be influenced by bisphenols through several mechanisms. When offspring is *in utero* exposed to BPA (25 mg BPA/kg food pellet) via diet from gestational day 7 to 19, BPA increases adrenal gland weight, increases plasma corticosterone levels in both sexes, and upregulates the expression of *Star* and *Cyp11a1* [100]. Adult male Wistar rats exposed to BPA (10 mg/kg) for 14 days have an increase in corticosterone synthesis possibly via inducing reactive oxygen species since antioxidant melatonin can antagonize it [101]. In mouse Y1 adrenal cortex cells, treatment with low doses of BPA (10–1000 nM) increases the *Cyp11a1* transcription, thereby increasing corticosterone production through the JNK/c-Jun signaling pathway [102]. In the human adrenal H295R cell line, BPA increases cell number and protein levels of proliferating cell nuclear antigen, a universal marker of cell proliferation, cyclin D1 and D2, key proliferation factors, as well as *Shh* and its key transcriptional regulator *Gli1* possibly via activating oestrogen receptor β [103].

Bisphenols may also affect adrenal steroidogenesis by interacting with enzymes involved in hormone production. For example, studies have suggested that bisphenols can inhibit enzymes such as 11 β -HSD2 [104]. Bisphenols show inhibitory potency against human 11 β -HSD2, depending on its structure, being bisphenol FL > bisphenol AP > bisphenol Z > bisphenol B > bisphenol C > bisphenol AF > BPA [104]. Halogenated bisphenols also potentially inhibit human 11 β -HSD2 activity [105].

Case-control study also shows that the maternal BPA levels are positively correlated with the serum cortisol levels in female infants [106]. A cross-sectional relationship between BPA exposure and cortisol among peripubertal boys in Canada shows that BPA concentrations were associated with a 16% decrease in serum cortisol levels [107].

4.5 Organotin

Organotin compounds are a group of chemicals that contain tin and carbon atoms bonded together [108]. They have been used in a variety of industrial and consumer applications, including as stabilizers in plastics, fungicides, and as antifouling agents in paints for boats and ships. However, their use has been restricted or banned in many countries due to their widespread environmental persistence and toxicity [109]. The relationship between organotin compounds and adrenal cortex steroidogenesis, the process involving the production of steroid hormones in the adrenal glands, has been the subject of research. While there is limited information specifically on this topic, some studies suggest that certain organotin compounds may disrupt adrenal cortex steroidogenesis by interfering with the function of enzymes involved in hormone production. Exposure of adult male Sprague Dawley rats to triphenyltin (0, 0.5, 1, and 2 mg/kg) from age of 56 days to 86 days decreases serum corticosterone levels without affecting aldosterone and ACTH levels possibly by downregulating the expression of *Scarb1*, *Star*, *Cyp11a1*, *Hsd3b*, *Cyp21*, *Cyp11b1*, and *Hsd11b1* while up-regulating the expression of *At1*, *Nr4a2*, and *Hsd11b2* [110]. Triphenyltin *in vitro* also inhibits corticosteroid secretion by inducing ROS production in H295R cells [110]. Young male rats exposed to 0, 0.5, 1, or 2 mg/kg/day triphenyltin for 18 days also have lower corticosterone and ACTH levels, possibly due to the suppression of

adrenal cortex development due to the reduced expression of transcription factor genes (*Nr4a1*, *Nr4a2*, *Nr4a3*, and *Ppard*) [111]. Female rats exposed to tributyltin have also high CRH and low ACTH expression and increased plasma corticosterone levels [112]. Triphenyltin and tributyltin, also inhibit human 11 β -HSD2 activity with IC₅₀ of 3.3 and 16.5 μ M [113]. This disruption can lead to alterations in the production and regulation of hormones such as cortisol, aldosterone, and adrenal androgens. However, it's important to note that the available research on the effects of organotin compounds on adrenal cortex steroidogenesis is still limited and further studies are needed to better understand the specific mechanisms and potential health impacts.

4.6 Pesticides

The potential effects of various types of pesticides, such as insecticides, fungicides, and biocides, on adrenal cortex steroidogenesis have been a subject of scientific investigation. Research has indicated that certain pesticides may have the potential to disrupt adrenal cortex steroidogenesis. These chemicals are known as endocrine disruptors, as they can interfere with the normal functioning of hormones in the body. The specific mechanisms through which pesticides disrupt adrenal function can vary depending on the individual compound and its mode of action. Insecticides, for example, have been shown to impact adrenal cortex steroidogenesis by directly affecting key enzymes involved in hormone synthesis.

3-Methylsulphonyl-DDE (3-MeSO₂-DDE) is a derivative of DDE (dichlorodiphenyldichloroethylene), which is a metabolite of the pesticide DDT (dichlorodiphenyltrichloroethane) [114]. 3-MeSO₂-DDE is formed in the human body through the metabolism of DDE. Foetal mice *in utero* exposure to 3-MeSO₂-DDE have mitochondrial degeneration and vacuolation in foetal adrenal cortex cells and dysfunction of corticosteroid steroidogenesis [115]. 1,1-Dichloro-2,2-bis(p-chlorophenyl)ethylene (p,p'-DDE) is a chemical compound that is derived from the pesticide DDT [116, 117]. It is formed through the breakdown of DDT in the environment or in the human body. p,p'-DDE is a persistent organic pollutant and has been widely detected in the environment, including in soil, water, and food sources [116, 117]. p,p'-DDE exposure (50 and 100 mg/kg) *in utero* to rats inhibits corticosteroid steroidogenesis in the foetal adrenal cortex [118].

Cis-bifenthrin is a synthetic pyrethroid insecticide commonly used for pest control in residential, agricultural, and public health settings [119]. Pyrethroids, including cis-bifenthrin, act on the nervous systems of insects, leading to paralysis and death [120]. Cis-bifenthrin inhibits cortisol and aldosterone biosynthesis via cAMP signaling cascade in human adrenocortical H295R cells [119].

Lindane is an organochlorine pesticide that has been widely used in the past for insect control, particularly against lice and scabies [121]. Research investigating the effects of lindane on H295R cells has indicated that it can disrupt adrenal steroidogenesis. Specifically, lindane has been shown to interfere with the synthesis and regulation of adrenal hormones, including cortisol. Lindane's mechanism of action involves interference with the enzymes involved in steroid hormone synthesis and STAR expression [122].

Triadimefon is a fungicide that belongs to the class of triazole compounds. It is commonly used in agriculture and horticulture to control fungal diseases in crops and ornamental plants [123, 124]. After in-utero exposure to triadimefon (0, 25, 50, and 100 mg/kg/day) for 10 days from gestational day 12 to 21, male foetal rat's zF thickness is reduced and serum aldosterone, corticosterone, and ACTH levels are reduced

possibly via downregulating the expression of *Agtr1*, *Mc2r*, *Star*, *Cyp11b1*, *Cyp11b2*, *Igf1*, and *Nr5a1* after activating the reactive oxygen species through reducing the expression of antioxidant *Sod2*, *Gpx1*, and *Cat* [125]. Triadimefon also inhibits human and rodent 11 β -HSD1 activity [126].

5. Conclusion

The steroidogenesis of corticosteroids plays a critical role in regulating various physiological processes in the body, including immune function, metabolism, and stress response. Genetic mutations in genes involved in adrenal cortex steroidogenesis can disrupt the synthesis and regulation of cortisol, aldosterone, and adrenal androgens, resulting in adrenal insufficiency and related symptoms. CAH represents a group of genetic disorders characterized by enzyme deficiencies that impair adrenal steroidogenesis. These deficiencies can lead to a range of clinical presentations and hormonal imbalances, depending on the specific gene mutations involved. Other disorders such as AHC and FGD are also due to the mutation of some critical genes in the adrenal cortex. In addition to genetic mutations, endocrine-disrupting compounds, such as certain pesticides, fungicides, biocides, and bisphenols, can interfere with adrenal cortex steroidogenesis. These chemicals disrupt the normal function of hormones, hormone receptors, and enzyme activity, thereby impacting the synthesis and regulation of corticosteroids. The resulting endocrine disruption can contribute to adrenal insufficiency and associated health effects. Understanding the interplay between genetic mutations, endocrine disruption, and adrenal insufficiency is crucial for diagnosis, management, and prevention of related health conditions. Genetic testing, hormone monitoring, and tailored hormone replacement therapies are often employed in the management of adrenal insufficiency. Additionally, awareness of potential exposure to endocrine-disrupting compounds and adopting safety measures can help to minimize health risks. Further research is needed to explore the mechanisms by which genetic mutations and endocrine-disrupting compounds impact adrenal cortex steroidogenesis, as well as their long-term consequences on overall health. This knowledge will enable the development of strategies to mitigate the effects of these factors and improve patient outcomes.

Author contribution

Y.S. and R.S.G wrote the chapter and R.S.G. edited the chapter.

Declaration

The authors declare no conflict of interest.

Abbreviations

11 β -HSD1	11 β -hydroxysteroid dehydrogenase 1
11 β -HSD2	11 β -hydroxysteroid dehydrogenase 2
3 β -HSD2	3 β -hydroxysteroid dehydrogenase/ $\Delta^{5,4}$ -isomerase 2

ACTH	adrenocorticotrophic hormone
AHC	adrenal hypoplasia congenita
ANP	atrial natriuretic peptide
AT1	angiotensin II type 1 receptor
B5	cytochrome b5
CAH	congenital adrenal hyperplasia
CMO-II	corticosterone methyl oxidase type II deficiency
cAMP	cyclic adenosine monophosphate
CBG	corticosteroid-binding globulin
CLAH	congenital lipoid adrenal hyperplasia
<i>Crf1r</i>	corticotropin-releasing factor 1 receptor
CRH	corticotropin-releasing hormone
CYP11A1	cytochrome P450 cholesterol side chain cleavage
CYP11B1	cytochrome P450 11 β -hydroxylase
CYP11B2	cytochrome P450 aldosterone synthase
CYP17A1	cytochrome P450 17 α -hydroxylase/17–20-lyase
CYP21A2	cytochrome P450 21-hydroxylase 2
DAX1	dosage-sensitive sex reversal, adrenal hypoplasia critical region, on chromosome X, gene 1
DHEA	dehydroepiandrosterone
DEHP	di-(2-ethylhexyl) phthalate
DPeP	di-n-pentyl phthalate
FGD	familial glucocorticoid deficiency
HPA	hypothalamic-pituitary-adrenal axis
IC ₅₀	half maximal inhibitory concentration
Kcnk5	potassium channel 5
LDLR	low-density lipoprotein receptor
NR0B1	nuclear receptor family 0 member b1
NR3C1	glucocorticoid receptor
NR5A1	nuclear receptor family 5 member A1
MC2R	melanocortin 2 receptor
MRAP	melanocortin 2 receptor accessory protein
PBDE	polybrominated diphenyl ether
PFAS	perfluoroalkylated and polyfluoroalkylated substances
PFOA	perfluorooctanoic acid
PFOS	perfluorooctane sulfonate
PGC-1 α	peroxisome proliferator-activated receptor- γ coactivator 1 α
POR	P450 oxidoreductase
RAAS	renin-angiotensin-aldosterone system
Rxra	retinoid-X receptor α
Rxra	retinoid-X receptor β
SCARB1	scavenger receptor member BI
SF-1	steroidogenic factor 1
STAR	steroidogenic acute regulatory protein
zF	zona fasciculata
zG	zona glomerulosa
zR	zona reticularis

Author details


Ying Su^{1,2*}, Ren-Shan Ge^{1*} and Hong Xie²

1 Key Laboratory of Pediatric Anesthesiology, Ministry of Education, Department of Anaesthesiology, The Second Affiliated Hospital and Yuying Children's Hospital of Wenzhou Medical University, Wenzhou, Zhejiang, China

2 Department of Anaesthesiology, The Second Affiliated Hospital of Soochow University, Suzhou, Jiangsu, China

*Address all correspondence to: suyinglb@163.com and renshan_ge@wmu.edu

IntechOpen

© 2023 The Author(s). Licensee IntechOpen. This chapter is distributed under the terms of the Creative Commons Attribution License (<http://creativecommons.org/licenses/by/3.0>), which permits unrestricted use, distribution, and reproduction in any medium, provided the original work is properly cited. 

References

- [1] Wang Y, Li H, Zhu Q, Li X, Lin Z, Ge RS. The cross talk of adrenal and Leydig cell steroids in Leydig cells. *The Journal of Steroid Biochemistry and Molecular Biology*. 2019;**192**:105386
- [2] Tanaka S, Matsuzawa A. Comparison of adrenocortical zonation in C57BL/6J and DDD mice. *Experimental Animals*. 1995;**44**:285-291
- [3] Mitani F, Mukai K, Miyamoto H, Suematsu M, Ishimura Y. The undifferentiated cell zone is a stem cell zone in adult rat adrenal cortex. *Biochimica et Biophysica Acta*. 2003;**1619**:317-324
- [4] Mitani F. Functional zonation of the rat adrenal cortex: The development and maintenance. *Proceedings of the Japan Academy. Series B, Physical and Biological Sciences*. 2014;**90**:163-183
- [5] Mukai K, Nagasawa H, Agake-Suzuki R, Mitani F, Totani K, Yanai N, et al. Conditionally immortalized adrenocortical cell lines at undifferentiated states exhibit inducible expression of glucocorticoid-synthesizing genes. *European Journal of Biochemistry*. 2002;**269**:69-81
- [6] Winter JSD. The adrenal cortex in the fetus and neonate. In: Anderson DC, Winter JSD, editors. *Adrenal Cortex*. London: Butterworths; 1985
- [7] Huang CC, Kang Y. The transient cortical zone in the adrenal gland: The mystery of the adrenal X-zone. *The Journal of Endocrinology*. 2019;**241**:R51-R63
- [8] Mesiano S, Jaffe RB. Developmental and functional biology of the primate fetal adrenal cortex. *Endocrine Reviews*. 1997;**18**:378-403
- [9] Ehrhart-Bornstein M, Hinson JP, Bornstein SR, Scherbaum WA, Vinson GP. Intraadrenal interactions in the regulation of adrenocortical steroidogenesis. *Endocrine Reviews*. 1998;**19**:101-143
- [10] Mitani F, Mukai K, Miyamoto H, Suematsu M, Ishimura Y. Development of functional zonation in the rat adrenal cortex. *Endocrinology*. 1999;**140**:3342-3353
- [11] Ikeda Y, Lala DS, Luo X, Kim E, Moisan MP, Parker KL. Characterization of the mouse FTZ-F1 gene which encodes a key regulator of steroid hydroxylase gene expression. *Molecular Endocrinology*. 1993;**7**:852-860
- [12] Pignatti E, du Toit T, Fluck CE. Development and function of the fetal adrenal. *Reviews in Endocrine & Metabolic Disorders*. 2023;**24**:5-21
- [13] Zheng HS, Kang Y, Lyu Q, Junghans K, Cleary C, Reid O, et al. DHCR24, a key enzyme of cholesterol synthesis, serves as a marker gene of the mouse adrenal gland inner cortex. *International Journal of Molecular Sciences*. 2023;**24**:933
- [14] Zubair M, Parker KL, Morohashi K. Developmental links between the fetal and adult zones of the adrenal cortex revealed by lineage tracing. *Molecular and Cellular Biology*. 2008;**28**:7030-7040
- [15] Miller WL. Disorders in the initial steps of steroid hormone synthesis. *The Journal of Steroid Biochemistry and Molecular Biology*. 2017;**165**:18-37
- [16] Landschulz KT, Pathak RK, Rigotti A, Krieger M, Hobbs HH. Regulation of scavenger receptor, class

- B, type I, a high density lipoprotein receptor, in liver and steroidogenic tissues of the rat. *The Journal of Clinical Investigation*. 1996;**98**:984-995
- [17] Connelly MA, Williams DL. SR-BI and cholesterol uptake into steroidogenic cells. *Trends in Endocrinology and Metabolism: TEM*. 2003;**14**:467-472
- [18] Manna PR, Stocco DM. Regulation of the steroidogenic acute regulatory protein expression: Functional and physiological consequences. *Current Drug Targets. Immune, Endocrine and Metabolic Disorders*. 2005;**5**:93-108
- [19] Ye L, Su ZJ, Ge RS. Inhibitors of testosterone biosynthetic and metabolic activation enzymes. *Molecules*. 2011;**16**:9983-10001
- [20] Mitani F, Ogishima T, Miyamoto H, Ishimura Y. Localization of P450_{11β} and P450_{17α} in normal and regenerating rat adrenal cortex. *Endocrine Research*. 1995;**21**:413-423
- [21] Moore XL, Hoong I, Cole TJ. Expression of the 11 β -hydroxysteroid dehydrogenase 2 gene in the mouse. *Kidney International*. 2000;**57**:1307-1312
- [22] Zallocchi M, Matkovic L, Damasco MC. Adrenal 11 β -hydroxysteroid dehydrogenase activity in response to stress. *Canadian Journal of Physiology and Pharmacology*. 2004;**82**:422-425
- [23] Chapman K, Holmes M, Seckl JR. 11 β -hydroxysteroid dehydrogenases: Intracellular gate-keepers of tissue glucocorticoid action. *Physiological Reviews*. 2013;**93**:1139-1206
- [24] Ma X, Lian QQ, Dong Q, Ge RS. Environmental inhibitors of 11 β -hydroxysteroid dehydrogenase type 2. *Toxicology*. 2011;**285**:83-89
- [25] Guagliardo NA, Klein PM, Gancayco CA, Lu A, Leng S, Makarem RR, et al. Angiotensin II induces coordinated calcium bursts in aldosterone-producing adrenal rosettes. *Nature Communications*. 2020;**11**:1679
- [26] de Kloet ER, Joels M, Holsboer F. Stress and the brain: From adaptation to disease. *Nature Reviews. Neuroscience*. 2005;**6**:463-475
- [27] Zhu Q, Ge F, Li X, Deng HS, Xu M, Bu T, et al. Dehydroepiandrosterone antagonizes pain stress-induced suppression of testosterone production in male rats. *Frontiers in Pharmacology*. 2018;**9**:322
- [28] Hardy MP, McKittrick CR, McEwen BS, Blanchard RJ, Blanchard DC, Sakai RR. Reduced testosterone production by rat Leydig cells after psychosocial stress. *Biology of Reproduction*. 1998;**58**:164
- [29] Finkelstein GP, Vieites A, Bergada I, Rey RA. Disorders of sex development of adrenal origin. *Frontiers in Endocrinology*. 2021;**12**:770782
- [30] White PC, New MI. Molecular genetics of congenital adrenal hyperplasia. *Baillière's Clinical Endocrinology and Metabolism*. 1988;**2**:941-965
- [31] Stratakis CA, Rennert OM. Congenital adrenal hyperplasia: Molecular genetics and alternative approaches to treatment. *Critical Reviews in Clinical Laboratory Sciences*. 1999;**36**:329-363
- [32] Miller WL, Flück CE, Breault DT, Feldman BJ. Adrenal cortex and its disorders. In: Sperling MA, editor. *Pediatric Endocrinology*. Amsterdam: Elsevier; 2020

- [33] Strachan T, White PC. Molecular pathology of steroid 21-hydroxylase deficiency. *The Journal of Steroid Biochemistry and Molecular Biology*. 1991;**40**:537-543
- [34] Keen-Kim D, Redman JB, Alanes RU, Eachus MM, Wilson RC, New MI, et al. Validation and clinical application of a locus-specific polymerase chain reaction- and minisequencing-based assay for congenital adrenal hyperplasia (21-hydroxylase deficiency). *The Journal of Molecular Diagnostics*. 2005;**7**:236-246
- [35] Trakakis E, Laggas D, Salamalekis E, Creatsas G. 21-hydroxylase deficiency: From molecular genetics to clinical presentation. *Journal of Endocrinological Investigation*. 2005;**28**:187-192
- [36] Tonetto-Fernandes V, Lemos-Marini SH, DeMello MP, Ribeiro-Neto LM, Kater CE. 21-hydroxylase deficiency transiently mimicking combined 21- and 11beta-hydroxylase deficiency. *Journal of Pediatric Endocrinology & Metabolism: JPEM*. 2008;**21**:487-494
- [37] Ginalska-Malinowska M. Classic congenital adrenal hyperplasia due to 21-hydroxylase deficiency—The next disease included in the neonatal screening program in Poland. *Developmental Period Medicine*. 2018;**22**:197-200
- [38] Chen Cardenas SM, El-Kaissi S, Jarad O, Liaqat M, Korbonits M, Hamrahian AH. Unusual combination of MEN-1 and the contiguous gene deletion syndrome of CAH and Ehlers-Danlos syndrome (CAH-X). *Journal of the Endocrine Society*. 2020;**4**:bvaa077
- [39] Chabraoui L, Abid F, Menassa R, Gaouzi A, El Hessni A, Morel Y. Three novel CYP11B1 mutations in congenital adrenal hyperplasia due to steroid 11Beta-hydroxylase deficiency in a moroccan population. *Hormone Research in Paediatrics*. 2010;**74**:182-189
- [40] Parajes S, Loidi L, Reisch N, Dhir V, Rose IT, Hampel R, et al. Functional consequences of seven novel mutations in the CYP11B1 gene: Four mutations associated with nonclassic and three mutations causing classic 11beta-hydroxylase deficiency. *The Journal of Clinical Endocrinology and Metabolism*. 2010;**95**:779-788
- [41] Rosler A, White PC. Mutations in human 11 beta-hydroxylase genes: 11 beta-hydroxylase deficiency in Jews of Morocco and corticosterone methyl-oxidase II deficiency in Jews of Iran. *The Journal of Steroid Biochemistry and Molecular Biology*. 1993;**45**:99-106
- [42] White PC, Curnow KM, Pascoe L. Disorders of steroid 11 beta-hydroxylase isozymes. *Endocrine Reviews*. 1994;**15**:421-438
- [43] Krone N, Arlt W. Genetics of congenital adrenal hyperplasia. *Best Practice & Research. Clinical Endocrinology & Metabolism*. 2009;**23**:181-192
- [44] Liu Y, Chen M, Liu J, Mao A, Teng Y, Yan H, et al. Comprehensive analysis of congenital adrenal hyperplasia using long-read sequencing. *Clinical Chemistry*. 2022;**68**:927-939
- [45] Mornet E, Dupont J, Vitek A, White PC. Characterization of two genes encoding human steroid 11 beta-hydroxylase (P-450(11) beta). *The Journal of Biological Chemistry*. 1989;**264**:20961-20967
- [46] White PC, Dupont J, New MI, Leiberman E, Hochberg Z, Rosler A. A mutation in CYP11B1 (Arg-448---His) associated with steroid 11 beta-hydroxylase deficiency in Jews of

Moroccan origin. *The Journal of Clinical Investigation*. 1991;**87**:1664-1667

[47] Joehrer K, Geley S, Strasser-Wozak EM, Azziz R, Wollmann HA, Schmitt K, et al. CYP11B1 mutations causing non-classic adrenal hyperplasia due to 11 beta-hydroxylase deficiency. *Human Molecular Genetics*. 1997;**6**:1829-1834

[48] Merke DP, Tajima T, Chhabra A, Barnes K, Mancilla E, Baron J, et al. Novel CYP11B1 mutations in congenital adrenal hyperplasia due to steroid 11 beta-hydroxylase deficiency. *The Journal of Clinical Endocrinology and Metabolism*. 1998;**83**:270-273

[49] Portrat S, Mulatero P, Curnow KM, Chaussain JL, Morel Y, Pascoe L. Deletion hybrid genes, due to unequal crossing over between CYP11B1 (11beta-hydroxylase) and CYP11B2 (aldosterone synthase) cause steroid 11beta-hydroxylase deficiency and congenital adrenal hyperplasia. *The Journal of Clinical Endocrinology and Metabolism*. 2001;**86**:3197-3201

[50] Zhang G, Rodriguez H, Fardella CE, Harris DA, Miller WL. Mutation T318M in the CYP11B2 gene encoding P450c11AS (aldosterone synthase) causes corticosterone methyl oxidase II deficiency. *American Journal of Human Genetics*. 1995;**57**:1037-1043

[51] Shizuta Y, Kawamoto T, Mitsuuchi Y, Toda K, Miyahara K, Ichikawa Y, et al. Molecular genetic studies on the biosynthesis of aldosterone in humans. *The Journal of Steroid Biochemistry and Molecular Biology*. 1992;**43**:981-987

[52] Shizuta Y, Kawamoto T, Mitsuuchi Y, Miyahara K, Rosler A, Ulick S, et al. Inborn errors of aldosterone biosynthesis in humans. *Steroids*. 1995;**60**:15-21

[53] Koprulu O, Ozkan B, Acar S, Nalbantoglu O, Ozkaya Donmez B, Arslan G, et al. Clinical and genetic characteristics of patients with common and rare types of congenital adrenal hyperplasia: Novel variants in STAR and CYP17A1. *Sisli Etfal Hastanesi Tip Bulteni*. 2022;**56**:291-298

[54] Tee MK, Lin D, Sugawara T, Holt JA, Guiguen Y, Buckingham B, et al. T-->A transversion 11 bp from a splice acceptor site in the human gene for steroidogenic acute regulatory protein causes congenital lipid adrenal hyperplasia. *Human Molecular Genetics*. 1995;**4**:2299-2305

[55] Nakae J, Tajima T, Sugawara T, Arakane F, Hanaki K, Hotsubo T, et al. Analysis of the steroidogenic acute regulatory protein (StAR) gene in Japanese patients with congenital lipid adrenal hyperplasia. *Human Molecular Genetics*. 1997;**6**:571-576

[56] Bose HS, Baldwin MA, Miller WL. Incorrect folding of steroidogenic acute regulatory protein (StAR) in congenital lipid adrenal hyperplasia. *Biochemistry*. 1998;**37**:9768-9775

[57] Kaur J, Casas L, Bose HS. Lipoid congenital adrenal hyperplasia due to STAR mutations in a Caucasian patient. *Endocrinology, Diabetes & Metabolism Case Reports*. 2016;**2016**:150119

[58] Bizzarri C, Pisaneschi E, Mucciolo M, Pedicelli S, Galeazzi D, Novelli A, et al. Lipoid congenital adrenal hyperplasia by steroidogenic acute regulatory protein (STAR) gene mutation in an Italian infant: An uncommon cause of adrenal insufficiency. *Italian Journal of Pediatrics*. 2017;**43**:57

[59] Sahakitrunguang T, Tee MK, Blackett PR, Miller WL. Partial defect in the cholesterol side-chain cleavage

enzyme P450_{scc} (CYP11A1) resembling nonclassic congenital lipid adrenal hyperplasia. *The Journal of Clinical Endocrinology and Metabolism*. 2011;**96**:792-798

[60] Johnson KJ, McCahan SM, Si X, Champion L, Herrmann R, Barthold JS. The orl rat with inherited cryptorchidism has increased susceptibility to the testicular effects of in utero dibutyl phthalate exposure. *Toxicological Sciences*. 2008;**105**:360-367

[61] Dai W, Zhang X, Liu H, Sun Y, Fan Y, Yu Y. Two intronic variants of CYP11B1 and CYP17A1 disrupt mRNA splicing and cause congenital adrenal hyperplasia (CAH). *Journal of Pediatric Endocrinology & Metabolism: JPEM*. 2020;**33**:1225-1229

[62] Miller WL. Disorders of androgen synthesis--from cholesterol to dehydroepiandrosterone. *Medical Principles and Practice: International Journal of the Kuwait University, Health Science Centre*. 2005;**14**(Suppl 1):58-68

[63] Fluck CE, Pandey AV. Clinical and biochemical consequences of p450 oxidoreductase deficiency. *Endocrine Development*. 2011;**20**:63-79

[64] Saleem F, Baradhi KM. Adrenal hypoplasia. In: *StatPearls, Treasure Island (FL): StatPearls Publishing; 2023*

[65] Brett EM, Auchus RJ. Genetic forms of adrenal insufficiency. *Endocrine Practice*. 2015;**21**:395-399

[66] Guo W, Mason JS, Stone CG Jr, Morgan SA, Madu SI, Baldini A, et al. Diagnosis of X-linked adrenal hypoplasia congenita by mutation analysis of the DAX1 gene. *JAMA*. 1995;**274**:324-330

[67] Seminara SB, Achermann JC, Genel M, Jameson JL, Crowley WF Jr.

X-linked adrenal hypoplasia congenita: A mutation in DAX1 expands the phenotypic spectrum in males and females. *The Journal of Clinical Endocrinology and Metabolism*. 1999;**84**:4501-4509

[68] Rojek A, Krawczynski MR, Jamsheer A, Sowinska-Seidler A, Iwaniszewska B, Malunowicz E, et al. X-linked adrenal hypoplasia congenita in a boy due to a novel deletion of the entire NR0B1 (DAX1) and MAGEB1-4 genes. *International Journal of Endocrinology*. 2016;**2016**:5178953

[69] Gao J, Chen L. Primary adrenocortical insufficiency case series in the neonatal period: Genetic etiologies are more common than expected. *Frontiers in Pediatrics*. 2020;**8**:464

[70] Ferraz-de-Souza B, Achermann JC. Disorders of adrenal development. *Endocrine Development*. 2008;**13**:19-32

[71] Newfield RS. ACTH receptor blockade: A novel approach to treat congenital adrenal hyperplasia, or Cushing's disease. *Medical Hypotheses*. 2010;**74**:705-706

[72] Clark AJ, McLoughlin L, Grossman A. Familial glucocorticoid deficiency associated with point mutation in the adrenocorticotropin receptor. *Lancet*. 1993;**341**:461-462

[73] Novoselova TV, Hussain M, King PJ, Guasti L, Metherell LA, Charalambous M, et al. MRAP deficiency impairs adrenal progenitor cell differentiation and gland zonation. *FASEB Journal: Official Publication of the Federation of American Societies for Experimental Biology*. 2018;**32**:fj201701274RR

[74] Metherell LA, Chapple JP, Cooray S, David A, Becker C, Ruschendorf F,

et al. Mutations in MRAP, encoding a new interacting partner of the ACTH receptor, cause familial glucocorticoid deficiency type 2. *Nature Genetics*. 2005;37:166-170

[75] Novoselova T, King P, Guasti L, Metherell LA, Clark AJL, Chan LF. ACTH signalling and adrenal development: lessons from mouse models. *Endocrine Connections*. 2019;8:R122-R130

[76] Bach CC, Vested A, Jorgensen KT, Bonde JP, Henriksen TB, Toft G. Perfluoroalkyl and polyfluoroalkyl substances and measures of human fertility: A systematic review. *Critical Reviews in Toxicology*. 2016;46:735-755

[77] Zhu Q, Li H, Wen Z, Wang Y, Li X, Huang T, et al. Perfluoroalkyl substances cause Leydig cell dysfunction as endocrine disruptors. *Chemosphere*. 2020;253:126764

[78] Caroccia B, Seccia TM, Pallafacchina G, Piazza M, Caputo I, Zamberlan S, et al. Aldosterone biosynthesis is potentially stimulated by perfluoroalkyl acids: A link between common environmental pollutants and arterial hypertension. *International Journal of Molecular Sciences*. 2023;24:9376

[79] Salgado-Freiria R, Lopez-Doval S, Lafuente A. Perfluorooctane sulfonate (PFOS) can alter the hypothalamic-pituitary-adrenal (HPA) axis activity by modifying CRF1 and glucocorticoid receptors. *Toxicology Letters*. 2018;295:1-9

[80] van den Dungen MW, Rijk JC, Kampman E, Steegenga WT, Murk AJ. Steroid hormone related effects of marine persistent organic pollutants in human H295R adrenocortical carcinoma cells. *Toxicology in Vitro: An International Journal Published in Association with BIBRA*. 2015;29:769-778

[81] Zhao C, Wang S, Zhai Y, Wang M, Tang Y, Li H, et al. Direct inhibition of human and rat 11beta-hydroxysteroid dehydrogenase 2 by per- and polyfluoroalkyl substances: Structure-activity relationship and in silico docking analysis. *Toxicology*. 2023;488:153484

[82] Zhao B, Lian QQ, Chu Y, Hardy DO, Li XK, Ge RS. The inhibition of human and rat 11beta-hydroxysteroid dehydrogenase 2 by perfluoroalkylated substances. *Journal of Steroid Biochemistry and Molecular Biology*. 2011;125(1-2):143-147

[83] Ye L, Zhao B, Cai XH, Chu Y, Li C, Ge RS. The inhibitory effects of perfluoroalkyl substances on human and rat 11beta-hydroxysteroid dehydrogenase 1. *Chemico-Biological Interactions*. 2011;195:114-118

[84] Li X, Mo J, Zhu Q, Ni C, Wang Y, Li H, et al. The structure-activity relationship (SAR) for phthalate-mediated developmental and reproductive toxicity in males. *Chemosphere*. 2019;223:504-513

[85] Martinez-Arguelles DB, McIntosh M, Rohlicek CV, Culty M, Zirkin BR, Papadopoulos V. Maternal in utero exposure to the endocrine disruptor di-(2-ethylhexyl) phthalate affects the blood pressure of adult male offspring. *Toxicology and Applied Pharmacology*. 2013;266:95-100

[86] Martinez-Arguelles DB, Guichard T, Culty M, Zirkin BR, Papadopoulos V. In utero exposure to the antiandrogen di-(2-ethylhexyl) phthalate decreases adrenal aldosterone production in the adult rat. *Biology of Reproduction*. 2011;85:51-61

[87] Lee S, Martinez-Arguelles DB, Campioli E, Papadopoulos V. Fetal exposure to low levels of the plasticizer DEHP predisposes the adult male

adrenal gland to endocrine disruption. *Endocrinology*. 2017;**158**:304-318

[88] Martinez-Arguelles DB, Papadopoulos V. Prenatal phthalate exposure: Epigenetic changes leading to lifelong impact on steroid formation. *Andrology*. 2016;**4**:573-584

[89] Chen H, Liu M, Li Q, Zhou P, Huang J, Zhu Q, et al. Exposure to dipentyl phthalate in utero disrupts the adrenal cortex function of adult male rats by inhibiting SIRT1/PGC-1 α and inducing AMPK phosphorylation. *Environmental Toxicology*. 2023;**38**:997-1010

[90] Ahmad S, Sharma S, Afjal MA, Habib H, Akhter J, Goswami P, et al. mRNA expression and protein-protein interaction (PPI) network analysis of adrenal steroidogenesis in response to exposure to phthalates in rats. *Environmental Toxicology and Pharmacology*. 2022;**89**:103780

[91] Liu M, Chen H, Dai H, Wang Y, Li J, Tian F, et al. Effects of bis (2-butoxyethyl) phthalate on adrenocortical function in male rats in puberty partially via down-regulating NR5A1/NR4A1/NR4A2 pathways. *Environmental Toxicology*. 2022;**37**:2419-2433

[92] Supornsilchai V, Soder O, Svechnikov K. Stimulation of the pituitary-adrenal axis and of adrenocortical steroidogenesis ex vivo by administration of di-2-ethylhexyl phthalate to prepubertal male rats. *The Journal of Endocrinology*. 2007;**192**:33-39

[93] Hong D, Li XW, Lian QQ, Lamba P, Bernard DJ, Hardy DO, et al. Mono-(2-ethylhexyl) phthalate (MEHP) regulates glucocorticoid metabolism through 11 β -hydroxysteroid dehydrogenase 2 in murine gonadotrope cells.

Biochemical and Biophysical Research Communications. 2009;**389**:305-309

[94] Zhao B, Chu Y, Huang Y, Hardy DO, Lin S, Ge RS. Structure-dependent inhibition of human and rat 11 β -hydroxysteroid dehydrogenase 2 activities by phthalates. *Chemico-Biological Interactions*. 2010;**183**:79-84

[95] Araki A, Mitsui T, Goudarzi H, Nakajima T, Miyashita C, Itoh S, et al. Prenatal di(2-ethylhexyl) phthalate exposure and disruption of adrenal androgens and glucocorticoids levels in cord blood: The Hokkaido study. *The Science of the Total Environment*. 2017;**581-582**:297-304

[96] Chen X, Mo J, Zhang S, Li X, Huang T, Zhu Q, et al. 4-Bromodiphenyl ether causes adrenal gland dysfunction in rats during puberty. *Chemical Research in Toxicology*. 2019;**32**:1772-1779

[97] Song R, Duarte TL, Almeida GM, Farmer PB, Cooke MS, Zhang W, et al. Cytotoxicity and gene expression profiling of two hydroxylated polybrominated diphenyl ethers in human H295R adrenocortical carcinoma cells. *Toxicology Letters*. 2009;**185**:23-31

[98] Chen X, Dong Y, Cao S, Li X, Wang Z, Chen R, et al. Effects of polybrominated diphenyl ethers on rat and human 11 β -hydroxysteroid dehydrogenase 1 and 2 activities. *Pharmacology*. 2016;**98**:115-123

[99] Li X, Wen Z, Wang Y, Mo J, Zhong Y, Ge RS. Bisphenols and Leydig cell development and function. *Frontiers in Endocrinology*. 2020;**11**:447

[100] Medwid S, Guan H, Yang K. Prenatal exposure to bisphenol A disrupts adrenal steroidogenesis in adult mouse offspring. *Environmental Toxicology and Pharmacology*. 2016;**43**:203-208

- [101] Olukole SG, Lanipekun DO, Ola-Davies EO, Oke BO. Melatonin attenuates bisphenol A-induced toxicity of the adrenal gland of Wistar rats. *Environmental Science and Pollution Research International*. 2019;**26**:5971-5982
- [102] Lan HC, Lin IW, Yang ZJ, Lin JH. Low-dose bisphenol a activates Cyp11a1 gene expression and corticosterone secretion in adrenal gland via the JNK signaling pathway. *Toxicological Sciences: An Official Journal of the Society of Toxicology*. 2015;**148**:26-34
- [103] Medwid S, Guan H, Yang K. Bisphenol A stimulates adrenal cortical cell proliferation via ERbeta-mediated activation of the sonic hedgehog signalling pathway. *The Journal of Steroid Biochemistry and Molecular Biology*. 2018;**178**:254-262
- [104] Zhang B, Wang S, Tang Y, Hu Z, Shi L, Lu J, et al. Direct inhibition of bisphenols on human and rat 11beta-hydroxysteroid dehydrogenase 2: Structure-activity relationship and docking analysis. *Ecotoxicology and Environmental Safety*. 2023;**254**:114715
- [105] Shi L, Zhang B, Ying Y, Tang Y, Wang S, Zhu Y, et al. Halogen atoms determine the inhibitory potency of halogenated bisphenol A derivatives on human and rat placental 11beta-hydroxysteroid dehydrogenase 2. *Food and Chemical Toxicology: An International Journal Published for the British Industrial Biological Research Association*. 2023;**175**:113739
- [106] Giesbrecht GF, Ejaredar M, Liu J, Thomas J, Letourneau N, Campbell T, et al. Prenatal bisphenol a exposure and dysregulation of infant hypothalamic-pituitary-adrenal axis function: Findings from the APrON cohort study. *Environmental Health: A Global Access Science Source*. 2017;**16**:47
- [107] Mustieles V, Ocon-Hernandez O, Minguez-Alarcon L, Davila-Arias C, Perez-Lobato R, Calvente I, et al. Bisphenol A and reproductive hormones and cortisol in peripubertal boys: The INMA-Granada cohort. *The Science of the Total Environment*. 2018;**618**:1046-1053
- [108] de Araujo JFP, Podratz PL, Merlo E, Sarmiento IV, da Costa CS, Nino OMS, et al. Organotin exposure and vertebrate reproduction: A review. *Frontiers in Endocrinology*. 2018;**9**:64
- [109] Fent K. Ecotoxicology of organotin compounds. *Critical Reviews in Toxicology*. 1996;**26**:1-117
- [110] Wu K, Li Y, Liu J, Mo J, Li X, Ge RS. Long-term triphenyltin exposure disrupts adrenal function in adult male rats. *Chemosphere*. 2020;**243**:125149
- [111] Li X, Li L, Chen X, Li X, Wang Y, Zhu Q, et al. Triphenyltin chloride reduces the development of rat adrenal cortex during puberty. *Food and Chemical Toxicology: An International Journal Published for the British Industrial Biological Research Association*. 2020;**143**:111479
- [112] Merlo E, Podratz PL, Sena GC, de Araujo JF, Lima LC, Alves IS, et al. The environmental pollutant tributyltin chloride disrupts the hypothalamic-pituitary-adrenal axis at different levels in female rats. *Endocrinology*. 2016;**157**:2978-2995
- [113] Ohshima M, Ohno S, Nakajin S. Inhibitory effects of some possible endocrine-disrupting chemicals on the isozymes of human 11beta-hydroxysteroid dehydrogenase and expression of their mRNA in gonads and adrenal glands. *Environmental Sciences*. 2005;**12**:219-230

- [114] Lund BO, Bergman A, Brandt I. Metabolic activation and toxicity of a DDT-metabolite, 3-methylsulphonyl-DDE, in the adrenal zona fasciculata in mice. *Chemico-Biological Interactions*. 1988;**65**:25-40
- [115] Jonsson J, Rodriguez-Martinez H, Brandt I. Transplacental toxicity of 3-methylsulphonyl-DDE in the developing adrenal cortex in mice. *Reproductive Toxicology*. 1995;**9**:257-264
- [116] Kelce WR, Stone CR, Laws SC, Gray LE, Kemppainen JA, Wilson EM. Persistent DDT metabolite pp'-DDE is a potent androgen receptor antagonist. *Nature*. 1995;**375**:581-585
- [117] Andersen A, Warren DJ, Nome O, Vesterhus L, Slordal L. A high-pressure liquid chromatographic method for measuring mitotane [1,1-(o,p'-Dichlorodiphenyl)-2,2-dichloroethane] and its metabolite 1,1-(o,p'-Dichlorodiphenyl)-2,2-dichloroethene in plasma. *Therapeutic Drug Monitoring*. 1995;**17**:526-531
- [118] Adamsson A, Salonen V, Paranko J, Toppari J. Effects of maternal exposure to di-isononylphthalate (DINP) and 1,1-dichloro-2,2-bis(p-chlorophenyl)ethylene (p,p'-DDE) on steroidogenesis in the fetal rat testis and adrenal gland. *Reproductive Toxicology*. 2009;**28**:66-74
- [119] Yang Y, Wang C, Shen H, Fan H, Liu J, Wu N. Cis-bifenthrin inhibits cortisol and aldosterone biosynthesis in human adrenocortical H295R cells via cAMP signaling cascade. *Environmental Toxicology and Pharmacology*. 2022;**89**:103784
- [120] Hornychova M, Frantik E, Kubat J, Formanek J. Neurotoxicity profile of supermethrin, a new pyrethroid insecticide, cent. *European Journal of Public Health*. 1995;**3**:210-218
- [121] Chowdhury AR, Gautam AK. Steroidogenic impairment after lindane treatment in male rats. *Sangyo Ika Daigaku Zasshi*. 1994;**16**:145-152
- [122] Oskarsson A, Ulleras E, Plant KE, Hinson JP, Goldfarb PS. Steroidogenic gene expression in H295R cells and the human adrenal gland: Adrenotoxic effects of lindane in vitro. *Journal of Applied Toxicology: JAT*. 2006;**26**:484-492
- [123] Xi J, Yang Z, Zeng C, Hu X, Wang J. Suppressive effect of triadimefon, a triazole fungicide, on spatial learning and reference memory in rats. *Behavioural Pharmacology*. 2012;**23**:727-734
- [124] Goetz AK, Rockett JC, Ren H, Thillainadarajah I, Dix DJ. Inhibition of rat and human steroidogenesis by triazole antifungals. *Systems Biology in Reproductive Medicine*. 2009;**55**:214-226
- [125] Xu Q, Chen Q, Lin L, Zhang P, Li Z, Yu Y, et al. Triadimefon suppresses fetal adrenal gland development after in utero exposure. *Toxicology*. 2021;**462**:152932
- [126] Meyer A, Vuorinen A, Zielinska AE, Da Cunha T, Strajhar P, Lavery GG, et al. Carbonyl reduction of triadimefon by human and rodent 11beta-hydroxysteroid dehydrogenase 1. *Biochemical Pharmacology*. 2013;**85**:1370-1378

Efficacy of Glucocorticoid Therapy in Different Types of Multiple Sclerosis Progression

Vitaliy Vasylovskyy, Tetiana Nehreba, Nataliya Voloshyna, Maksym Chernenko and Tetiana Pohuliaieva

Abstract

Multiple sclerosis (MS) is an autoimmune disease, affecting the central nervous system that causes significant disability and healthcare burden. Pulse-dosage corticosteroid therapy (GCT) remains the mainstay of treatment of exacerbations of multiple sclerosis. A total of 98 patients were examined, including 28 patients with relapsing-remitting MS (24 women and 4 men) and 70 patients with secondary progressive MS (57 women and 13 men). The number of GCT therapy courses in 98 patients at all disease stages totalled 536: 98 in RR MS (9 at debuts and 89 at RRS) and 438 in SP MS (11 at debuts, 178 at RRS and 249 at SPS). The efficacy of repeated courses of GCT therapy in patients with RR and SP MS was evaluated at different stages of the disease progression: debut in RR and SP MS, RRS in RR and SP MS and SPS in SP MS, including retrospective analysis. Important conclusions have been made about complex systemic reorganisation at different stages of relapsing-remitting and secondary-progredient types of MS, efficiency of GCT in different types of MS and stages of pathological process and about influence of GTC on the prognosis of the disease.

Keywords: multiple sclerosis, corticosteroid therapy, exacerbation, secondary progression, uncertain prognosis

1. Introduction

The modern algorithm of multiple sclerosis (MS) treatment includes management of exacerbations with glucocorticoids (GCT), immunotherapy with MS disease-modifying drugs (MS DMDs), symptomatic therapy to eliminate various clinical disease manifestations and adaptive strategies to develop a set of rehabilitation measures to reduce the degree of disability [1–8].

First-line drugs that manage MS exacerbations are GCTs (prednisolone, methylprednisolone), whose clinical effect is due to their immunosuppressive, anti-inflammatory and anti-oedematous action. GCTs have a wide spectrum of therapeutic action, influencing immune reactions in various ways: by lymphocytolysis, by accelerating the catabolism of immunoglobulins, by reducing the production of pro-inflammatory cytokines (interleukins-1, –6, –8 and tumour necrosis factor-alpha

(TNF- α), by suppressing the transcription and enhancing the degradation of genes controlling the synthesis of interleukin-2, which is central to the development of the immune response, by improving axonal conduction, and by stabilising the permeability of the blood-brain barrier (BBB). Recent studies point to the ability of GCTs to inhibit the formation of ‘black holes’ (sites of neuronal death) and prevent the development of brain atrophy. The discovered effects of GCTs prevent early persistent disability by slowing the development of brain atrophy, which is accompanied by a steady accumulation of residual neurological deficit [9–11].

Hormonal therapy in MS is important not only as a factor suppressing the autoimmune process but also as a type of substitution therapy due to the development of glucocorticoid deficiency, which changes immunological reactivity towards increased allergic manifestations and contributes to the demyelination process. Hyperactivity of the hypothalamic-pituitary-adrenal (HPA) system in MS is caused by reduced functional activity of GCT receptors and results in impaired immunoreactivity of the body. At the same time, the experience of using GCTs in MS accumulated over many decades has not solved a series of problems related to their administration. There is no consensus on adequate dosages, regimens, methods and duration of administration taking into account the severity of exacerbations, expediency of prescription in the debut and evaluation of the efficacy of GCT therapy in isolated use and in combination with other alternative treatment methods. Frequent administration of inadequate hormone regimens by increasing the daily dose of the drug at the next exacerbation contributes to the suppression of the HPA system and the development of steroid addiction, which leads to persistent hormone-dependent forms and further progression of the process [1, 3, 12].

A breakthrough in this field occurred in recent decades thanks to the implementation of highly effective pulse therapy with methylprednisolone (Metypred, Solu-Medrol) for the management of relapses in the relapsing-remitting (RR) type of MS progression. The drug has a significant advantage over prednisolone due to the presence of a methyl group capable of penetrating the cell membrane and binding to intracellular receptors. Solu-Medrol (Metypred) is administered in high doses (up to 1000 mg) by intravenous drip for 5–7 days. The effect of the drug in the process of restoration of central nervous system (CNS) functions affected by demyelinating processes is maintained for 1.5 months due to a powerful anti-inflammatory and anti-oedematous action, leading to a significant reduction in brain volume and normalisation of BBB permeability [1, 8, 13, 14].

2. Rationale

Until recently, the spectrum of therapeutic measures in the secondary progressive (SP) type of MS progression was forcefully limited to the use of cytostatics, which cause a significant number of complications in case of long-term treatment [15, 16]. Due to the therapeutic effects of GCTs, the sceptical attitude to their prescription in SP MS was reconsidered because, unlike RR MS, SP MS is characterised by an unfavourable prognosis because of the progression of the process leading to the accumulation of neurological deficit and persistent disability. It is proved that in this disease type, degenerative-axonal lesions are combined with autoimmune inflammatory changes of varying severity. Despite a different temporal algorithm of the inflammatory process development and significant differences between these MS types, which are manifested by clinical-immunological and clinical-morphological dissociations (‘iceberg phenomenon’ according to C. Poser), the activity of the demyelinating

process at the secondary progression stage (SPS) in SP MS can be comparable with the activity of relapses in RR MS. Therefore, timely and adequate administration of GCTs at early stages of SP MS, that is, at the debut and at the beginning of the relapsing-remitting stage (RRS), can delay further progression of the process. This statement is the evidence-based justification for the use of active immunosuppressive GCT therapy in this category of patients at all stages of the disease progression [1, 5, 17].

3. Aim of the study

To evaluate the comparative efficacy of hormonal glucocorticoid pulse therapy and to develop an algorithm of differential administration at different stages of relapsing-remitting and secondary-progredient types of multiple sclerosis.

4. Materials and methods

The study was conducted at the Department of Autoimmune and Degenerative Pathology of the Nervous System at the Multiple Sclerosis Centre of the State Enterprise 'Institute of Neurology, Psychiatry and Narcology of the National Academy of Medical Sciences of Ukraine' (SE INPN NAMS of Ukraine).

The study involved clinical neurological and statistical research methods. The clinical neurological method included retrospective analysis of the disease progression from the manifestation of clinical symptoms in each patient and dynamic neurological examination during periods of relapses and remissions at the RRS in RR MS and during progression and stabilisation at the SPS in SP MS. Statistical processing of the data was carried out using the 'Statgraph' statistical software package with a defined number of patients (n), mean index value (M) and the standard deviation of the index (m).

A total of 98 patients were examined, including 28 patients with RR MS (24 women and 4 men) and 70 patients with SP MS (57 women and 13 men).

The number of GCT therapy courses in 98 patients at all disease stages totalled 536: 98 in RR MS (9 at debuts and 89 at RRS) and 438 in SP MS (11 at debuts, 178 at RRS and 249 at SPS).

The efficacy of repeated courses of GCT therapy in patients with RR and SP MS was evaluated at different stages of the disease progression: debut in RR and SP MS, RRS in RR and SP MS and SPS in SP MS, which are of strategic importance for the final prognosis of the disease. The following clinical parameters were considered at different stages of RR and SP MS: age at onset, disease duration, age and severity of debuts, duration of remission after debut, duration of RRS, number and severity of relapses at RRS, mean relapse rate (MRR) at RRS, duration of SPS at the end of the study, progression variants at SPS, duration of remissions (stabilisation) after the first and before the last GCT course in RR and SP MS, progression rate in RR and SP MS, dynamics of EDSS disability scale scores after the first and before the last GCT course in RR and SP MS [18–20].

5. Results

At the time of evaluation of GCT treatment efficacy, the age of patients and disease duration in RR MS were significantly lower than in SP MS ($p < 0.05$), whereas the age of debut in the two disease types was not significantly different (Table 1).

Parameter	RR (n = 28)	SP (n = 70)
Mean age	39.2 ± 2.0 ¹	45.9 ± 2.5 ¹
Mean disease duration	9.5 ± 1.2 ²	19.8 ± 2.3 ²
Mean age at onset	29.5 ± 2.1	27.6 ± 2.0

Notes: n, number of patients; M, mean value; m, standard deviation; ¹p < 0.05 – significant differences in age between RR and SP MS; ²p < 0.05 – significant differences in disease duration between RR and SP MS.

Table 1.

Age, disease duration and age at onset in RR and SP MS (years), M ± m.

Parameter	RR (n = 28)		SP (n = 70)	
	abs. value	%	abs. value	%
Mild debuts	16	57.2 ± 9.3 ¹	19	27.5 ± 7.4 ¹
Moderate debuts	10	35.7 ± 9.0 ²	44	62.5 ± 8.1 ²
Severe debuts	2	7.1 ± 4.8	7	10.0 ± 5.1

Notes: n, number of patients; M, mean value; m, standard deviation; ¹p < 0.05 – significant differences in the frequency of mild debuts between RR and SP MS; ²p < 0.05 – significant differences in the frequency of moderate debuts between RR and SP MS.

Table 2.

Debuts of varying severity in RR and SP MS, M ± m.

Parameter	Percentages			
	RR (n = 28)		SP (n = 70)	
	abs. value	%	abs. value	%
After GCT administration in RR	9	32.1 ± 8.8	—	—
Without GCT administration in RR	19	67.9 ± 8.8	—	—
After GCT administration in SP	—	—	12	17.1 ± 4.5
Without GCT administration in SP	—	—	58	82.9 ± 4.5

Notes: n – number of patients; M – mean value; m – standard deviation.

Table 3.

GCT pulse therapy at the debut stage in patients with RR and SP MS, M ± m.

The pattern of debut severity in RR and SP MS was alternating, mild debuts were predominant in RR and moderate debuts were predominant in SP MS. Accordingly, a comparative assessment of debut severity between the two types of disease showed a significant predominance of mild debuts in RR and moderate debuts in SP MS; severe debuts were rare in all patients with almost equal incidence (**Table 2**).

GCT pulse therapy at the debut stage was performed in only 21 (21.4%) of 98 patients, including in 9 (32.1 ± 8.8)% of 28 with RR and in 12 (17.1 ± 4.5)% of 70 with SP MS. Such a low percentage, especially in patients with future SP MS (2 times less), was due to untimely diagnosis of MS (**Table 3**).

The experience of GCT administration proved its high efficacy in mild and moderate debuts, especially in RR MS. The first course of the GCT therapy resulted in rapid and significant regression of neurological symptoms and full clinical remission. In the group of patients with severe debuts, which were extremely rare, especially in RR MS,

Parameter	Percentages	
	RR (n = 28)	SP (n = 70)
After GCT administration	3.5 ± 1.3	5.7 ± 2.8
Without GCT administration	2.6 ± 0.8 ¹	6.2 ± 2.9 ¹

Notes: n – number of patients; M, mean value; m, standard deviation; ¹p < 0.05 – significant differences in the duration of remission after debuting in SP MS without GCT administration.

Table 4.
Duration of remission after debut depending on the administration of the first GCT therapy course in RR and SP MS, M ± m.

the recovery from debuts was prolonged and accompanied by minimal regression of neurological deficit with the outcome of incomplete clinical remission despite GCT administration.

Despite the high efficacy of the first GCT therapy course, no significant differences in the duration of remission after the debut were found in patients with RR and SP MS, whereas this parameter was significantly higher in patients with SP MS without GCT administration (**Table 4**).

The specific features of the RRS (duration, frequency and severity of relapses and neurological deficit accumulation rate) play a key role in triggering the process of RRS to SPS transformation. The implementation of this process requires a complex selective structural reorganisation of clinical indicators at RRS, among which the severity of relapses is of particular significance. An increase in the frequency of severe relapses during the RRS is a trigger that accelerates the RRS to SPS transformation [19, 21].

According to its duration, RRS was divided into short (2 to 5 years), moderate (5 to 8 years) and long (more than 8 years). The average duration of RRS at the background of repeated hormonal therapy courses was (6.8 ± 0.8) years in RR MS and (10.4 ± 3.9) years in SP MS. Thus, at the time of pulse therapy efficacy evaluation, the duration of RRS was shorter (p > 0.05) in RR MS than in SP MS due to the incomplete nature of the relapse process and indicated the absence of an immediate threat of its transformation into SPS.

Neurological symptoms during exacerbation periods at the RRS affected the leading functional systems with predominance of pyramidal and cerebellar syndromes. As a rule, relapses of different severity (mild, moderate and severe) alternated in the vast majority of patients as the RRS progressed. Mild relapses were characterised by rapid rates of clinical symptom development, short duration (no more than 3–4 weeks), mono- or oligosyndromic symptoms with minimal signs of rapidly regressing neurological deficit. In moderate relapses, oligo- or polysyndromic symptoms prevailed with the formation of moderate neurological deficit and its subsequent regression at moderate rates (up to 2 or more months). In severe relapses, pronounced polysyndromic symptoms developed and their partial regression occurred at a slower rate (within 3 or more months), as a rule with the outcome of short and incomplete clinical remissions.

19 of 28 patients with RR MS and 47 of 70 patients with SP MS were first administered GCT therapy at the RRS. As a consequence, all patients with RR MS and 59 of 70 patients with SP MS received GCT therapy at the debut or at the RRS. The other 11 patients with SP MS first received hormonal therapy at the SPS due to the absence of the RRS.

A total of 267 GCT therapy courses were administered at the RRS in both patient groups: 89 courses for RR MS (72 for moderate relapses and 17 for severe relapses) in 67.8% of patients and 178 courses for SP MS (104 for moderate relapses and 74 for severe relapses) in 84.3% of patients. The mean number of courses per patient was 3.1 for RR MS and 3.0 for SP MS.

Thus, hormonal therapy at the RRS covered the vast majority of patients with moderate to severe relapses. In mild relapses, patients did not receive GCT therapy despite a significant proportion of this subgroup having radiological activity based on MRI. Violation of the protocol, according to which hormonal therapy is recommended for all relapses regardless of their severity, led to an increase in the frequency and severity of relapses, accumulation of residual neurological deficits, shortened RRS duration and increased risk of RRS transformation into secondary progression.

The total number of relapses at the RRS in all patients at the background of repeated courses of GCT therapy was 505, including 139 (27.5%) in RR MS and 366 (72.5%) in SP MS. The average number of relapses per patient was 4.9 in RR MS and 6.3 in SP MS. The prevalence of relapses at the RRS in patients with SP MS indicates a more unfavourable development of the process and can serve as one of the clinical markers of probable RRS to SPS transformation.

The analysis of the frequency of relapses of different severity (mild, moderate, severe) showed no significant differences between RR and SP MS. During the entire RRS in the two types of disease progression, the relapses of moderate severity prevailed with the same incidence; mild relapses were more frequent in RR MS ($p > 0.05$); severe relapses prevailed in SP MS ($p > 0.05$). A significant predominance of moderate over severe and mild over severe relapses was observed in RR MS. In turn, moderate relapses were significantly more frequent than mild or severe relapses in SP MS (**Table 5**).

The mean relapse rate (MRR – the ratio of the number of relapses to the RRS duration) was not significantly different between the studied patient groups and was 0.9 ± 0.1 for RR MS and 1.1 ± 0.2 for SP MS (MRR for each patient ranged from 0.1 to 2.8). Decreasing MRR (<1.0) indicated infrequent relapses and longer RRS duration, increasing MRR (>1.0) was associated with more frequent relapses and shorter RRS duration (**Table 6**).

Relapses were significantly more frequent in SP MS with MRR > 1.0 than with MRR < 1.0 , whereas there was just a trend between these two parameters in RR MS ($p > 0.005$) (**Table 6**).

Relapse severity at the RR stage	Percentages	
	RR (n = 28)	SP (n = 59)
Mild	35.9 ± 9.1^2	28.8 ± 5.9^3
Moderate	51.9 ± 9.4^1	$49.1 \pm 6.5^{3,4}$
Severe	$12.2 \pm 6.2^{1,2}$	22.1 ± 5.4^4

Notes: n, number of patients; M, mean value; m, standard deviation; ¹ $p < 0.05$ – significant differences in the incidence of moderate and severe relapses in RR MS; ² $p < 0.05$ – significant differences in the incidence of mild and severe relapses in RR MS; ³ $p < 0.05$ – significant differences in the incidence of mild and moderate relapses in SP MS; ⁴ $p < 0.05$ – significant differences in the incidence of moderate and severe relapses in SP MS.

Table 5.
Severity of relapses at the relapsing-remitting stage (RRS) in RR and SP MS at the background of repeated GCT therapy courses, $M \pm m$.

MRR	Percentages	
	RR (n = 28)	SP (n = 70)
<1.0	0.6 ± 0.3	0.5 ± 0.1 ¹
>1.0	1.5 ± 0.9	1.6 ± 0.7 ¹

Notes: n, number of patients; M, mean value; m, standard deviation; ¹p < 0.05 – significant difference between MRR <1.0 and MRR >1.0 in SP MS.

Table 6.

Mean relapse rate at the relapsing-remitting stage in RR and SP MS at the background of repeated GCT therapy courses, M ± m.

The clinical effect under the influence of GCT therapy courses was characterised by differentiated regression of neurological deficit. This led to conditional distinction between 'well-controlled' and 'poorly controlled' symptoms in each functional system. In the pyramidal syndrome, spastic tonus disorders were primarily subject to reverse development, while recovery of leg strength depended on the severity of paresis. In the cerebellar-atactic syndrome, 'well-controlled' symptoms included a decrease in the amplitude of horizontal nystagmus and shakiness when walking, as well as an improvement in the performance of the finger-nose test. Performance of the patellofemoral test and static ataxia in the Romberg test were much less frequently subject to reverse development. The regression of sensory disorders was differentiated and depended on their nature. The most 'well-controlled' symptoms were disorders of pain sensitivity and astereognosis, whereas normalisation of proprioceptive and temperature sensitivity was slow and, as a rule, partial. In stem disorders, vestibular syndrome, vertical nystagmus and facial muscle dysfunctions as a result of facial nerve damage were more often subjected to significant regression; less frequently, various oculomotor disorders were observed. Sphincter disorders, depending on the degree of their decompensation, were usually subject to partial regression with significant individual differences.

Thus, the analysis of GCT pulse therapy efficacy indicates that a 'dissociation syndrome' with selective and differentiated regression of clinical symptoms in separate functional systems was developed during RRS at relapses of varying severity in patients with RR and SP MS.

The process of RRS to SPS transformation occurred as the efficacy of hormonal therapy decreased and proceeded at different rates in different patients. At the time of assessment of GCT treatment results in 70 patients with SP MS, the average duration of SPS was (7.2 ± 1.4) years (ranging from 3 to 17 years).

The number of GCT therapy courses at SPS in 70 patients with SP MS was 249, which on average corresponded to 3.5 courses per patient. There were no significant differences in the average frequency of courses during RRS and SPS in SP MS (3.0 and 3.5, respectively).

Clinical analysis of the SPS identified the main variants and rates of progression, which indicate its complex structural and functional organisation and are of strategic importance for further disease development and prognosis.

Three main variants of progression have been identified: steady, proceeding without clinically marked stabilisation periods; relapsing, in the form of abrupt exacerbations, resembling relapses, recovery from which was accompanied by stabilisation periods of different duration; and progressive, representing an alternation of the periods of slow progression of neurological symptoms and stabilisation of different duration [7, 20, 21].

The first two variants (steady and relapsing), usually unfavourable, are characterised by the development of gross and persistent polysyndromic neurological symptoms, absence or relative rarity of dissociation syndromes and a high progression rate. As a result of such development, a deep disability degree and therapeutic resistance to GCT therapy of varying degrees are developed. The progressive variant of progression is more favourable in comparison with the first two and is characterised by the absence of gross neurological deficit, higher efficacy of pathogenetic therapy, longer period of residual working ability and better sociopsychological adaptation. The nature of further progression was determined not only by the variants but also by the intensification rates of neurological symptoms – rapid, moderate and slow. In rapid rates, steady and relapsing variants or their alternation prevail; in moderate and especially slow rates, progressive variants prevail.

The analysis of clinical features of the SPS revealed interdependence between the MRR at RRS and variants of secondary progression. The most favourable progressive variant of progression (40.0 ± 5.8 %), which prevailed in patients with $MRR < 1.0$, was the most frequent (**Table 7**).

The second most frequent variant of progression was the most unfavourable one, that is, steady (30.0 ± 5.4 %), which occurred in one half of the patients at $MRR > 1.0$, and in the second half at the SPS development, which followed remission after the debut, bypassing the RRS. The relapsing variant, which has an intermediate position between the previous variants in terms of its prognostic significance, was observed in (24.3 ± 4.5 %) of patients. In this category of patients, $MRR < 1.0$ and $MRR > 1.0$ were almost equally frequent. Very rarely, in (5.7 ± 2.8 %) of cases, alternation of different variants of progression throughout the course of SPS was observed (**Table 7**).

When assessing GCT treatment efficacy in RR and SP MS at the beginning (after the first course) and at the end (before the last course), the following parameters were taken into account: mean remission duration (MRD) and (or) stabilisation duration, the dynamics of scores on the EDSS disability scale and the rate of progression.

In RR MS, a comparative assessment of MRD was performed after the first and before the last GCT course at the end of the study when the RRS was not completed and there was no immediate risk of transformation into SPS. The studies showed a significant prevalence of MRD after the first course – (2.8 ± 0.8) years (ranging from 6 months to 10 years) versus the last course – (1.5 ± 0.2) years (ranging from 4 months to 3 years).

Parameter	SP MS (n = 70)	
	abs. value	%
Progressive variant	28	$40.0 \pm 5.8^{1,2}$
Relapsing variant	17	$24.3 \pm 4.5^{1,3}$
Steady variant	21	30.0 ± 5.4^4
Alternation of different variants	4	$5.7 \pm 2.8^{2,3,4}$

Notes: n, number of patients; M, mean value; m, standard deviation; ¹ $p < 0.05$ – significant differences between progressive and relapsing variants of progression; ² $p < 0.05$ – significant differences between progressive variant and alternation of different variants of progression; ³ $p < 0.05$ – significant differences between relapsing variant and alternation of different variants of progression; ⁴ $p < 0.05$ – significant differences between steady variant and alternation of different variants of progression.

Table 7.
Progression variants in SP MS.

In SP MS, the MRD or stabilisation duration during the SPS was significantly longer (1.8 ± 0.5) years (ranging from 3 months to 5 years) after the first course than before the last course (1.0 ± 0.1) years (ranging from 2 months to 2 years). A comparative analysis of this parameter between the two disease types, a tendency towards predominance after the first course and a significant predominance before the last course was noted in patients with RR MS.

The prevalence of MRD at the initial stages of the disease and its significant decrease at the end of the study despite repeated courses of hormonal therapy indicates the depression of the HPA system with the development of steroid addiction, which in some patients leads to the depletion of adaptation-compensatory processes and increased risk of transformation into SPS.

The above finding is supported by the increased degree of neurological deficit according to the EDSS disability scale in the two disease types. In RR MS, the mean disability score was (2.1 ± 1.1) points (ranging from 1.0 to 3.0 points) after the first course of GCT therapy and (3.5 ± 0.7) points (ranging from 2.0 to 4.5 points) before the last course. In SP MS, the EDSS score was (3.1 ± 0.4) points (ranging from 2.8 to 5.0 points) after the first course and (6.0 ± 0.9) points (ranging from 5.5 to 7.0 points) before the last course at the end of the study. Comparative analysis of the mean EDSS score after the first and before the last course of GCT therapy shows a deepening of neurological deficit, especially in patients with SP MS at the SPS ($p < 0.05$).

The negative dynamics of EDSS scores corresponds to such an integral indicator as the rate of progression (the sum of the difference of scores on the EDSS disability scale between the first and before the last GCT course for each patient in relation to the total number of patients), which was 1.1 in RR MS and 2.3 in SP MS.

Based on the findings, criteria for the efficacy of GCT treatment in RR and SP MS were developed. High (61.0 ± 9.2) % and moderate (39.0 ± 9.2) % efficacy was obtained for RR MS, and moderate (30.0 ± 5.4) %, low (30.0 ± 5.4) % and no (40.0 ± 5.8) % efficacy was obtained for SP MS.

With high efficacy of GCT therapy, the risk of transformation into SPS was considered minimal, and the MRR was less than 1.0. The treatment process in these patients was accompanied by a decrease in the duration of debuts and complete clinical remission after the debut. At the background of increasing RRS duration, mild (more often) and moderate (less often) short or mid-duration relapses, complete remissions between relapses with minimal residual neurological deficit (EDSS not more than 2.0 points), long-term preservation of full (more often) or partial (less often) working ability prevailed. With moderate efficacy, patients with RR MS were not at immediate risk of transformation to SPS either (with MRR values of less than 1.0 (more often) and more than 1.0 (less often)). However, despite repeated courses of GCT therapy, the course of the RRS was less favourable in contrast to patients with high treatment efficacy. This was manifested by an increase in the duration of the debut, predominance of incomplete clinical remissions after the debut, an increase in the frequency of relapses of moderate severity during the RRS, a gradual increase in neurological deficit (EDSS from 2.0 to 3.0 points) in remissions between relapses and partial loss of working ability (**Table 8**).

Differences in MRD in patients with high and moderate efficacy after the first and before the last GCT course were not significant. Low rate of progression (1.1) correlated with insignificant negative dynamics of EDSS disability score between the first and before the last GCT course (from 2.1 ± 1.1 to 3.5 ± 0.7), which was mainly attributed to patients with moderate efficacy.

Parameter	RR (n = 28)		SP (n = 70)	
	abs. value	%	abs. value	%
High	17	61.0 ± 9.2	—	—
Moderate	11	39.0 ± 9.2	21	30.0 ± 5.4
Low	—	—	21	30.0 ± 5.4
No efficacy	—	—	28	40.0 ± 5.8

Notes: n, number of patients; M, mean value; m, standard deviation.

Table 8.
GCT therapy efficacy in RR and SP MS.

In SP MS, there was no high efficacy at the background of repeated courses of GCT therapy. Moderate efficacy was obtained in patients with $MRR < 1.0$ and $MRR > 1.0$, whose clinical symptoms at the background of GCT therapy were characterised by incomplete remissions after the management of debuts of different severity and duration, development of the RRS of different duration, against which moderate relapses prevailed. After transformation into SPS, which occurred at a slow pace, progressive (more often) or relapsing (less often) variants of progression were predominant with neurological deficit (< 6.0 points on the EDSS scale) and partial or complete loss of working ability (**Table 8**).

Low efficacy was characterised by the development of a short RRS after the management of severe or moderate long-term debuts and incomplete and short-term remission. During the RRS, there was a regular tendency to more frequent and more severe relapses ($MRR > 1.0$) with a steady accumulation of neurological deficit. As a result, there was an inevitable transformation into SPS, occurring in the form of relapsing (more often) or steady (less often) variants of progression with persistent neurological deficit (from 5.5 to 6.5 points on the EDSS scale) and complete loss of working ability.

There was no efficacy in some patients with $MRR > 1.0$. In part of these patients, RRS was absent and SPS developed immediately after a prolonged and severe debut. This category of patients was characterised by a steady variant of progression that developed rapidly, high scores (more than 6.5 on the EDSS scale) with profound disability and complete loss of working ability (**Table 8**). The comparison of treatment results with the nature of prognosis depending on the disease type indicates that patients with an uncertain prognosis are characterised by moderate treatment efficacy, whereas an unfavourable prognosis prevails in patients with low or no efficacy.

6. Discussion of results

The conducted study indicate that hormonal therapy was the most effective in patients with RR MS. Under the influence of repeated courses of GCT therapy, high and moderate efficacy of treatment was achieved in the form of positive dynamics of most clinical parameters. At different stages of RR MS, there was a rapid and complete regression of the leading syndromes in the debuts, completeness and duration of remission after the debut increased, the number of patients with $MRR < 1.0$ rose, the duration of the RRS increased, the frequency and severity of relapses decreased

and minimal neurological deficit was preserved at the background of low progression rate. As a result of the above reorganisation, the duration of the RRS was prolonged and the immediate risk of RRS to SPS transformation was averted.

In SP MS, hormonal therapy was less effective and was assessed according to three gradations as moderate, low or no efficacy. With moderate efficacy, the SPS developed later after the onset of the disease compared to low efficacy. In this process, which was accompanied by a complex structural rearrangement of the leading clinical indicators, the duration of remission after the debut increased, the number of patients with MRR >1.0 decreased, the duration of the RRS increased against the background of reduced number of severe relapses, and there was a slow accumulation of neurological deficit. The positive dynamics of these parameters under the influence of GCT treatment were partial and differentiated, and despite significant individual differences, led to the development of a progressive variant of progression, which has a more favourable prognostic value.

In patients with low or no efficacy of GCT therapy, recovery from debuts was prolonged and accompanied by minimal regression of neurological deficit and short remission after the first attack. The duration of the RRS was shorter and the frequency of severe relapses was higher than in the group of patients with moderate efficacy. This led to an increase in the number of patients with a high MRR, steady accumulation of neurological deficit, increased rate of progression and rapid development of the SPS, whose structure is dominated by unfavourable variants of progression (steady and relapsing).

The analysis of the dynamics of clinical symptoms at different stages of RR and SP MS under the influence of repeated courses of GCT therapy indicates that the treatment efficacy is closely related to the nature of the disease prognosis. It is known that, in the overwhelming majority of patients, RR MS has a favourable character. However, a variety of variants should be distinguished in RR MS, differing in their clinical course and prognostic significance. Thus, the presence of clinical markers indicating the risk of transformation into SP MS leads to treating the current prognosis in RR MS as uncertain. Progredient types of disease, including SP MS, are usually characterised by a rapid accumulation of neurological deficit due to the progression of the process with the development of a high degree of disability and an unfavourable prognosis in the vast majority of patients. However, a relatively 'benign' or uncertain, variant of prognosis should also be distinguished in SP MS, which is characterised by longer RRS, progressive variant of progression with long periods of stabilisation, slow accumulation of neurological deficit and positive response to various methods of pathogenetic therapy (GCT, MS DMDs, etc.). Consequently, the prognosis, as an expected result of the previous course of the demyelinating process, depends on the clinical interpretation of the entire disease pattern, including retrospective analysis of disease stages [7, 20, 22, 23].

Clinical and mathematical analysis for the evaluation of the studied indicators in different types of MS resulted in the development of clinical criteria for different prognosis variants: favourable and uncertain for RR MS and unfavourable and uncertain for SP MS [23–25].

A comparison of treatment results with the prognosis in RR MS indicates a favourable prognosis with high efficacy and an uncertain prognosis with moderate efficacy of repeated courses of GCT. In SP MS, uncertain prognosis prevailed in patients with moderate efficacy, while low or no efficacy under the influence of GCT treatment suggested an unfavourable prognosis.

7. Conclusions

1. Under the influence of repeated courses of GCT therapy, clinical parameters undergo a complex systemic reorganisation at different stages of relapsing-remitting and secondary-progredient types of MS.
2. As a result of retrospective analysis of the dynamics of clinical parameters occurring in the course of relapsing-remitting and secondary-progredient MS, criteria for the efficacy of hormonal GCT therapy were developed: high and moderate efficacy for the relapsing-remitting type; moderate, low and no efficacy for the secondary-progredient type.
3. Treatment efficacy in repeated GCT courses is closely associated with the nature of prognosis (favourable, unfavourable, uncertain) obtained as a result of clinical and mathematical analysis of indicators characterising different types of MS. In the relapsing-remitting type, high efficacy prevailed for the favourable prognosis, and moderate efficacy prevailed for the uncertain prognosis; in the secondary-progredient type, moderate efficacy correlated with the uncertain prognosis, and low or no efficacy correlated with the unfavourable prognosis.
4. High efficacy of GCT therapy in patients with relapsing-remitting MS with a favourable prognosis was characterised by complete clinical remissions after the debut, predominance of mild short relapses at the relapsing stage, minimal neurological deficit, low progression rate, long-term preservation of working ability and minimal risk of transformation into the secondary-progredient type. With moderate efficacy of GCT therapy in patients with an uncertain prognosis, the probability of transformation into the secondary-progredient type increased due to decreased compensatory reserves of the body. In this process, the duration of debut and the prevalence of incomplete clinical remissions after debut increased. At the relapsing-remitting stage, relapses of moderate severity prevailed against the background of a gradual increase in neurological deficit with partial loss of working ability.
5. In the secondary-progredient type, the efficacy of treatment with repeated courses of GCT was significantly lower than in the relapsing-remitting type, but the process of transformation of the relapsing-remitting stage into secondary progression occurred at different rates and was characterised by significant individual differences. In the case of an uncertain prognosis, moderate efficacy prevailed, which led to a decrease in the number of severe relapses against the background of increased duration of the relapsing-remitting stage and the development of a more favourable progressive variant of progression. The unfavourable prognosis was characterised by low or no efficacy. These subgroups of patients showed no positive dynamics of most clinical parameters at all stages of the disease. As a result, a steady or recurrent variant of progression, a pronounced neurological deficit, and a high degree of disability were developed.
6. The expediency of timely administration of and treatment with repeated courses of GCT pulse therapy in patients with relapsing-remitting MS with a favourable and uncertain prognosis and in patients with the secondary-progredient type

with an uncertain prognosis has been proved. In case of low efficacy in patients with secondary-progredient MS type and an unfavourable prognosis, it is necessary to develop new approaches to the MS treatment strategy.

Abbreviations

SP	secondary progredient type
HPAS	hypothalamic-pituitary-adrenal system
GCT	glucocorticoids
BBB	blood-brain barrier
MS DMDs	multiple sclerosis disease-modifying drugs
MS	multiple sclerosis
RR	relapsing-remitting type
RRS	relapsing-remitting stage
MRD	mean remission duration
MRR	mean relapse rate
CNS	central nervous system
SPS	secondary progression stage

Author details

Vitaliy Vasylovskyy*, Tetiana Nehreba, Nataliya Voloshyna, Maksym Chernenko and Tetiana Pohuliaieva
Institute of Neurology, Psychiatry and Narcology of National Academy of Medical Sciences of Ukraine, Multiple Sclerosis Centre, Ukraine

*Address all correspondence to: vvasylovskyy72@gmail.com

IntechOpen

© 2023 The Author(s). Licensee IntechOpen. This chapter is distributed under the terms of the Creative Commons Attribution License (<http://creativecommons.org/licenses/by/3.0>), which permits unrestricted use, distribution, and reproduction in any medium, provided the original work is properly cited. 

References

- [1] Gusev EI, Boiko AN. Multiple Sclerosis: From Studying Immunopathogenesis to New Treatment Techniques. Gubernskaya Medicine. Russia; 2001. 128 p
- [2] Gusev EI, Zavalishin IA, Noiko AN. Multiple Sclerosis and Other Demyelinating Diseases. Miklosh. Moscow. 2004. 540 p
- [3] Levin OS. Immunotherapy of multiple sclerosis. Russian Medical Journal. 2001;6:48-52
- [4] Yevtushenko SK, Derevyanko IN. The pathogenesis and basis for treatment in multiple sclerosis. International Neurological Journal. 2006;2(6):2-12
- [5] Compston AC. Current approaches to the treatment of multiple sclerosis: Achievements, disappointments, hopes (2nd communication). Neurology and Neurosurgery. 2004;106:246
- [6] Dobson R, Giovannoni G. Multiple sclerosis – A review. EAN. 2018;26(1):27-40. DOI: 10.1111/ene.13819
- [7] Voloshyna NP, Taitlin VI, Leshchenko AH, et al. Multiple sclerosis in Ukraine: prevalence, course, prognosis, treatment, pharmacoeconomics. Ukrainian Bulletin of Psychoneurology. 2007;15(1):6-21
- [8] Voloshyn NP, Voloshyna NP, Taitlin VI, et al. Current aspects of multiple sclerosis: pathogenesis, peculiarities of disease course in Ukraine, diagnosis, standards of pathogenetic therapy. Neuron-Review (Journal of Clinical Neurosciences). 2007;3:4-26
- [9] Tarianyk KA, Shkodina AD, Lytvynenko NV, Boiko DI. Combined therapy of relapsing-remitting multiple sclerosis exacerbations with plasmapheresis and glucocorticoids with regard to patients' quality of life. Ukrainian Neurological Journal. 2020;3:29-34. DOI: 10.30978/UNJ2020-3-29
- [10] Voloshyna NP, Nehreba TV, Vasylosvyy VV, et al. Comparative efficacy of hormonal pulse therapy in relapsing-remitting and secondary-progressive types of multiple sclerosis with different prognosis patterns (Communication I. Efficacy of hormonal pulse therapy in the debut and relapsing phase in relapsing and secondary-progressive types of multiple sclerosis with different prognosis patterns). International Neurological Journal. 2018;4(98):21-31
- [11] Voloshyna NP, Nehreba TV, Vasylosvyy VV, et al. Comparative efficacy of hormonal pulse therapy in relapsing-remitting and secondary-progressive types of multiple sclerosis with different prognosis patterns (Communication II. Efficacy of hormonal pulse therapy in the progression phase in the secondary-progressive type of multiple sclerosis with different prognosis patterns). International Neurological Journal. 2018;7(101):14-16
- [12] Douglas S. Glucocorticoids for the treatment of multiple sclerosis. Clinical Neurology. 2014;122:455-464. DOI: 10.1016/B978-0-444-52001-2.00020-0
- [13] Sharrack B, Hughes RA, Morris RW, et al. The effect of oral and intravenous methylprednisolone treatment on subsequent relapse rate in multiple sclerosis. Journal of Neurological Science. 2000;73:73-77

- [14] Alam SM, Kyriakides TM, Lawdwn PK. Newman Methylprednisolone in multiple sclerosis. *Journal of Neurology*. 2008;**56**: 1219-1220
- [15] Voloshyna NP, Vasylovskyy VV, Chernenko MY. Use of mitoxantrone in combination with cortexin for the treatment of progressive multiple sclerosis. *International Neurological Journal*. 2008;**6**(22):13-16
- [16] Vasylovskyy VV, Voloshyna NP, Nehreba TV, Chernenko MY. Efficacy of mitoxantrone in patients with progredient types of multiple sclerosis. *International Neurological Journal*. 2015;**7**(77):17-27
- [17] Poser C. Multiple sclerosis. *Journal of Neurology and Psychiatry*. 1993;**4**:77-78
- [18] Zavalishin IA, Zakharova MN, Peresadova AV, Steude NN, et al. Progressive course of multiple sclerosis. *S. S. Korsakov Journal of Neuropathology and Psychiatry*. 2002;**2**:26-31
- [19] Nehreba TV. Comparative clinical characteristics of debuts and relapse stages in relapsing-remitting and secondary-progressive multiple sclerosis. *Ukrainian Bulletin of Psychoneurology*. 2004;**12**(1):66-69
- [20] Nehreba TV. Course and prognosis of modern forms of multiple sclerosis. *Ukrainian Bulletin of Psychoneurology*. 2006;**14**(1):44-46
- [21] Voloshyna NP, Vasylovskyy VV, Levchenko IL, Yehorkina OV, Tkachova TM, Chernenko MY, et al. New approaches to the clinical diagnosis of different types of multiple sclerosis and their differentiated therapy. Practical recommendations. Copyright for a scientific work No 47786 dated 13.02.2013
- [22] Nehreba TV. Prognostic criteria for different types of multiple sclerosis. Copyright for a scientific work No 39160 dated 14.07.2011. Application No. 39386 dated 04.05.2011
- [23] Voloshyna NP, Nehreba TV, Vasylovskyy VV, Kirzhner VM, Chernenko MY, Voloshyn-Haponov IK. Development of prognosis depending on the development of the progression stage and progression options in progressive types of multiple sclerosis. *Ukrainian Bulletin of Psychoneurology*. 2021;**29**(3):18-22
- [24] Voloshyna NP, Nehreba TV, Vasylovskyy VV, Sukhorukov VV, Kirzhner VM. Clinical and mathematical analysis of relationships between prognosis and debut patterns in different types of multiple sclerosis. *Georgian Medical News*. 2021;**9**(318):127-133
- [25] Voloshyna NP, Vasylovskyy VV, Kirzhner VM, Pohulaieva TM, Chernenko MY, Voloshyn-Haponov IK, et al. Correlation analysis between clinical parameters in different types of multiple sclerosis. *Ukrainian Bulletin of Psychoneurology*. 2022;**30**(110): 21-27. DOI: 10.36927/2079-0325-V30-is3-2022-94

Edited by Diana Loreta Păun

The book is an exploration of the biology and pathophysiology of cortisol, a crucial hormone for survival, from the perspective of a multidisciplinary team of international experts. From presenting the current state of knowledge in the field of hormone physiology to discussing aspects related to cortisol measurement methods, the book raises a series of challenges for both endocrinologists and physicians from other specialties. It addresses interesting topics such as the role of enzymes involved in adrenal steroidogenesis, the connection between cortisol and obesity, and the role of hormone therapy in multiple sclerosis.

Published in London, UK

© 2024 IntechOpen
© DrWD40 / iStock

IntechOpen

